Spring 2015

Comprehensive benefits of green roofs

Madison R. Gibler

Department:

COMPREHENSIVE BENEFITS OF GREEN ROOFS

by

MADISON R. GIBLER

A THESIS

Presented to the Faculty of the Graduate School of the

MISSOURI UNIVERSITY OF SCIENCE AND TECHNOLOGY

In Partial Fulfillment of the Requirements for the Degree

MASTER OF SCIENCE IN ENVIRONMENTAL ENGINEERING

2015

Approved by

Joel Burken, Advisor
Eric Showalter
Stuart Baur
Kelly Homan

PUBLICATION THESIS OPTION

This thesis has been prepared in the style used by Environmental Science and Technology. Pages 19-39 will be submitted for publication in that journal. Appendices A and B have been added for purposes normal to thesis writing.

ABSTRACT

Green infrastructure uses vegetation, soils, and natural processes to manage water and create healthier urban environments, providing traditional roof services and alternative stormwater management technologies. Other benefits and impacts are not yet fully understood or valued. Research conducted assesses specific stormwater benefits of green roofs, providing information on nutrient leaching from media; and analyzes potential energy benefits through side-by-side comparisons of full-scale white, traditional black rubber, and green roofs in the mid-continent Missouri climate. Roofing media selection impacted leaching of nutrients, suspended solids, and organic carbon from the tested green roof media. Thermal properties were investigated at the building level, as were benefits related to urban heat island effects. Water and energy models are combined to illustrate impacts of evapotranspiration (ET) on green roof temperatures and urban heat dissipation. As ET is dependent on a variety of climate parameters including temperature, humidity, wind speed, and solar radiation, the potential to dissipate energy from a roof surface by means of water vaporization was modeled. Models using climate data to estimate potential ET may be used as predictive tools on impacts of green roof design and can be applied in stormwater management, allowing green roofs to reach maximum benefits of reduced nutrient loading, decreased runoff, peak flow attenuation, urban heat island mitigation, and economic savings. Findings also raise questions as many ancillary benefits such as aesthetics, stormwater management, and urban energy dissipation are society-level benefits, yet capital costs as well as operation and maintenance costs are generally incurred only by the building owner. Economic vehicles could help maximize community benefits and alleviate financial burden on building owners.

ACKNOWLEDGMENTS

I would like to express my sincerest thanks to Dr. Joel Burken, my advsor, who took me on as a graduate student in Environmental Engineering, despite my Civil Engineering background and lack of chemistry knowledge. Although Dr. Burken was on the opposite side of the globe for a large portion of my research, it felt as though he was still on campus, gracing me with his countless ideas, extensive knowledge, and much appreciated guidance. Thanks to Dr. Eric Showalter for allowing me to lean on him for facilities knowledge and for being a great resource of all things green roof. Also, I want to thank Dr. Stuart Baur, for guidance during the development of the weather station for my research. I'm extending a special thanks to Dr. Kelly Homan and Dr. Curt Elmore for their expertise in solar radiation. While Dr. Matt Limmer was not my advisor, his wealth of knowledge and experience greatly helped in the data analysis and general guidance throughout my research experience. His input and collegial assistance was invaluable.

The supplies and funding for this research came from a variety of sources. The creation and use of the built-in-place green roof atop Emerson Hall was possible in part by Missouri S&T's physical facilities. Members of the RCI Foundation donated green roof materials. Helene Hardy-Pierce and Brian Smith from GAF facilitated donated supplies for both the green roof trays and built-in-place GAF GardenScapes™ roof. Kelly Luckett supplied Arkalyte growing media and Green Roof Blocks™. The USGS lent the Sutron Datalogger necessary for automated data collection.

I would like to thank Brian Swift for extensive technical knowledge and other members of the Civil, Architectural, and Environmental Engineering Department Technical Team: Gary Abbott and John Bullock. I would also like to thank Joann Stiritz from Missouri S&T for assistance with images used in this thesis.

I am thankful to the lab group and fellow researchers who were of great help and support: Grace Philpy (formerly Harper), Tyler Hall, Marshall Usrey, Kirstin Kurilla, Katherine Bartels, Jace O'Brien, Jordan Wilson, and Lea Ahrens.

Last, but certainly not least, I want to thank my friends and family, especially my parents, for their continued love and support as I pursued even more education, missing holidays, birthdays, vacations, and family events.

TABLE OF CONTENTS

Page

PUBLICATION THESIS OPTION iii

ABSTRACT iv

ACKNOWLEDGMENTS v

LIST OF FIGURES ix

LIST OF TABLES x

SECTION

1. INTRODUCTION 1
    1.1. URBAN STORMWATER MANAGEMENT 1
    1.2. GREEN INFRASTRUCTURE 1
    1.3. GREEN ROOF APPLICATION AND PERFORMANCE 2
2. GOALS AND OBJECTIVES 3
    2.1. GOALS 3
    2.2. OBJECTIVES 3
3. LITERATURE REVIEW 5
    3.1. ECOSYSTEM SERVICES 5
    3.2. URBANIZATION 5
    3.3. EUTROPHICATION 7
    3.4. GREEN INFRASTRUCTURE 9
        3.4.1. Non-vegetated Green Infrastructure 10
        3.4.2. Vegetated Green Infrastructure 10
    3.5. GREEN ROOFS 11
        3.5.1. Water Quality 13
            3.5.1.1 Suspended solids 13
            3.5.1.2 Organic carbon 14
            3.5.1.3 Nutrients 14
        3.5.2. Runoff Reduction 14
        3.5.3. Urban Heat Island Effects 16
        3.5.4. Additional Benefits 17

PAPER
GREEN ROOF VALUATION: SAVING POLLUTANTS AND ENERGY 19
ABSTRACT 19
INTRODUCTION 20
EFFECTS OF URBANIZATION 20
GREEN ROOF IMPLEMENTATION 21
MATERIALS AND METHODS 22
GREEN ROOF MEDIA AND VEGETATION 22
WATER QUANTITY/QUALITY ANALYSIS 22
METEOROLOGICAL DATA 23
WATER AND ENERGY BALANCE 24
RESULTS AND DISCUSSION 28
LEACHATE CONCENTRATIONS 28
RUNOFF REDUCTION 32
URBAN HEAT ISLAND EFFECTS 34
CONCLUSION 38
REFERENCES 39
SECTION
4. COMBATTING URBAN HEAT ISLAND EFFECTS 40
4.1. MATLAB MODELING 40
4.2. CROP COEFFICIENTS 40
5. SUMMARY AND CONCLUSIONS 42
6. RECOMMENDATIONS FOR FUTURE WORK 43
6.1. NUTRIENT LOADING 43
6.2. PEAK FLOW ATTENUATION 43
6.3. WATER AND ENERGY BALANCE 43
6.4. MEDIA SELECTION 44
6.5. GREEN ROOF TEXTILES 44
6.6. THERMAL ANALYSIS OF URBAN WATERSHEDS 45
APPENDICES
A. MATLAB CODE 46

B. MATLAB OUTPUT FOR 08/30/14-09/03/14, 12/13/14-12/17/14, & 01/11/15-01/15/15 63

BIBLIOGRAPHY 100

VITA 104

LIST OF FIGURES

Page

Figure 3.1. The effect of urbanization on stormwater runoff 6

Figure 3.2. Green roof section showing typical components..... 12

Figure 3.3. Peak flow attenuation of varying roof types..... 15

PAPER

Figure 1. Schematic of full-scale green, white TPO, and black EPDM roofs atop Emerson Hall on Missouri S&T campus 25

Figure 2. Thermocouple layout to record temperature at various layers of all three roofs 26

Figure 3. Green roof experimental arrangement to collect real-time data on moisture content in green roof media 27

Figure 4. TP concentrations for precipitation events during the 30-month study 29

Figure 5. TN concentrations for precipitation events during the 30-month study..... 30

Figure 6. TOC concentrations for precipitation events during the 30-month study 31

Figure 7. Median TSS concentrations for precipitation events during the 30-month study 32

Figure 8. Cumulative runoff for precipitation events during the 30-month study..... 33

Figure 9. Surface temperatures of the three roof types (left axis) as well as cumulative precipitation and water storage in the media (right axis) for two rainstorm events over a 48-hour period..... 35

Figure 10. Thermal roof image showing qualitative temperature differences between three roof types on September 9, 2014 at 3:35:18pm CST 36

Figure 11. Thermal roof image showing qualitative temperature differences between three roof types on September 9, 2014 at 3:37:14pm CST 37

LIST OF TABLES

PAPER Page

Table 1. Tested green roof conditions..... 23

1. INTRODUCTION

1.1. URBAN STORMWATER MANAGEMENT

Stormwater management is challenging for urban watersheds. The increased percentage of urban impervious areas reduces infiltration and evapotranspiration (ET), resulting in excess flow to sewer systems and local surface waters. Until the early 20th century, sewer systems had been combined sewer systems (CSSs), where stormwater and wastewater were conveyed together through the same pipe network. Since then, the application of new sanitary sewer systems (SSSs) and municipal separate storm sewer systems (MS4s) convey municipal wastewater and stormwater, respectively (EPA 2004). The separation of CSSs to SSS and MS4 in the U.S. would be an exorbitant expense, thus CSSs remain in use today. When wet weather events exceed CSS capacitance, combined sewer overflow (CSO) events occur, introducing microbial pathogens, nutrients, and other toxic substances into our nation's lakes, rivers, streams, and coastal waters (EPA 2004). Aside from sewer separation, two CSO solutions are common: 1) construct massive reservoirs to contain the CSS wastewater until water treatment capacity is available; or 2) minimize the volume of stormwater entering and leaving the sewer system.

1.2. GREEN INFRASTRUCTURE

Green infrastructure mimics natural stormwater flows, unlike gray infrastructure. Green infrastructure can reduce overland flow by increasing pervious surface area, attenuating flow, and/or creating storage, thus reducing the stormwater load on CSSs. A variety of green infrastructure, such as rainwater harvesting, permeable pavement, rain gardens, and green roofs, have been incorporated into best management practices (BMPs), and used for urban stormwater control (Villarreal, et al. 2004). Although full benefits have yet to be realized, the value of green infrastructure is well recognized and supported by the American Society of Civil Engineers (ASCE), Environmental Protection

Agency (EPA), and the White House Council on Environmental Quality (CEQ), forming the Green Infrastructure Collaborative along with twenty organizations (EPA 2014).

1.3. GREEN ROOF APPLICATION AND PERFORMANCE

There are two types of green roofs: extensive and intensive. Extensive green roofs have media depths ranging from 5-15 cm, whereas, intensive green roofs have media depths greater than 15 cm, capable of sustaining vegetation with deeper root structures and that is less drought tolerant (Luckett 2009). Aside from rooftop gardens for personal use, when a building owner decides to incorporate green roofs into the building plan, they are designed to meet aesthetic, environmental, and/or regulatory goals (Luckett 2009). The ancillary benefits (aesthetic, environmental, and regulatory) are difficult to assess, as are societal benefits, but roofing costs are bore solely by the building owner, creating a unique technical/social situation.

Green roofs can provide traditional roof services and even an increased roof life, yet also reduce stormwater runoff and encourage peak flow attenuation. Additionally, green roofs can provide ecosystem services concurrently with economic and environmental benefits, such as potential energy savings and improved air quality. Urbanization intensifies summer urban heat islands, leading to more heat-related deaths, respiratory disease, and heightened peak energy consumption (Sproul, et al. 2014). Although reducing urban heat island effects with green roofs has not been well studied, air temperature reductions due to change in albedo and increased vegetation have been projected in modeling by Taha (1997) for urban settings.

2. GOALS AND OBJECTIVES

2.1. GOALS

The primary goal of this study was to describe and model the comprehensive benefits of green roofs through evaluation of stormwater retention, water quality impacts, building energy savings potential, and reduction of urban heat island effects. To further understand the benefits of green roofs the following studies were performed.

2.2. OBJECTIVES

To reach the aforementioned goal, the following objectives were established:

- First Objective. Measure runoff volume from and retention in different types of green roof media for planted and unplanted test bed conditions, extending the initial eight-month pilot study under field conditions.
    - Hypothesis: GAF GardenScapes^{TM} media will reduce runoff more effectively than Arkalyte media.
- Second Objective. Evaluate the effect of media type on concentrations of suspended solids, organic carbon, and nutrients (phosphorus and nitrogen) in green roof leachate over time. Extend initial eight-month pilot study to determine time-sensitivity of nutrient concentrations in green roof leachate.
    - Hypothesis: Nutrient concentrations will decrease until reaching a plateau level (steady state) and total mass leaching can be shown.
- Third Objective. Perform a side-by-side thermal comparison of white thermoplastic polyolefin (TPO), black ethylene propylene diene monomer (EPDM) rubber, and green roofs to determine building energy savings potential.
    - Hypothesis: Green roofs will have the greatest potential for building energy savings in terms of building heating and cooling, followed by white TPO roofs, followed by black EPDM roofs.

- Fourth Objective. Perform a side-by-side evaluation of a white TPO roof, a black EPDM roof, and a green roof to determine potential impacts of urban heat island effects by green roofs in terms of energy dissipated.
    - Hypothesis: Green roofs will have the greatest urban heat island reduction potential due to evapotranspiration (ET) cooling.
- Fifth Objective. Develop FAO Penman-Monteith model to compare reference evapotranspiration to actual evapotranspiration measured via collection of load cell data for GRBs.
    - Hypothesis: FAO Penman-Monteith model for reference evapotranspiration will underestimate measured evapotranspiration.

The aforementioned goals and objectives are addressed in the following documentation. Results and conclusions generally supported hypotheses presented. Although full benefits of green roofs have yet to be realized, the following research makes strides in the advancement of urban heat island reduction and energy savings benefits of green roofs as it relates to evapotranspiration potential. This research poses further potential for developing forecasting models to determine where green roofs have the ability to make the largest impact in stormwater management and urban heat island mitigation.

3. LITERATURE REVIEW

3.1. ECOSYSTEM SERVICES

Ecosystem services in our environment from forested land cover provide flood protection, atmospheric regulation of carbon dioxide and oxygen, climate control, and reduce the spread of diseases (Holzman 2012). However, ecosystem services are often considered free and go unappreciated for their environmental capital, upon which human well-being is dependent (PCAST 2011). Natural resources such as clean water, wildlife, vegetation, fertile soil, and fresh air are a result of biodiverse ecosystems (Holzman 2012). Engineered ecosystems, such as constructed wetlands, bioswales, and green roofs are designed to provide specific infrastructure services as well as ecosystem services. Green roofs can reduce heat transfer through roofs of buildings, retain stormwater, trap airborne particulate matter, and sequester carbon, all while providing habitat, amenity, and aesthetic value (Lundholm, et al. 2015). Human well-being is greatly influenced by healthy ecosystems and their services.

3.2. URBANIZATION

Urbanization, although a sign of healthy growth for a city, has detrimental impacts on our environment. A large influx of population to urban areas leads to expansion of the metropolis area. Urbanization creates disconnection between the earth and the atmosphere in the hydrologic water cycle. Construction of buildings and roadways to account for this population rise adds impervious surfaces. Roofs account for approximately 40-50% of impervious area in most developed cities (Stovin, et al. 2012). An increase of impervious area by 10 - 20% doubled peak flows associated with the 1.5 – 2 year recurrence intervals for most watersheds, resulting in the potential to severely destabilize streams (Bledsoe and Watson 2001). The addition of this impervious cover, by means of roofs, parking lots, and streets, increases the volume of stormwater available for runoff by reducing infiltration as seen in Figure 3.1 below (Chow, et al. 1988). Aquatic ecosystems are greatly affected by urbanization as streams must widen or deepen

to account for greater flows, occurring more often, for longer durations (Bledsoe and Watson 2001).

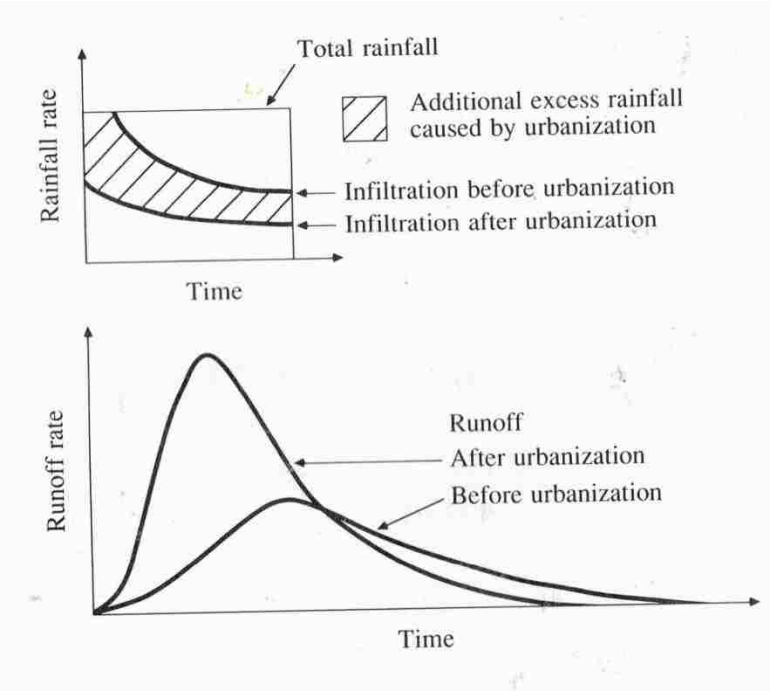

Figure 3.1. The effect of urbanization on stormwater runoff (Chow, et al. 1988)

Changes in discharge, and thus stream instability, are affected by more than impervious area (Bledsoe and Watson 2001). Land development processes including tree removal, surface leveling, and surface compaction also affect infiltration, increasing the quantity of surface runoff (Akan and Houghtalen 2003). Hydraulically improved drainage systems, such as man-made sewer systems, increase peak flows through use of artificial channels, gutters, and storm drain collection systems (Bedient, et al. 2013; Chow, et al. 1988). Times of concentration associated with conveyance systems are less than that of overland flow. The designed network of pipes and channels used to convey stormwater throughout an urban environment increases discharge (Akan and Houghtalen 2003). Land use practices in conjunction with conveyance systems result in greater flowrates, meaning

higher velocities and accelerated scouring of stream channels; or, in the case of excess erosion caused by land development, channel aggradation (Brooks, et al. 2003). Urban streams are often hardened to prevent scour, transporting the problems downstream.

Urbanization affects water quality as well as water quantity. The buildup of pollutants on urban surfaces impairs water quality (Akan and Houghtalen 2003). Heavy metals and rust from decaying motor vehicles, petroleum based hydrocarbons such as gas range organics (GROs) and diesel range organics (DROs), fertilizers, feces, and debris are all potential pollutants introduced to receiving water bodies from surfaces found in urban environments. Additionally, thermal pollution is a problem associated with urbanization. The surface temperature of a waterbody is affected by the temperature of the inflowing water (Brooks, et al. 2003). Due to the low albedos of most impervious surfaces such as roofs and pavements, inflows from urban environments are susceptible to higher temperatures. Land use practices involving the addition of low albedo impervious surfaces to a watershed, raise temperatures of receiving waters, reducing dissolved oxygen levels of those water bodies, inhibiting the habitability of those aquatic ecosystems (Brooks, et al. 2003).

3.3. EUTROPHICATION

Eutrophication has developed into a wide spread problem for both freshwater and coastal saltwater systems. Eutrophication is the excessive addition of nutrients to natural waters, impairing water quality by means of excessive plant growth, loss of dissolved oxygen, reduced biodiversity, taste issues, and odor problems (Schnoor 1996). Anthropogenic sources of nutrient enrichment include: agriculture, municipal wastewater, industrial waste, and the burning of fossil fuels, where many detergents and fertilizers contain nitrogen and/or phosphorus (Rabotyagov, et al. 2014). Nutrients encourage growth of algal blooms that upon death fall through the water column and decompose in the hypolimnion, depleting oxygen by stimulating bacterial respiration (Rabotyagov, et al. 2014; Scavia, et al. 2014).

Point and nonpoint sources of nutrients, mainly nitrogen and phosphorus, which may both act as limiting nutrients, result in eutrophication (Michalak, et al. 2013; Rabotyagov, et al. 2014). The National Pollutant Discharge Elimination System (NPDES) permit program developed by the Clean Water Act (CWA) handles discharge of pollutants from point sources such as industrial process water, non-contact cooling water, and channeled stormwater runoff (Bell, et al. 2014). Nonpoint sources, however, are more difficult to regulate. Surface runoff from fertilized lawns, cropland, and agricultural production exemplify nonpoint sources of nutrients with minimal to no oversight.

Recently publicized examples of eutrophication in the United States include record-setting algal blooms in Lake Erie and The Dead Zone in the Gulf of Mexico. In 2011, Lake Erie experienced record-setting algal blooms containing cyanobacteria, also known as blue-green algae (Michalak, et al. 2013). The development of the large algal biomass, and in turn the toxic blue-green algae was attributed to many causes, including long-term agricultural practices, increased precipitation, and a warm quiescent lake environment (Michalak, et al. 2013). Hypoxic conditions have also been problematic in the Gulf of Mexico. The Dead Zone in the Gulf of Mexico is characterized by oxygen levels that are too low to sustain a variety of aquatic organisms (Rabotyagov, et al. 2014).

Although hypoxia can be a naturally occurring process, anthropogenic sources have been linked to the expanding number, size, a severity hypoxic regions (Rabotyagov, et al. 2014). Gulf hypoxia occurrence should be no surprise as the Gulf of Mexico is the receiving water body for all pollutants in the entire Mississippi watershed, an area of vast agricultural landscape, where long-term agricultural practices such as autumn season fertilizer application, surface fertilizer application as opposed to soil injection, and conservation tillage contribute to runoff with high phosphorus concentrations (Michalak, et al. 2013). To remedy problems associated with eutrophic conditions, a change in land use management practices such as incorporating green infrastructure to reconnect the hydrologic cycle with terrestrial systems (soil, vegetation, etc.) must occur.

3.4. GREEN INFRASTRUCTURE

Green infrastructure identifies any infrastructure designed to mimic naturally occurring processes. Green infrastructure can be used in conjuncture with low impact development (LID) , a site design technique capable of fulfilling the Energy Independence and Security Act of 2007 (Bedient, et al. 2013). The Energy Independence and Security Act of 2007, Section 438 states the necessity "to maintain or restore, to the maximum extent technically feasible, the predevelopment hydrology of the property with regard to the temperature, rate, volume, and duration of flow" (EISA 2007).

Best management practices (BMPs) are structural and nonstructural controls used to reduce or prevent water pollution (Brooks, et al. 2003). These stormwater controls manage quantity and quality, which are closely related in effective stormwater management (WEF, et al. 2012). Ideal stormwater management techniques strike a balance between aesthetics, expense, and functionality. Cost-effective stormwater management approaches, such as green infrastructure, are multi-faceted, capable of utilizing detention, infiltration, evapotranspiration, attenuation, and pollutant removal (WEF, et al. 2012).

Choosing the most appropriate type of green infrastructure to be implemented into the site design is a crucial component for BMPs. Each stormwater management technique must be analyzed for its ability to provide water quality protection, channel protection, overbank flow protection, extreme flow protection, groundwater recharge and evapotranspiration (WEF, et al. 2012). Drainage area, site layout, climate, environmental factors, permitting, right of way, construction access, maintenance, safety, appearance, capital cost, and operation and maintenance costs are all constraints to be considered in BMP selection (WEF, et al. 2012).

There can be both non-structural and structural BMPs. Non-structural BMPs include stormwater management plans (SWMP), pollution prevention, and public education (Akan and Houghtalen 2003). Structural BMPs are those stormwater controls, such as green infrastructure that often require engineering design. Examples of green infrastructure include permeable pavement, filters, infiltrators, detention basins, retention basins, constructed wetlands, filter strips, bioswales, and green roofs.

3.4.1. Non-vegetated Green Infrastructure. Non-vegetated green infrastructure utilizes processes such as infiltration, retardation, and sedimentation to promote groundwater recharge and pollutant removal. Permeable pavement, infiltrators, and filters are all types of non-vegetative green infrastructure that reconnect the soil-water component of the hydrologic cycle.

Permeable pavement is an overarching term that encompasses pervious concrete, porous asphalt, and permeable interlocking concrete pavers (PICP). Permeable pavement provides more void space in the surface course and greater storage depth in the base course to allow for extensive infiltration. Permeable pavement can be used as a replacement for traditional pavement in low traffic volume locations.

Infiltrators, such as infiltration trenches and water quality trenches, are channels excavated to depth, replaced with coarse aggregate backfill, and topped with rip-rap or aggregate (Akan and Houghtalen 2003). The top course retards flows, and the porous backfill promotes percolation into the subgrade. The distinguishing factor between water quality trenches and infiltration trenches is that water quality trenches are deigned to capture only the water quality volume, runoff from frequent storm events, or the first flush from larger storm events (Akan and Houghtalen 2003). Infiltration trenches and water quality trenches can be incorporated along roadways.

Sand filters utilize a bed of porous media for storage and subsequent filtration. Sand filters, like water quality trenches, are designed to treat the runoff of frequent storm events and the first flush of larger storm events (Akan and Houghtalen 2003). Sand filters remove a majority of suspended solids and sorbed pollutants in the pretreatment or sedimentation stage of the sand filter (WEF, et al. 2012). Sand filters must be sized appropriately for the acting drainage area.

3.4.2. Vegetated Green Infrastructure. Vegetated green infrastructure, like non-vegetated green infrastructure, uses infiltration, retardation, and sedimentation for flow control and pollutant removal. However, vegetated green infrastructure additionally utilizes evapotranspiration in stormwater management, reconnecting the soil-vegetation-water component of the hydrologic cycle. Examples of vegetated green infrastructure include basins, engineered wetlands, filter strips, bioswales, and green roofs.

Basins provide surface storage of stormwater. Storage time allows for sedimentation and thus pollutant removal. Detention and retention basins differ in that retention basins, also known as wet ponds, have a permanent pool, whereas detention basins do not. Basins have a forebay with riprap bottom to dissipate erosive energy of inflows and retention basins include an aquatic bench of wetland vegetation around the perimeter (WEF, et al. 2012). Flow attenuation and volume reduction from evaporation, transpiration, and/or infiltration are key processes of stormwater management for basins. Basins require a large area of land for installation.

Four classifications of stormwater wetlands include shallow marsh systems, pond/wetland systems, extended detention wetlands, and pocket wetlands, which are applicable in varying development sites (Akan and Houghtalen 2003). Wetlands remove pollutants, retard flows, reduce flow volumes, and provide potential wildlife habitats; however, wetlands consume large areas of land and require time dedicated for management needs (Akan and Houghtalen 2003).

Filter strips and bioswales are often vegetated with turf grasses, native vegetation, and other wetland plants to retard flows and strain suspended pollutants (WEF, et al. 2012). Filter strips dissipate overland flow, whereas bioswales, also known as rain gardens, convey shallow channelized flow (WEF, et al. 2012). Filter strips and rain gardens can be incorporated into smaller sites to receive runoff from rain gutters or parking lots.

3.5. GREEN ROOFS

Green roofs, commonly known as rooftop gardens, are vegetated beds constructed in lieu of traditional membrane roofs. Green roofs are an engineered best management practice of layered waterproof membrane, root barrier, drainage layer, filter fabric, growing media, and vegetation atop the existing roof section as seen in Figure 3.2 below. There are two types of green roofs: extensive green roofs and intensive green roofs. Extensive green roofs, characterized by shallow media depths, are most common, and usually vegetated with drought tolerant *Sedum* or native grasses. Intensive green roofs

provide larger media depths for plants with deeper root structures. Additionally intensive green roofs can house less drought tolerant plant species due to the additional water storage capacity of the media. Necessary load bearing capability and costs associated with intensive green roofs are greater than that of extensive green roofs.

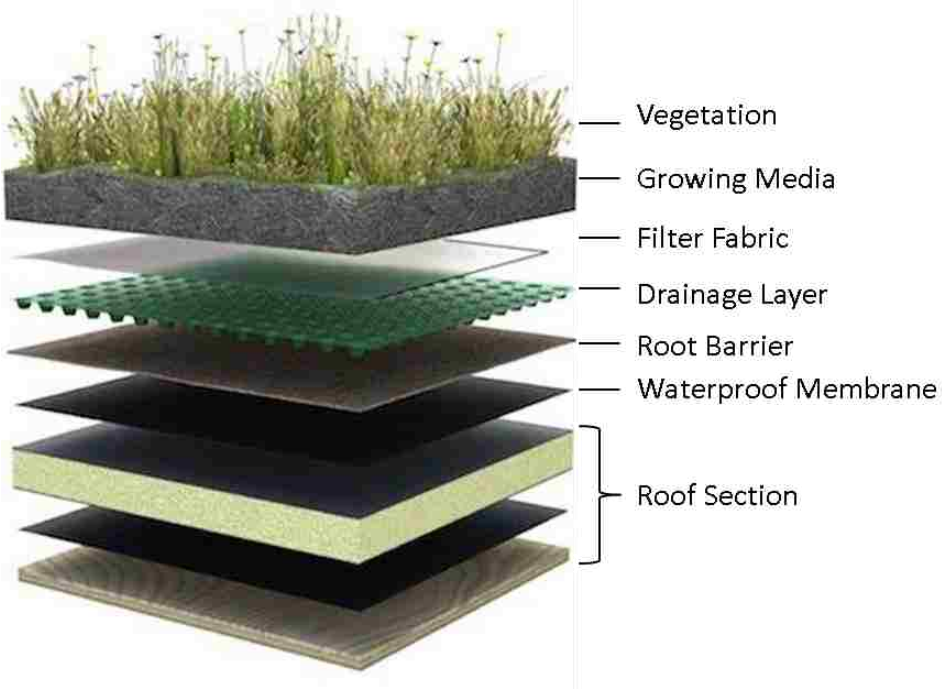

Figure 3.2. Green roof section showing typical components (greenerheights.wordpresss.com 2012)

Green roofs have grown in popularity in recent years. With the emergence of Leadership in Energy & Environmental Design (LEED) certification programs, green roofs, as well as other types of green infrastructure, have more commonly been incorporated into both existing and new construction sites. If properly designed into the site plan, green roofs have the potential to earn LEED points within the Sustainable Sites category, in which 5 LEED points are available, for Rainwater Management and Heat Island Reduction credits (USGBC 2015). Although full benefits of green roofs have yet

to be realized, their noted potential in stormwater management and urban heat island reduction exemplify versatile application capabilities.

LEED certification and other economic tools, such as tax incentives or service fee reductions drive green roof installation as capital costs associated with green roof construction exceed membrane roof installation. Despite green roofs having a 40-year lifespan compared to a membrane roof's 20-year lifespan, the capital costs associated with green roofs are difficult to overcome because installation of extensive green roofs is at least $10 per square foot, whereas membrane installation runs around $1.88 per square foot (Sproul, et al. 2014). Ancillary benefits of green roofs must be realized to justify large capital costs of green roofs.

3.5.1. Water Quality. Green roofs have been shown to impact water quality by increasing suspended solids, organic carbon, and nutrient (nitrogen and phosphorus) concentrations in green roof leachate.

3.5.1.1 Suspended solids. Total suspended solids (TSS) include those particulates such as clay, silts, and fine organic matter that remain suspended in the water column, threatening water clarity among other issues (Morgan, et al. 2011). The particulate matter, in addition to being an aesthetic issue, affects water quality. After sedimentation, solids within the water column, carrying pollutants, are allowed to dissolve into the water body. Although most studies use turbidity as a direct measurement of water clarity, where turbidity is determined by the amount of light capable of passing through the water column without being refracted by the suspended particles, gravimetric methods of determining suspended solids are also used. Morgan, et al. (2011) found mean TSS results decreasing from 119 mg/L to 13 mg/L in runoff from vegetated Arkalyte green roof media and from 377 mg/L to 38 mg/L in runoff from non-vegetated Arkalyte green roof media after 15 watering events for vegetated pots and 11 watering events for non-vegetated pots. From the literature, vegetated green roof media has lower leachate concentrations of suspended solids than non-vegetated green roof media, most likely due to the stabilizing action of the vegetation's root structures. Long-term impacts have not been tracked as roof age and leaching concentrations change.

3.5.1.2 Organic carbon. Similar to total suspended solids, organic carbon has an indirect ability to affect water quality. As organic carbon falls through the water column and decays, it increases the biochemical oxygen demand (BOD), decreasing dissolved oxygen in the water body, negatively impacting aquatic life. Beck, et al. (2011) showed total organic carbon concentrations in green roof leachate ranging from 46 mg/L to 188 mg/L, with average concentrations of 139.8 mg/L and 78.8 mg/L in non-vegetated and *Sedum* vegetated green roof media, respectively. Since organic carbon found in green roof leachate may very well be due to the suspended organic matter, leachate from vegetated green roof media has lower concentrations of total organic carbon than non-vegetated green roof media. Impacts of aging have not been assessed.

3.5.1.3 Nutrients. Because green roof media are designed to sustain vegetation, fertilizer additives containing nitrogen, phosphorus, and potassium are observed in green roof leachate (van Seters, et al. 2009). The fertilizers used in green roof media to promote plant growth also threaten water quality of receiving waters with algae and excessive aquatic plant growth due to high levels of total phosphorus in green roof leachate, which exceed the Ontario water standard of 0.03 mg/L as observed by van Seters, et al. (2009). Fertilizer additives were also related to higher levels of total nitrogen in runoff from green roof media, reported as high as 1.52 mg/L by van Seters, et al. (2009). As a result of studies performed by van Seters, et al. (2009), both nitrogen and phosphorus showed a decline in leachate concentrations over the 18-month monitoring period.

A field study of green roofs performed by Hathaway, et al. (2008) revealed total nitrogen and total phosphorus concentrations in green roof leachate to be greater than those nutrient concentrations in the rainfall outflow for the first two years of the study. In the first seven months of the study, total nitrogen concentrations decreased from 5.4 mg/L to 0.7 mg/L. Additionally total phosphorus concentrations decreased from 1.0mg/L to 0.6 mg/L in the first seven months of the study (Hathaway, et al. 2008).
Total phosphorus and nitrogen concentrations in green roof leachate displayed trends of decreasing over time due to roof age and fertilizing routines (Berndtsson 2010).

3.5.2. Runoff Reduction. Green roofs are an effective form of urban stormwater management. Green roofs effectively detached interconnected impervious areas from subsequent sewer systems as a method of inner city stormwater control (Villarreal, et al.

2004). Green roofs control stormwater runoff by peak flow attenuation and volume reduction.

Assuming that runoff would be observed almost immediately from a membrane covered roof, extensive green roof performance by Stovin, et al. (2012) revealed a mean 59% peak attenuation, resulting in a mean lag time of 143 minutes from the beginning of rainfall to start of runoff. VanWoert, et al. (2005) also illustrated the effects of an extensive green roof on peak flow attenuation as seen in Figure 3.3 below where runoff was delayed, peak flows were reduced, and volume was spread over time.

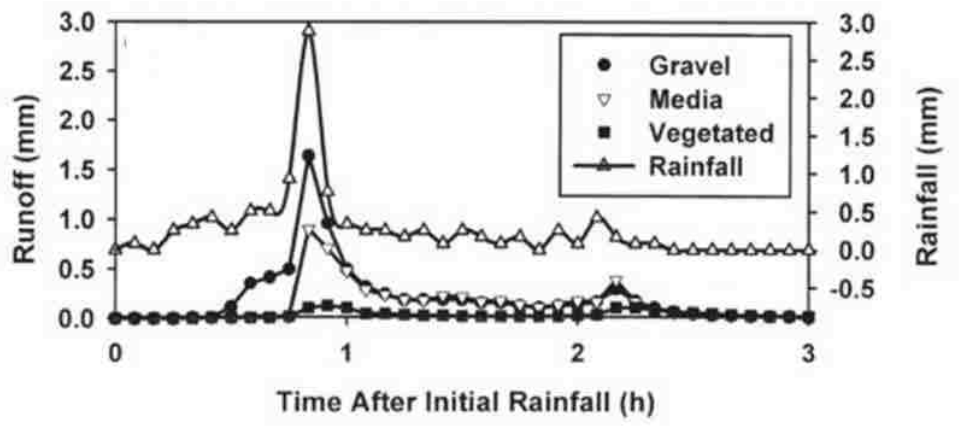

Figure 3.3. Peak flow attenuation of varying roof types (VanWoert, et al. 2005)

The volume of runoff from a green roof is equal to precipitation minus the sum of interception, retention, transpiration from vegetation, and evaporation from media (Nagase and Dunnett 2012). Nagase and Dunnett (2012) performed a greenhouse study of vegetation impacts on runoff volume, yielding results indicating that grass species were most effective in reducing runoff volume, followed by forbs, followed by *Sedum*. Although vegetation plays a role in runoff reduction, media type significantly impacted stormwater runoff (Harper, et al. 2014). Stovin, et al. (2012) shows that on average 50% of 825 mm of mean annual rainfall can be retained by an extensive green roof with 8 cm of media. Stovin, et al. (2012) additionally concludes that 100% retention of rainfall from

storm events with return periods between one and two years is possible. Research by VanWoert, et al. (2005) demonstrated 61% retention of 556 mm of cumulative rainfall for an extensive vegetated green roof over a 14-month study.

van Seters, et al. (2009) performed studies of green roof runoff on a full-scale vegetated green roof with media 14 cm in depth and observed varying percentages of stormwater retention: 54% retained from May to November 2003, 75% retained from June to November 2004, and about 75% retained from April to August 2005. Results from van Seters, et al. (2009) alert the importance of precipitation factors such as rainfall volume, intensity, and frequency on green roof runoff reduction. This importance is reaffirmed in work done by Morgan, et al. (2013) where 4 ft^2 built-in-place (BIP) vegetated green roofs with media 10 cm deep revealed different stormwater retention results between two different study periods: 51% retained during a period from September 2005 to March 2007 where 124 cm of precipitation was observed and 54% retained during a period from April 2007 to June 2008 where 140 cm of precipitation was observed. Not only do media and vegetation type impact runoff from green roofs, so do climate parameters.

3.5.3. Urban Heat Island Effects. A variety of factors influence how urban surfaces interact with the atmosphere including: albedo, moisture available for evapotranspiration, and anthropogenic heating (Dousset and Gourmelon 2003). Most urban areas have higher air temperatures, on average 2°C higher, than their rural counterparts (Taha 1997). Akbari, et al. (2001) reports peak summertime temperatures to be as much as 2.5°C higher in a typical city than in surrounding rural areas. Rosenzweig, et al. (2006) reports nocturnal heat island averages as high as 4°C.

Improving surface cover of buildings through installation of green roofs and highly reflective white roofs are suggestive measures to mitigate urban heat island effects (Takebayashi and Moriyama 2007). Energy savings can be attained through changes in building cover by switching from traditional roof surfaces to green or white roofs. Green roofs and highly reflective white roofs both have low sensible heat fluxes due to the large latent heat flux from evapotranspiration and the small net radiation from solar reflectance, respectively (Takebayashi and Moriyama 2007). Since vegetation cools

surfaces more effectively than increases in albedo, green roofs provide greater cooling potential than their lower-albedo, white roof competitor (Rosenzweig, et al. 2006).

As higher summertime air temperatures lead to general discomfort, additional cooling loads are incurred. Akbari, et al. (2001) concluded that peak urban electric demands increase by 2-4% for every rise of 1°C in daily maximum air temperature above a threshold of 15-20°C; and urban heat islands are responsible for billions of dollars in increased annual peak electricity demand. In a study by Sailor (2008) between Chicago and Houston, annual electricity consumption was lowered by 2% by switching from a membrane roof to a green roof. Savings in annual air conditioning costs for Los Angeles, New York, and Chicago, estimated by Lawrence Berkeley National Laboratory, are $35 million, $16 million, and $10million, respectively (Akbari and Konopacki 2005).

Not only are green roofs capable of building cooling from evapotranspirative effects, green roofs have the potential to reduce heat flux through the roof by acting as an insulation barrier (Palomo Del Barrio 1998). Sailor (2008) also discovered the insulative potential of green roofs by increasing green roof media thickness to 0.3 m, reducing natural gas consumption associated with heating during winter months.

3.5.4. Additional Benefits. In addition to the water and energy advantages of green roofs, other benefits have been identified. Atmospheric deposition is a major source of heavy metals, pesticides, and other pollutants in urban areas (Berndtsson 2010). Urban pollutant concentrations can exceed ten times the pollutant concentrations of clean atmospheres (Taha 1997). Green roofs can theoretically act as a filter and absorb these contaminants before being flushed from rooftops into receiving waters (Berndtsson, et al. 2006).

Green roofs can both directly and indirectly improve air quality. Green roofs contribute to a healthier environment by reducing outdoor air pollution as vegetation removes carbon dioxide, carbon monoxide, nitrogen oxides, air-born ammonia, sulfur dioxide, and ozone (Wu and Smith 2011). Intensive green roofs with media depths capable of sustaining trees can reduce carbon dioxide by sequestering carbon from the atmosphere during photosynthesis (Akbari, et al. 2001). Nitrogen oxides and carbon dioxide emissions from power plants are reduced indirectly by installation of green roofs due to decreased electric demands (Akbari, et al. 2001; Taha, et al. 1998). These

Greenhouse Gases (nitrogen oxides, carbon dioxide, and methane) as well as other harmful constituents (sulfur dioxide, small particulate matter, and volatile organic compounds) produced during power generation are also reduced with lowered peak electrical demands (Wu and Smith 2011). Those harmful constituents, the nitrogen oxides, sulfur dioxide, particulate matter, and ozone, cause respiratory diseases and threaten heart health (Brunekreef and Holgate 2002).

Aside from practical applications, green roofs can be aesthetic relief in urban areas often characterized by drab rooftops. Occupants of neighboring buildings can enjoy a change of scenery from the typical membrane roof. Additionally, onlookers are not bothered by highly reflective white membrane roofs of nearby buildings on sunny days. Green roofs provide habitats for birds, bees, and other insects attracted to pollinate the vegetation. Rooftop gardens can also serve as an oasis within the concrete jungle of the city for building residents.

Full economic benefits of green roofs have yet to be realized as stormwater retention, urban heat island mitigation, and air quality improvement are societal gains. Despite lack of economic quantification of comprehensive green roof benefits, green roofs have an increased roof life expectancy with a 40-year lifespan compared to the 20-year lifespan of a membrane roof (Sproul, et al. 2014).

PAPER

GREEN ROOF VALUATION: SAVING POLLUTANTS AND ENERGY

ABSTRACT

Green infrastructure uses vegetation, soils, and natural processes to manage stormwater and create healthier urban environments. Green roofs, a component of green infrastructure, can provide ecosystem services concurrently with economic and environmental benefits. Conducted research assesses specific stormwater benefits of green roofs, quantifying runoff reduction and nutrient leaching from various media types. Research was also undertaken to analyze potential energy benefits through side-by-side comparisons of full-scale white, black rubber, and green roofs on the S&T campus. In a unique effort to link water and energy research, water and energy models are combined to illustrate impacts of evapotranspiration (ET) on green roof temperatures and urban heat dissipation. The forecasting model inputs location-specific climate data to determine potential ET and water budgets for specific roof designs. The new predictive tool for green roof design and can be applied for green roofs to assess collective benefits of: reduced nutrient loading, runoff reduction, peak flow attenuation, reduction of urban heat island effects, and economic savings. Findings presented also raise societal questions as many benefits assessed occur at the societal level with lower peak urban temperatures and improved stormwater quality, yet capital investment as well as operation and maintenance costs are generally incurred only by the building owner.

INTRODUCTION

EFFECTS OF URBANIZATION

Stormwater management has become an issue for urban areas. The roadways and buildings necessary to sustain such a large population increase impervious area in the form of pavement and roofs. This increased percentage of impervious area disconnects terrestrial systems from the hydrologic cycle, by reducing infiltration and evapotranspiration (ET), resulting in excess flow to sewer systems and local surface waters. Land urbanization alters runoff processes from a subsurface flow regime to a surface flow regime through vegetation clearing, soil compaction, ditch construction, and installation of paved surfaces [1]. The man-made pipe network designed to convey stormwater and municipal wastewater from collection to treatment is strained, as populations and percentage of impervious area continues to increase. The hydraulically efficient combined sewer systems (CSSs), often used in cities, transports runoff and raw sewage at rates and volumes exceeding capacities of downstream treatment plants, resulting in combined sewer overflows (CSOs). Three solutions to minimize CSOs are common: 1) separate municipal wastewater and stormwater into sanitary sewer systems (SSSs) and municipal separate storm sewer systems (MS4s), respectively [2]; 2) construct massive reservoirs to contain the CSS wastewater until water treatment capacity is available; or 3) minimize the volume of stormwater entering and leaving the sewer system. As sewer separation and reservoir construction are costly solutions, urban areas are implementing green infrastructure into urban watersheds to manage urban stormwater.

In addition to stormwater management issues, urbanization leads to increased temperatures of urban areas, also known as urban heat islands. The intensity of urban heat islands is related to land use, water, and build-up [3]. The lowered surface albedo of dark pavements and rooftops in combination with high specific heat adds to urban heat islands. A typical city observes a 2.5°C increase between its urban and rural air temperatures [4].

GREEN ROOF IMPLEMENTATION

Although full benefits of green roofs have yet to be fully realized, the value of green infrastructure is well recognized and supported by the American Society of Civil Engineers (ASCE), Environmental Protection Agency (EPA), and the White House Council on Environmental Quality (CEQ), forming the Green Infrastructure Collaborative along with twenty organizations [5]. Green roofs have potential to combat both stormwater management issues and urban heat island effects associated with urbanization, simultaneously. Green roofs can reduce the stormwater loads on CSSs by increasing pervious surface area, attenuating flow, and creating storage, thus reducing the stormwater load on CSSs. Green roofs act as a stormwater management technique while providing traditional roof services and even an increased roof life. Additionally, green roofs can provide ecosystem services concurrently with economic and environmental benefits, such as potential energy savings and improved air quality. Although mitigating urban heat island effects by incorporating green roofs has not been well studied, air temperature reductions due to change in albedo and increased vegetation have been projected in modeling by Taha [6] for urban settings.

MATERIALS AND METHODS

GREEN ROOF MEDIA AND VEGETATION

Individual combinations of media plantings were tested in Green Roof Blocks™ (GRBs) as modular green roof trays 2 foot by 2 foot (60.8 cm by 60.8 cm), used in previous studies [8]. GRBs were filled 10 cm deep with either Arkalyte, an 80/20 composition of heat expanded clay rock/composted pine bark, or GAF GardenScapes™ media, a commercially produced blend of lightweight rock, organics, and carbon additives. The Arkalyte media was aged one year prior to use in the study. Plant selection targeted drought tolerant plants and a Midwest Mix of different *Sedum* species was selected: *Sedum acre, acre 'Octoberfest', album, aizoon, ellacombianum, floriferum, hispanicum, hybridum 'Czar's Gold', kamtschaticum, oreganum, pulchellum, reflexum, rupestre, seiboldii, sexangulare, spurium, stoloniferum, telephium,* and *Phedimus takesimensis.* Materials from GAF GardenScapes™ were also used to construct a full-scale extensive green roof atop Emerson Hall on the Missouri University of Science and Technology (Missouri S&T) campus, located in Rolla, Missouri, in 2012 [8].

WATER QUANTITY/QUALITY ANALYSIS

In preliminary research by Harper, et al. [7], thirteen GRBs were set up on top of Butler-Carlton Hall on the Missouri S&T campus to allow for collection and sampling. Six GRBs were filled with GAF media and six with Arkalyte media. Three GRBs of each media type were planted and three were left unplanted. The thirteenth GRB remained empty as a control. GRB test bed conditions can be seen in Table 1 below. Each GRB was connected to an 18.9 L bucket with a lid, by approximately 0.5 m of vinyl tubing.

Table 1. Tested green roof conditions

GRB	Quantity
Planted Arkalyte	3
Unplanted Arkalyte	3
Planted GAF	3
Unplanted GAF	3
Control (Empty GRB)	1
Total	13

Volume of runoff collected in the 18.9 L buckets was measured with a graduated cylinder periodically, following precipitation events. Samples of GRB runoff were collected and tested for total suspended solids (TSS), total phosphorus (TP), total nitrogen (TN), and total organic carbon (TOC). Materials and methods followed those presented in Harper, et al. [7]. Measurement of TSS was performed per Method 2540 D of Standard Methods for the Examination of Water and Wastewater. Using Hach Method 8190 and 8040 for a Hach DR/2400 Spectrophotometer, total phosphorus was measured, following EPA Method 365.2 for freshwater samples. Testing for TN and TOC was completed using a Shimadzu TOC-L TOC analyzer with standard catalyst per 720°C catalytic thermal decomposition/chemiluminescence and 680°C combustion catalytic oxidation methods, respectively. Samples were stored in refrigeration until the aforementioned water quality analyses were completed.

METEOROLOGICAL DATA

An on-site weather station captured precipitation, wind speed, wind direction, solar radiation, temperature, and relative humidity data for the microclimate atop Emerson Hall. Wind data was measured at a distance two meters above the green roof surface. Relative humidity measurements were taken at a distance of one meter above the

green roof surface. The meteorological data was collected and stored via Sutron Datalogger for convenient manual download.

A secondary ultrasonic wind sensor was set up at a distance of one meter above the green roof surface. When supplementary wind data was necessary, Equation 47 from Allen, et al. [9] was used to convert wind speeds at a height of one meter above the green roof surface to wind speeds at a height of two meters above the green roof surface.

In an attempt to validate collected data for solar radiation at the Emerson Hall site, pyranometer data was compared to hourly weather data by the Missouri Historical Agricultural Weather Database from Cook Station, Crawford County, Missouri, about 25 miles southeast of Rolla, Missouri, and collected pyranometer data was also compared to solar radiation data managed by Dr. Curt Elmore's team at their Stonehenge weather station location on the Missouri S&T campus.

Additional precipitation measurements for the water quantity/water quality analysis of the thirteen GRBs on Butler-Carlton Hall were provided by the Missouri S&T weather station, reported to the National Weather Service, and organized by the National Climatic Data Center (NCDC).

WATER AND ENERGY BALANCE

The Emerson Hall rooftop is approximately one-third green roof, one-third black ethylene propylene diene monomer (EPDM) rubber roof, and one-third white thermoplastic polyolefin (TPO) roof by surface area, with each area being approximately 370 m^2 [8]. Sixteen thermocouples were positioned at varying locations on the rooftop, seen in Figure 1.

Figure 1. Schematic of full-scale green, white TPO, and black EPDM roofs atop Emerson Hall on Missouri S&T campus

The thermocouples were secured at each location: 0.6 m above the roof surface, at the roof surface, and on the underside of the concrete slab of the roof (sub-slab) for each the green, EPDM, and TPO roofs. White, schedule 40, polyvinyl chloride (PVC) thermocouple shrouds were fixated to each the TPO, EPDM, and green roof to provide

shelter from incoming solar radiation for thermocouples housed at 0.6 m above the roof surfaces. For the green roof, thermocouples were also placed atop and beneath the planted media as seen in Figure 2.

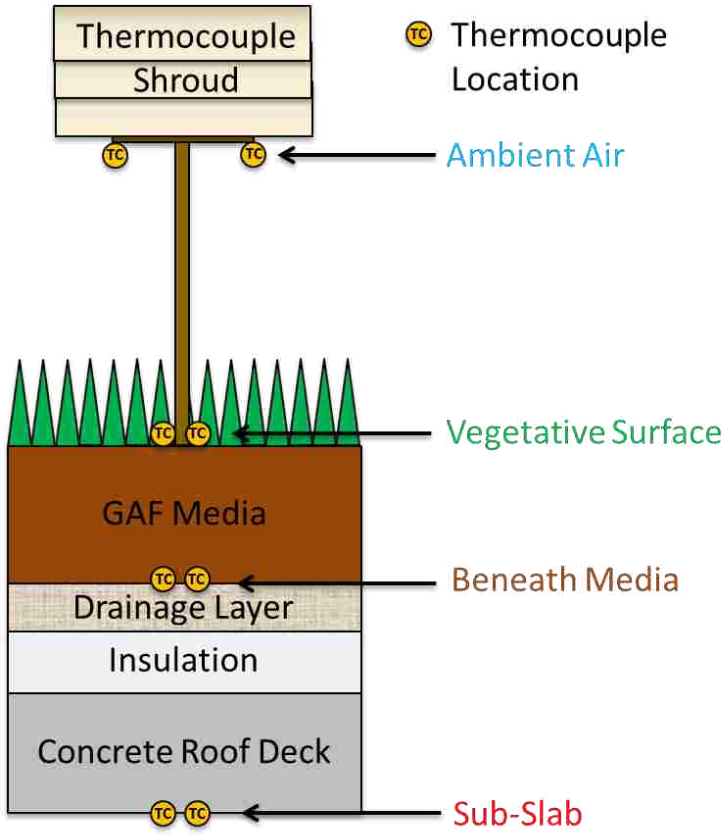

Figure 2. Thermocouple layout to record temperature at various layers of all three roofs

Additionally, four GRBs filled with GAF media and four GRBs filled with Arkalyte were placed on load cells to accurately record real-time water content of the green roof media. Two GRBs of each media type were planted with the Midwest Mix and two were left unplanted. GRBs were angled at roughly 2° slope to mimic roof angle. Collection buckets were attached by vinyl tubing to the GRBs to verify the validity of the

load cell data. Figure 3 represents the green roof experimental arrangement, describing the water quantity, water quality, and load cell setup used.

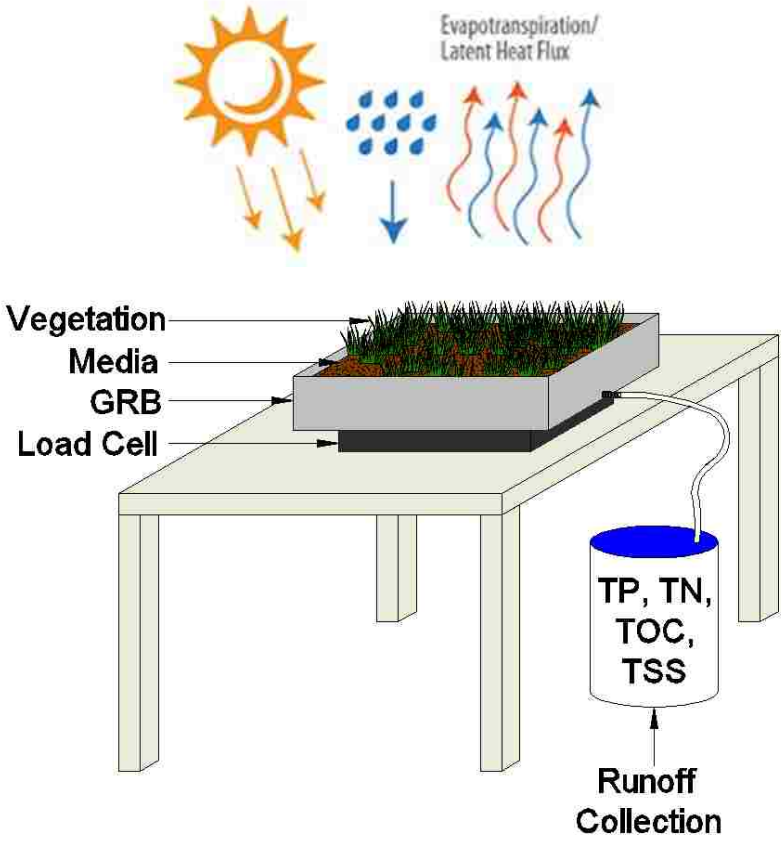

Figure 3. Green roof experimental arrangement to collect real-time data on moisture content in green roof media

The eight load cells, calibrated via two-point linear calibration from 0-90 kg, were connected by CRIO along with the sixteen thermocouples to a National Instruments interface. The data collection system allowed for real-time continuous measurement averaged on five-minute intervals, for ambient air, surface, and sub-slab temperatures of all three roof types; and for water content in the media. This data along with the on-site weather station is also measured continuously and averaged on five-minute intervals.

RESULTS AND DISCUSSION

LEACHATE CONCENTRATIONS

Nutrients leached from both media, with higher concentrations from GAF media than Arkalyte. Lower leachate concentrations observed in Arkalyte media could be attributed to the one year aging of the Arkalyte prior to use in the study. In summer 2014, planted GAF media leachate ranged from 5.3 – 9.1 mg/L TP and from 4.2 – 8.3 mg/L TN, whereas, Arkalyte leachate ranged from 1.2 – 1.9 mg/L TP and from 1.6 – 3.6 mg/L TN. Although nutrient concentrations for both TP and TN generally decreased over the duration of the 30-month study for both media types, observed TP and TN concentrations observed throughout the duration of the study exceeded literature values. Although TP concentrations remained above literature values, by the conclusion of the 30-month study TN concentrations fell within ranges observed by Hathaway, et al. [10]. Hathaway, et al. [10] observed TP concentrations ranging from 0.6 – 1.4 mg/L and TN concentrations ranging from 0.7 - 5.4 mg/L in green roof outflow. Over this 30-month study, TP concentrations decreased to 1.0 – 7.1 mg/L and TN concentrations ranged from 1.4 – 5.1 mg/L in months 24 to 30. Values of TP and TN concentrations in the green roof leachate can be found in Figure 4 and Figure 5, respectively.

Nutrients in green roof leachate are most certainly due to the fertilizer component of the media, where higher concentrations were leached from the commercially produced GAF media over the study period. Excess nutrients in green roof leachate are a concern to downstream water bodies, where high levels of nitrogen and phosphorus can cause eutrophic conditions. Results indicate that nutrient leaching varies with media type and planting. Nutrient leaching may cause concern for areas prone to eutrophication.

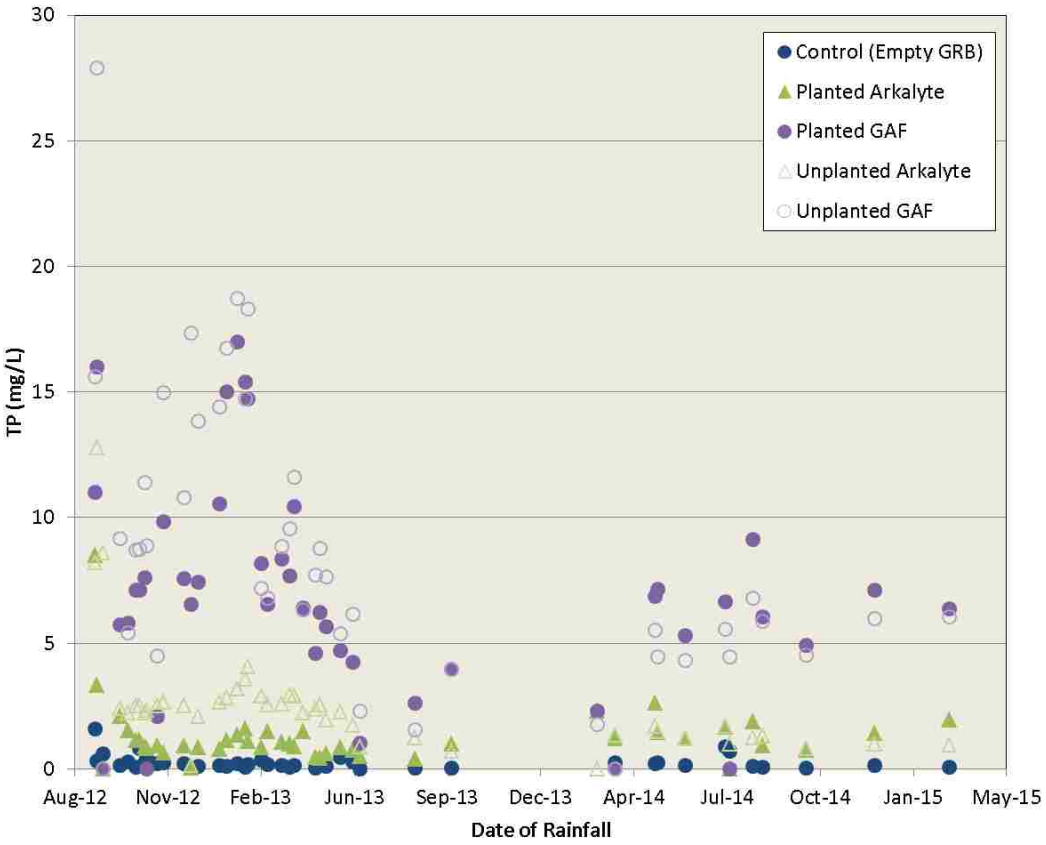

Figure 4. TP concentrations for precipitation events during the 30-month study

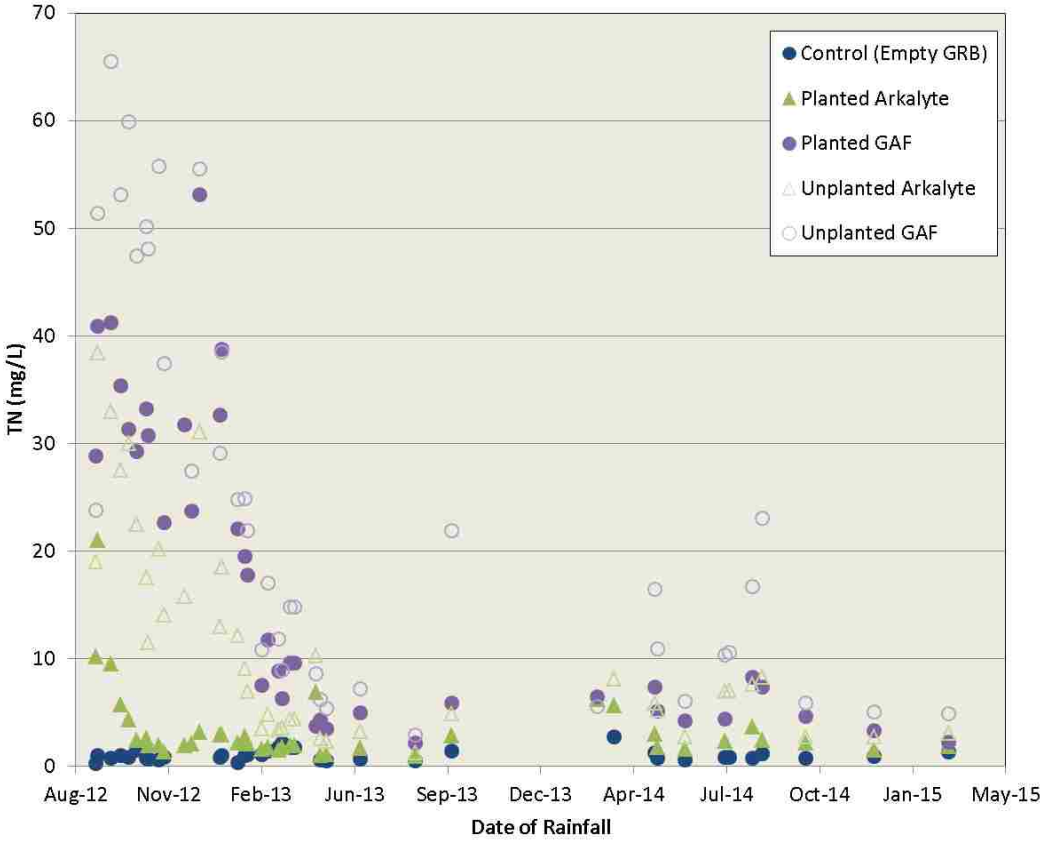

Figure 5. TN concentrations for precipitation events during the 30-month study

Similar to nutrient leaching, TOC concentrations generally decreased over time and were higher for leachate from GAF media than Arkalyte. TOC concentrations ranged from 9.0 – 15.8 mg/L in months 30 of this study. Organic carbon affects the water quality of downstream water bodies by increasing the biological oxygen demand (BOD). TOC concentrations in the green roof leachate can be found in Figure 6 below.

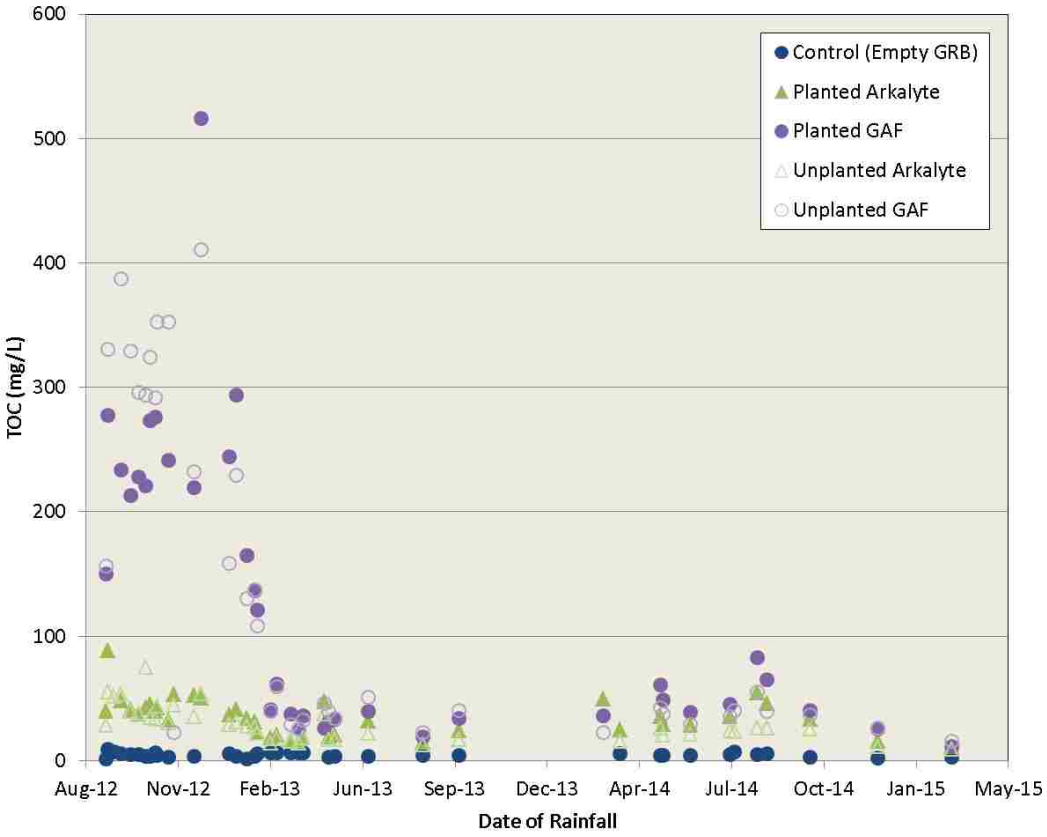

Figure 6. TOC concentrations for precipitation events during the 30-month study

Additionally, TSS concentrations were greater for GAF media than Arkalyte, and greater for the unplanted test bed condition than planted. Median values for TSS over all 30 months of the study for GAF were 6.8 mg/L and 9.5 mg/L for planted and unplanted conditions, respectively, whereas, Arkalyte concentrations were 2.0 mg/L and 2.6 mg/L for planted and unplanted conditions, respectively. Results indicated that the planted test bed condition better stabilizes the growing media, preventing transport of suspended solids. TSS concentrations in the green roof leachate can be found in Figure 7 below.

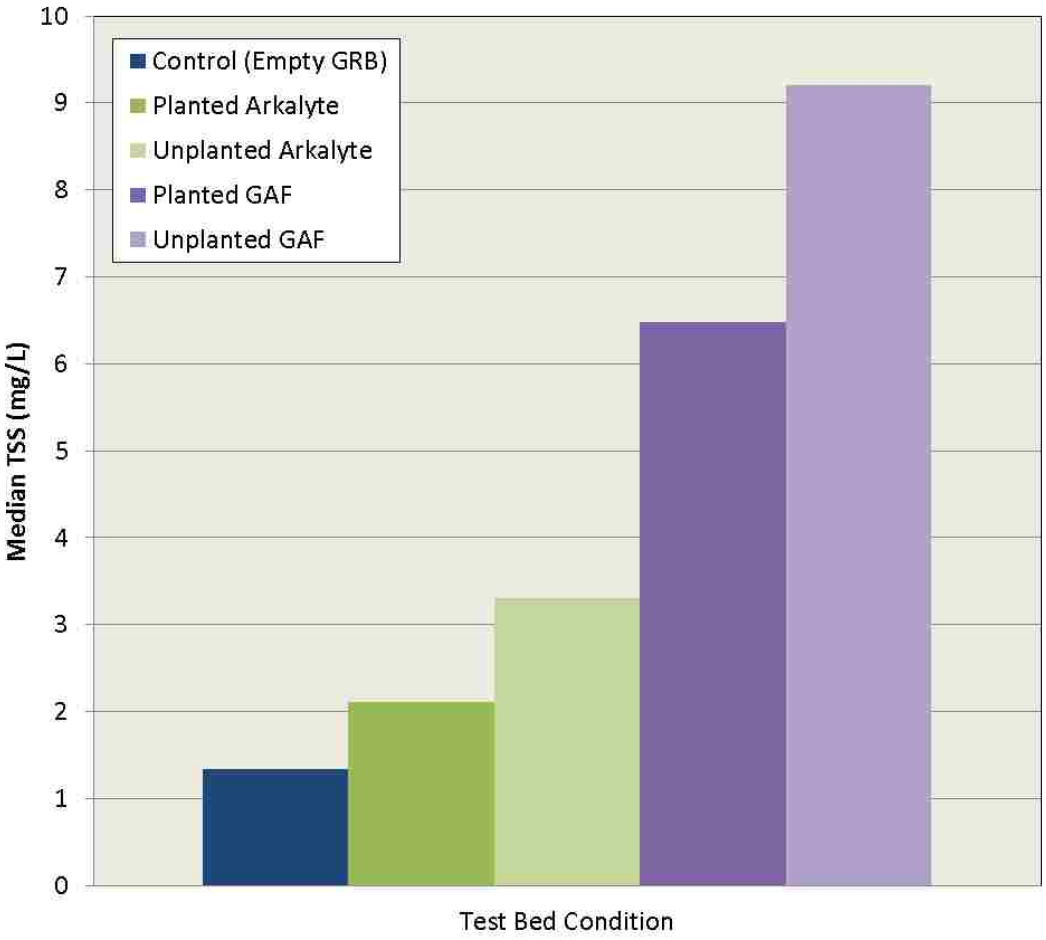

Figure 7. Median TSS concentrations for precipitation events during the 30-month study

RUNOFF REDUCTION

Results of this 30-month study under field conditions yielded findings similar to Morgan, et al. [11], where 10 cm of green roof media retained 54% of 139.8 cm total precipitation over fifteen months. Results from the 30-month Missouri S&T study revealed an average of 53.2 cm/yr (52%) runoff reduction for green roof media alone, and an average of 58.0 cm/yr (56%) runoff reduction for green roof media with established *Sedum* vegetation as can be seen in Figure 8 below. Arkalyte and GAF media reduced an average of 51.8 cm/yr (50%) and 59.3 cm/yr (58%) of runoff, respectively. Runoff reduction varied based on seasonal changes, with smaller runoff reduction in winter

months. Minimal runoff reduction in winter months was expected with low ET conditions and vegetation dormancy.

Green roofs provide runoff reduction and peak flow attenuation, with reductions related to storm frequency and total precipitation. The volume of storage associated with a green roof is directly related to its field capacity. Any precipitation occurring after field capacity of the media is reached results in runoff, shown in Figure 8. The time it takes the green roof to exceed field capacity reflects in peak flow attenuation. Peak flow attenuation is desirable to create lag time between the rainfall hydrograph and runoff hydrograph, reducing peak flows downstream. The stored water volume in the green roof media has potential to be evapotranspired, reducing total volume of runoff. Reduction of runoff volume and peak flow attenuation decrease stream incision and likelihood of flooding downstream.

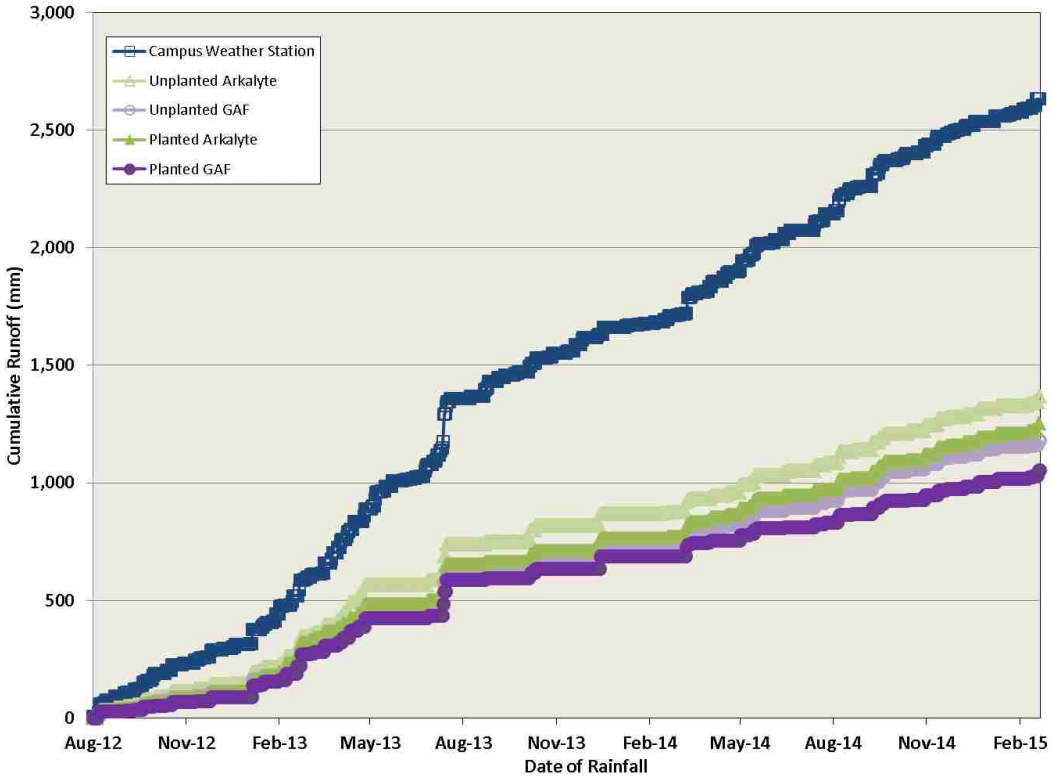

Figure 8. Cumulative runoff for precipitation events during the 30-month study

URBAN HEAT ISLAND EFFECTS

In addition to decreasing stormwater quantity, the volume of precipitation stored is later evapotranspired from the green roof media. The energy to evaporate the water, known as latent heat of vaporization, is dissipated from the roof. The ET process cools the building and urban surroundings. Therefore, green roofs have the potential to dissipate summer heat, lower energy costs, and lessen peak electrical demand for urban areas.

Besides summer cooling, green roof media also provides an insulative boundary for the building in winter, resulting in energy savings for both heating and cooling [12]. From the load cell and thermocouple study, data collection in late summer 2014 showed evaporative cooling effects similar to those noted in Sailor's [12] work. For example, Figure 9 illustrates both the insulative properties of green roof media and evaporative cooling effects for the 48-hour period of August 30, 2014 through August 31, 2014. Precipitation data was collected from the Emerson Hall on-site weather station. Storage was determined from the load cell values. Temperature values for each roof were obtained from the thermocouple study.

In Figure 9, two rainstorms occurred on August 30, 2014. The first event of 6.1 mm began at 10:15 am and the second event, a 36.3 mm event, began at 4:55 pm. The media stored essentially all precipitation from the first event and an additional 7.5 mm from the second storm event, combining for a total storage capacity of 13.5 mm for these two events [13].

On August 30th, following the conclusion of the first storm event at 10:40 am until the start of the second storm event at 4:55 pm, roughly 2 mm of precipitation were evapotranspired. At 5:40 pm, the green roof had reached field capacity and by the end of the second storm event at 5:45 pm, precipitation had resulted in nearly 29.9 mm of runoff. TPO roof surface temperatures were consistently lower than EPDM roof surface temperatures during daylight hours and equilibrated at night, enforcing Taha's [6] conclusion that an increase in albedo decreases temperatures. During the hours of 7:30 pm to 8:40 am between August 30th and August 31st, 0.6 mm of storage volume was evaporated. From 8:40 am to 7:30 pm on August 31st, about 4.8 mm of precipitation was

evapotranspired, removing energy from the rooftop. Measured ET from load cell data was also compared to reference crop evapotranspiration.

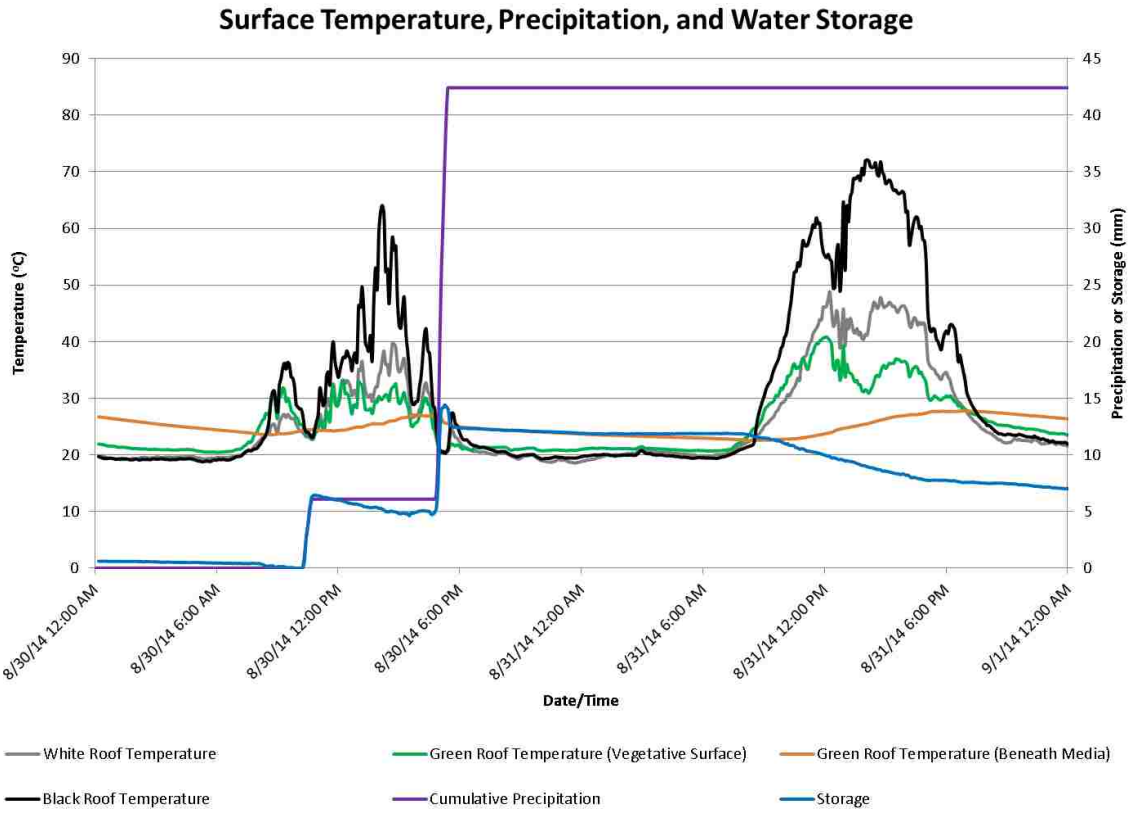

Figure 9. Surface temperatures of the three roof types (left axis) as well as cumulative precipitation and water storage in the media (right axis) for two rainstorm events over a 48-hour period

The amount of energy removed from the roof during ET can be determined by multiplying latent heat flux by the area of the green roof. The volume of precipitation removed via ET was multiplied by the latent heat of vaporization to find the latent heat flux as seen in Equation 1, below, where λET is latent heat flux, λ is latent heat of vaporization (2260 J/g), and ET is amount of evapotranspiration. The latent heat flux for 4.8 mm of precipitation evapotranspired was about 10.9 MJ/m^2.

$$\lambda ET = \lambda * ET \qquad (1)$$

Experimental results effectively demonstrated the connection between water storage and subsequent energy loss due to ET. Cooling impacts were evident as surface temperatures of the green roof were considerably lower than the membrane roofs for ideal ET time periods. At approximately 2 pm on August 31st, the green roof was 40°C cooler than the EPDM roof. Qualitative temperature differences between white TPO, black EPDM, and green roofs can be seen in Figure 10 and Figure 11 below for late afternoon on September 9, 2014 following a September rain event.

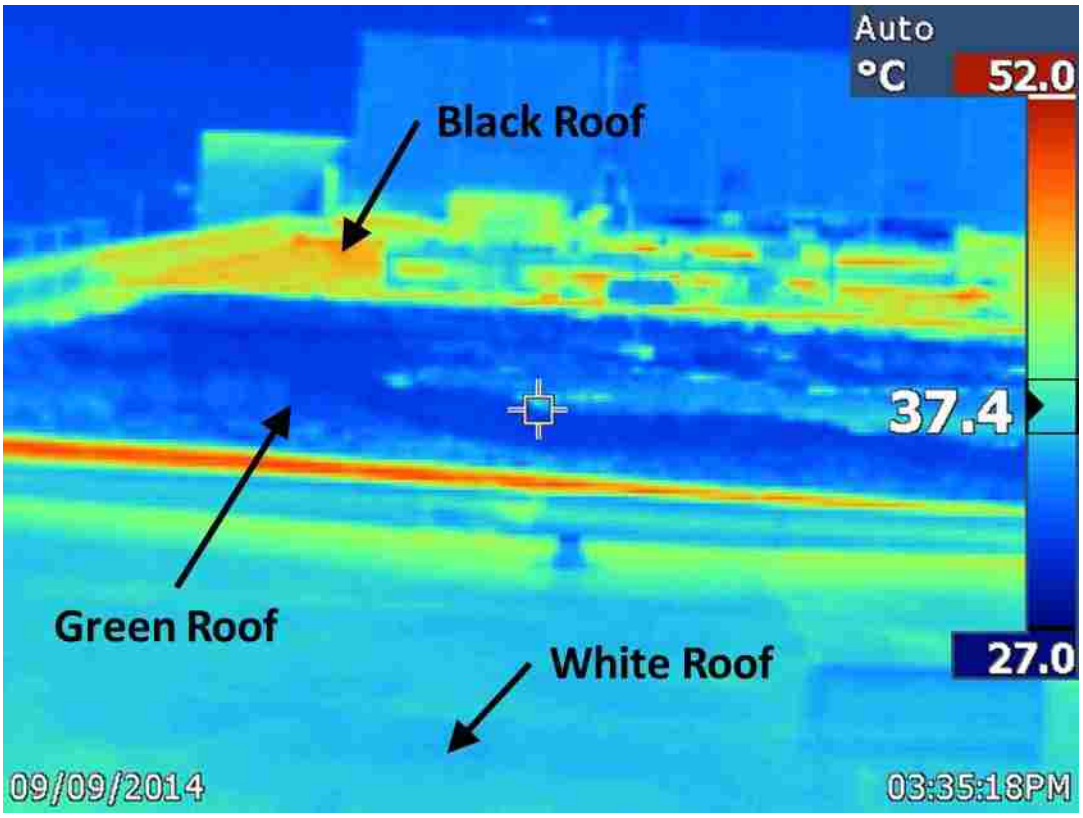

Figure 10. Thermal roof image showing qualitative temperature differences between three roof types on September 9, 2014 at 3:35:18pm CST

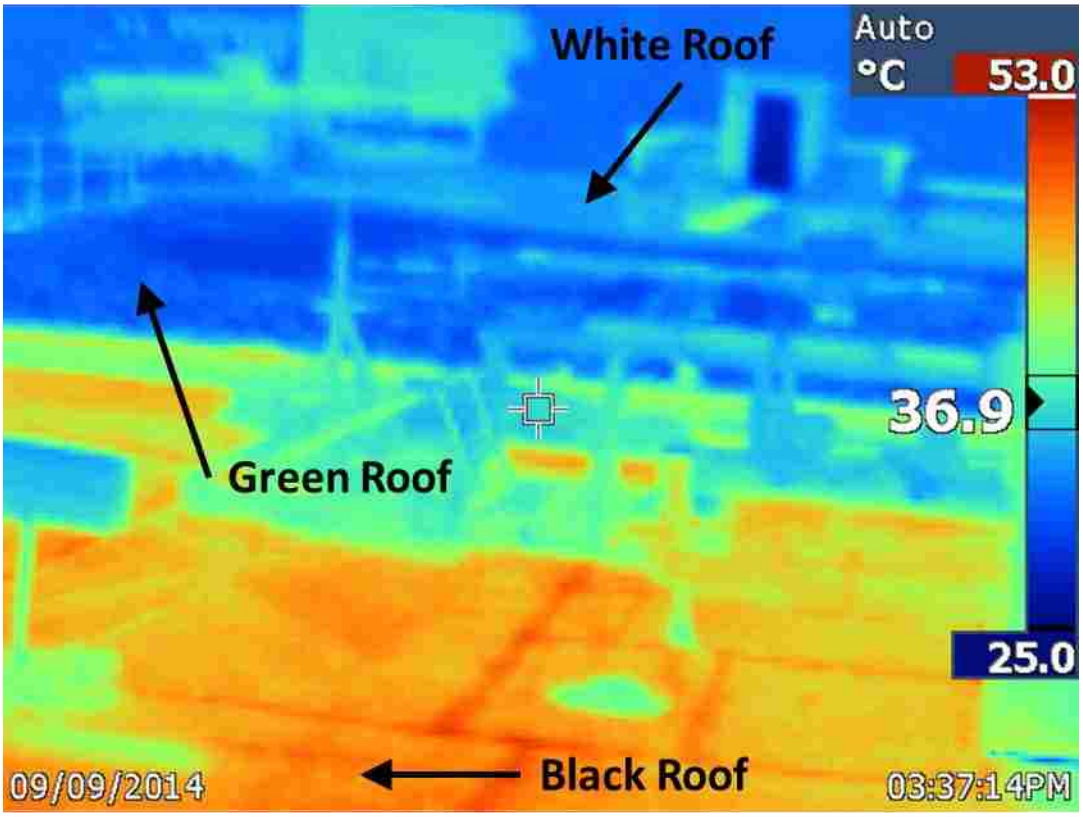

Figure 11. Thermal roof image showing qualitative temperature differences between three roof types on September 9, 2014 at 3:37:14pm CST

Reasonable increases in albedo vegetation have been hypothesized to potentially decrease air temperatures up to 4°C [6]. Evaporative cooling of roof surfaces on a larger scale, an urban scale, would have the potential to reduce urban heat island effects. The findings here may be the first to directly access and link evaporative cooling potential of green roofs. Ongoing work continues to access higher spacial and temporal resolution for heat modeling.

CONCLUSION

Green roofs have exhibited comprehensive benefits in social, environmental, and economical categories. With social trends toward sustainable infrastructure and increasing awareness of climate change, green roofs embrace these social principles all while providing aesthetic appeal. The environmental benefits of green roofs include runoff reduction and peak flow attenuation. Knowledge and predictability of environmental benefits are ever increasing, relating to energy savings, mitigating urban heat island effects, and potential air quality improvement. In most current cases, the only economic benefits of green roofs are increased roof life expectancy and potential energy savings in terms of direct building heating/cooling costs, which usually do not outweigh added capital or operation and maintenance costs of a green roof (Sproul, et al. 2014). Once both social and environmental benefits are fully elucidated, green roofs can be implemented to fulfill their triple bottom line potential.

These results quantify and illustrate evaporative cooling potential of green roofs, capable of projecting the urban cooling benefits of green roofs, when incorporated into a climate-based model. ET can be projected, using local meteorological data, coupled with designed field capacity to forecast stormwater retention performance. Such modeling can be used as a predictive tool to design green roofs for use in watershed management and urban planning, projecting large-scale benefits prior to construction. Through better understanding, design, and planning, green roof comprehensive benefits can be realized, including: runoff reduction, peak flow attenuation, reduction of urban heat island effects, energy savings, improved air quality, and minimized nutrient loading [13]. Societal benefits of green roofs, where the community profits from minimized flooding, cooler summer temperatures, less greenhouse gases, and visual appeal for nearby residents are afforded by the building owner, essentially as a donation to the community. Economic vehicles such as subsidies, tax incentives, or service fee reductions could successfully be implemented to facilitate installation of green roofs where modeled benefits warrant the cost to alleviate capital costs bore only by the building owner.

REFERENCES

1. Booth, D. B.; Jackson, C. R., Urbanization of aquatic systems: Degradation thresholds, stormwater detection, and the limits of mitigation. *J. AM. WATER RESOUR. ASSOC.* **1997,** *33*, (5), 1077-1090.
2. EPA *Report to Congress on the Impacts and Control of CSOs and SSOs*; United States Environmental Protection Agency: August 2004, 2004; p 633.
3. Chen, X. L.; Zhao, H. M.; Li, P. X.; Yin, Z. Y., Remote sensing image-based analysis of the relationship between urban heat island and land use/cover changes. *Remote Sens. Environ.* **2006,** *104*, (2), 133-146.
4. Akbari, H.; Pomerantz, M.; Taha, H., Cool surfaces and shade trees to reduce energy use and improve air quality in urban areas. *Sol. Energy* **2001,** *70*, (3), 295-310.
5. EPA, U. S. United States Environmental Protection Agency http://www.epa.gov/ (11/18/14),
6. Taha, H., Urban climates and heat islands: Albedo, evapotranspiration, and anthropogenic heat. *Energy and Buildings* **1997,** *25*, (2), 99-103.
7. Harper, G. E.; Limmer, M. A.; Showalter, W. E.; Burken, J. G., Nine-month evaluation of runoff quality and quantity from an experiential green roof in Missouri, USA. *Ecological Engineering* **2014**.
8. CArE, D. o. C., Architectural and Enivronmental Engineering Missouri S&T Green Roof. http://care.mst.edu/facilities/greenroof/ (January 4),
9. Allen, R. G.; Pereira, L. S.; Raees, D.; Smith, M., FAO Irrigation and Drainage Paper No. 56. In Rome, Itlay, 1998; p 333.
10. Hathaway, A. M.; Hunt, W. F.; Jennings, G. D., A field study of green roof hydrologic and water quality performance. *Trans. ASABE* **2008,** *51*, (1), 37-44.
11. Morgan, S.; Celik, S.; Retzlaff, W., Green roof storm-water runoff quantity and quality. *Journal of Environmental Engineering (United States)* **2013,** *139*, (4), 471-478.
12. Sailor, D. J., A green roof model for building energy simulation programs. *Energy and Buildings* **2008,** *40*, (8), 1466-1478.
13. Gibler, M. R. In *Comprehensive Benefits of Green Roofs*, World Environmental and Water Resources Congress, Austin, TX, 2015; EWRI, Environmental & Water Resources Institute: Austin, TX, 2015; p 8.

SECTION

4. COMBATTING URBAN HEAT ISLAND EFFECTS

4.1. MATLAB MODELING

By relating measured evapotranspiration from load cell data to the reference evapotranspiration (ET_0) obtained from the FAO Penman-Monteith model, a crop coefficient (K_c) was fitted to data from August 2014 to March 2015. Load cell values were used to obtain moisture content of the media, signifying wet and dry conditions. Data for all ET_0 calculations were averaged over a one-hour period, as FAO Penman-Monteith modeling of ET_0 is not realistic for time periods shorter than one hour. Load cell data was also averaged over one hour to minimize noise and to have data on the same time scale for comparison to calculated reference evapotranspiration. Thermocouple data and precipitation data (as precipitation data is not used in FAO Penman-Monteith reference evapotranspiration calculations) were used in their original 5-minute interval format. More details of the MATLAB modeling can be found in Appendix A. Graphical outputs of MATLAB modeling exemplified by August 30, 2014 to September 3, 2014, December 13, 2014 to December 17, 2014, and January 11, 2015 to January 15, 2015 date sequences can be found in Appendix B, illustrating urban heat island effects of green roofs for different weather conditions.

4.2. CROP COEFFICIENTS

Fitting a crop coefficient to data, excluding most spring and summer months, neglects seasons with the greatest potential for maximum ET. Since the FAO Penman-Monteith model is an energy-based model that omits precipitation inputs for calculations, crop coefficients were calculated assuming sufficient water for ET. Additionally, K_c

values were computed assuming that all water within the media was equally available for removal, neglecting intermolecular forces and cohesion of water to media particles.

Average crop coefficients for Arkalyte media are 2.49 and 0.915 for planted and unplanted conditions, respectively. Likewise, K_c values for GAF media are 3.385 and 1.555 for planted and unplanted conditions, respectively. Preliminary K_c values demonstrate the importance of both media type and vegetation. Results show that vegetation has a greater impact on crop coefficient than media type.

A majority of the crop coefficients listed previously are greater than one, indicating that the FAO Penman-Monteith model underestimates evapotranspiration from green roofs. This can be attributed to the thermal edge effects of the GRBs, which differ greatly from the thermal conditions associated with row crops. Also, green roof media is considerably more porous than farmland top soil, with greater void spaces increasing the availability for evaporation from the media. As the FAO Penman-Monteith model considers only reference crop characteristics, soil parameters are neglected.

Continued data collection in summer months is necessary for true K_c values, as existing values not only lack data for an entire year, the data used to determine K_c values is from a time period with the worst projected evapotranspirative effects.

5. SUMMARY AND CONCLUSIONS

Growing popularity of green roofs and green infrastructure is justified as green roofs exhibit multifaceted benefits of environmental, social, and economical importance. Environmental benefits of green roofs alluded to in literature include improved air quality, wildlife habitat, volume reduction, and peak flow attenuation. As volume reduction and peak flow attenuation reduce sewer loadings of local communities, they along with aesthetic appeal fulfill societal benefits. Knowledge and predictability of environmental benefits are ever increasing, relating to energy savings and urban heat island mitigation as urban communities are impacted by peak power demand and increased air temperatures. Economic benefits of green roofs are increased roof life expectancy and potential energy savings in terms of building heating/cooling costs, but those benefits do not outweigh additional capital or operation and maintenance costs of a green roof. The added green roof cost is bore solely by the building owner, despite a majority of benefits associated with green roofs being societal benefits, where the entire urban community prospers from minimized flooding, cooler summer temperatures, less greenhouse gases, and visual appeal for nearby residents. To combat costs afforded only by the building owner, economic vehicles such as subsidies, tax incentives, or service fee reductions could successfully be implemented to facilitate installation of green roofs.

Better understanding and design of green roofs will stimulate more efficient use in urban planning. Findings presented directly link evaporative cooling potential of green roofs with the capability of projecting urban cooling benefits, when incorporated into a climate-based model. Using local typical meteorological year (TMY) data, ET projections, coupled with designed field capacity can forecast stormwater retention performance and subsequent energy dissipation. This forecasting can be applied to project large-scale benefits of green roof projects before they are constructed, aiding as a predictive tool to design green roofs for use in watershed management and urban planning. As green roof comprehensive benefits are realized, including: runoff reduction, peak flow attenuation, urban heat island mitigation, energy savings, improved air quality, and minimized nutrient loading, supplemental funding for green roof construction can be allocated to green roof projects on a prioritized level.

6. RECOMMENDATIONS FOR FUTURE WORK

6.1. NUTRIENT LOADING

Future work should include studies to determine effects of storm size, storm intensity, and media depth on nutrients, suspended solids, and organic carbon. Studies must be performed in a laboratory environment to control design storm size and duration. Understanding impacts of storm characteristics on nutrient leaching could assist in qualifications for media washing. Additionally, implications of media depth on nutrient loading would help in water quality management and eutrophication prevention.

6.2. PEAK FLOW ATTENUATION

Flow meters installed to better quantify peak flow attenuation should measure flow from a green roof and a TPO flume. Each flume measures approximately ten inches wide by sixteen feet long, at roughly a 2° slope to mimic roof conditions. The green roof flume contains GAF media five inches deep with a “Midwest Mix” of *Sedum* vegetation. Peak flow attenuation can be monitored by comparing hydrographs for each flume. Lag time, peak flow reduction, and volume of storage can be computed through analyzing the hydrograph data of each flume for varying storm sizes.

6.3. WATER AND ENERGY BALANCE

Weather station data, thermocouple data, and load cell data should continue to be monitored for a minimum of 5 months following the submission of this thesis. Continuous data collection was not achieved until August 2014, and again modified for ease of collection in December 2014. Since large amounts of evapotranspiration occur in spring and summer months, a model incorporating eight months of data is not completely indicative of seasonal trends, nor is it suggestive of a comprehensive average crop coefficient. Research presented here only contains late summer, autumn, winter, and

early spring season data for a green roof in Rolla, Missouri, providing primary ET without a cooling season.

6.4. MEDIA SELECTION

The research presented here suggests that media type affects both water quality and runoff reduction. Media washing of excess nutrients prior to installation would reduce water quality impacts downstream. Additionally, variation in water holding capacity of differing media types suggests that further research is needed in green roof media mix design. An ideal green roof media is lightweight and drains with ease. When retro-fitting green roofs into existing buildings, this is true. The thermal benefits and water quality apprehensions of green roofs from this study guides media mix design toward a balance between water holding capacity, nutrient loading, and drainage. Incorporating a more complex media mix design would be applicable in situation where green roof design was tied into the original building plans. Although a less porous media may increase dead loads on a building, an increased water holding capacity would not only increase storage, it would spread energy dissipation out over a larger duration of time. Potential energy savings benefits of a more climate controlled ET cooling effect would possibly decrease the wear on air conditioning units. Much literature discusses varying media depths and their effect on storage and peak flow attenuation. It would be interesting to observe the effect media composition would have on both stormwater management and thermal implications.

6.5. GREEN ROOF TEXTILES

A difference between the Arkalyte and GAF GRBs from this experiment is the sub-media textiles used. Arkalyte GRBs used only filter fabric beneath the Arkalyte media, which follows the schematic of the designed system from Green Roof Blocks™. The GAF GRBs, however, used GAF's DuraGro™ 4-in-1 Drainage in lieu of the filter

fabric below the GAF media. The textile DuraGro^{TM} 4-in-1 Drainage used in GAF GRBs is thicker than the filter fabric used in Arkalyte GRBs, allowing for additional storage and air circulation. Testing should be performed on various sub-media green roof textiles as it relates to water storage and thermal benefits.

6.6. THERMAL ANALYSIS OF URBAN WATERSHEDS

It would be interesting to translate the evaporative cooling effects found in green roof urban heat island mitigation research to greenspaces found in urban settings. Land compaction during site development decreases hydraulic conductivity of the earth. Amending the earth with a sandy soil mix prior to sodding/seeding would increase infiltration capabilities of the ground. If media with greater porosity does in fact increase ET as indicated in the results of this research, then urban heat island mitigation could be compounded with land management strategies and green roof implementation.

Effectiveness of the aforementioned soil amenity can be evaluated by treating a large section of land with the soil amenity and leaving a neighboring section untouched as a control. Both thermocouple data and thermal imaging could be gathered for the two respective land sections to determine cooling potential of soil amenities. This experiment would be unrealistic in a high traffic area without proper barricades, as it would be important to places thermocouples on the surface and at varying depths within the media, and to protect the datalogger. Thermocouple depths within the media should be the same for both the amended and control land sections.

APPENDIX A
MATLAB CODE

```
%%%%%%%%%%%%%%%%%%%%%%%%%%%%
% Green Roof               %
% Evapotranspiration Calcs %
% 3/25/15                  %
%%%%%%%%%%%%%%%%%%%%%%%%%%%%

clear
clc

choice=input('\nWhat would you like to run?\n  Enter 1 for plots of data\n  Enter 2 for
comparison of buckets and tray weights\n  Enter 3 to calculate crop coefficient\n');

if choice==3
    Monthly_flag=input('  Enter 1 to calculate Kc on a monthly basis,\n   otherwise
calculation will be performed for entire period\n');
    Plot_flag=input('  Enter 1 for diagnostic plots\n');
end

%% Conversions
%J_per_MJ=10^6;
%s_per_min=60;
%min_per_hr=60;
%hr_per_day=24;
%s_per_hr=3600;
%kg_per_m3=1000;
%mm_per_m=1000;
lb_per_ft3=62.4;
n_Trays=8;
n_TC=16;

A_Tray=4; %ft^2
in_per_ft=12;

mm_per_in=25.4;

%% Inputs
%Screening Values
Min_Tray_Weight=30; %lbs for screening out bad data
Max_Tray_Weight=100; %lbs for screening out bad data
Max_Tray_ET=1; %maximum amount of ET (mm) measured by trays

%Tray Weights
Dry_wt=[45.26221 58.733551 38.493779 43.079821 59.587114 45.310085 51.245102 47.965783];
Water_wt=[24.420456 22.08352 33.110198 32.469373 18.818822 24.037026 24.593673 29.47446];

%% Weather Station Data for ET Calcs
file='S:\Research-031815\Research\Energy Model\Matlab\Data for ET Calcs.xlsx';
%file='C:\Users\Malqn3\Documents\MST\Greenroof\Data for ET Calcs.xlsx';
sheet='Data for FAO at 5 min Intervals';
%FullRange='C10960:K12215';  %Aug 29 - Sept 3, 2014
%FullRange='C41138:K42458';  %Dec 13 - Dec 17, 2014
%FullRange='C49778:K50806';   %Jan 11 - Jan 15, 2015
FullRange='C10952:K65785';   %Aug 29 - March 8, 2014-2015

%Column Numbers
DateTimeNum=1;
T=2;
RH=3;
u_2=4;
u_1=5;
pyran=6;
J=7;
Precip=8;


[FullDataNumeric]=xlsread(file, sheet, FullRange);

% Imput Weather Station Data for ET Calcs
%Numeric Date in MATLAB Time (Date)
Date=FullDataNumeric(:,DateTimeNum)+datenum('30-Dec-1899');
%air temperature (T)
```

```
T=FullDataNumeric(:,T); %in C
%relative humidity at z=1m above surface (RH)
RH=FullDataNumeric(:,RH); %in %
%measured wind speed at 2m above surface (u2)
u_2=FullDataNumeric(:,u_2); %in m*s^-1
%measured windspeed at z=1m above surface (u_z)
u_1=FullDataNumeric(:,u_1); %in m*s^-1
%pyranometer data (pyran)
pyran=FullDataNumeric(:,pyran); %in W*m^-2 or in J*s^-1*m^-2
%day of the year (J)
J=FullDataNumeric(:,J); %unitless
%Precipitation
Precip=FullDataNumeric(:,Precip); %in inches

% Convert Precip into mm
Precip=Precip*mm_per_in;

% Precip During the 5-minute Event (non cumulative)
Precip_Instantaneous=[0; Precip(2:length(Precip))-Precip(1:length(Precip)-1)];
Precip_Instantaneous=max(0, Precip_Instantaneous);

% Cumulative Precip
CumPrecip=cumsum(Precip_Instantaneous); %in mm

% Take Hourly Averages/Sums
[~,Precip_Instantaneous_hr]=HOUR_SUM(Date,Precip_Instantaneous);
CumPrecip_hr=cumsum(Precip_Instantaneous_hr);

clear FullDataNumeric


%% Thermocouple and Load Cell Data
%file='S:\Research-031815\Research\Energy Model\Matlab\Data for ET Calcs.xlsx';
sheet='NI Data';
%FullRange='B28:Y1283';  %Aug 29 - Sept 2, 2014
%FullRange='B25656:Y27121';  %Dec 13 - Dec 17, 2014
%FullRange='B34375:Y35404';  %Jan 11 - Jan 15, 2015
FullRange='B20:Y50378';   %Aug 29 - March 8, 2014-2015

%Column Numbers
TC1=1;
TC2=2;
TC3=3;
TC4=4;
TC5=5;
TC6=6;
TC7=7;
TC8=8;
TC9=9;
TC10=10;
TC11=11;
TC12=12;
TC13=13;
TC14=14;
TC15=15;
TC16=16;
T1=17;
T2=18;
T3=19;
T4=20;
T5=21;
T6=22;
T7=23;
T8=24;

[FullDataNumeric]=xlsread(file, sheet, FullRange);

% Input Thermocouple Data

%White (TPO) Roof Temperatures in C
TC16=FullDataNumeric(:,TC16); %White Sub-slab
```

```
TC2=FullDataNumeric(:,TC2); %White Surface North
TC1=FullDataNumeric(:,TC1); %White Surface South
TC12=FullDataNumeric(:,TC12); %White Ambient North
TC13=FullDataNumeric(:,TC13); %White Ambient South
%Green Roof Temperatures in C
TC14=FullDataNumeric(:,TC14); %Green Sub-slab
TC9=FullDataNumeric(:,TC9); %Green Beneath Media
TC11=FullDataNumeric(:,TC11); %Green Beneath Media
TC10=FullDataNumeric(:,TC10); %Green Vegetative Surface
TC8=FullDataNumeric(:,TC8); %Green Ambient North
TC3=FullDataNumeric(:,TC3); %Green Ambient South
%Black (EPDM) Roof Temperatures in C
TC15=FullDataNumeric(:,TC15); %Black Sub-slab
TC7=FullDataNumeric(:,TC7); %Black Surface North
TC5=FullDataNumeric(:,TC5); %Black Surface South
TC6=FullDataNumeric(:,TC6); %Black Ambient North
TC4=FullDataNumeric(:,TC4); %Black Ambient South
% Input Tray Weight Data (in lb)
T1=FullDataNumeric(:,T1); %GAF Unplanted
T2=FullDataNumeric(:,T2); %Arkalyte Unplanted
T3=FullDataNumeric(:,T3); %GAF Planted
T4=FullDataNumeric(:,T4); %Arkalyte Planted
T5=FullDataNumeric(:,T5); %GAF Unplanted
T6=FullDataNumeric(:,T6); %Arkalyte Unplanted
T7=FullDataNumeric(:,T7); %GAF Planted
T8=FullDataNumeric(:,T8); %Arkalyte Planted

TC=[TC1 TC2 TC3 TC4 TC5 TC6 TC7 TC8 TC9 TC10 TC11 TC12 TC13 TC14 TC15 TC16];
Tray=[T1 T2 T3 T4 T5 T6 T7 T8];

clear FullDataNumeric T1 T2 T3 T4 T5 T6 T7 T8 TC1 TC2 TC3 TC4 TC5 TC6 TC7 TC8 TC9 TC10
TC11 TC12 TC13 TC14 TC15 TC16

Tmin=zeros(1,n_Trays);
%Minimum Tray Weights
for i=1:n_Trays
    Tmin(i)=min(Tray(Tray(:,i)>Min_Tray_Weight,i));
end

%% Date/Time Data
%file='S:\Research-031815\Research\Energy Model\Matlab\Data for ET Calcs.xlsx';
sheet='NI Data';
%FullRange='AX28:AX1283';  %Aug 29 - Sept 2, 2014
%FullRange='AX25656:AX27121';  %Dec 13 - Dec 17, 2014
%FullRange='AX34375:AX35404';  %Jan 11 - Jan 15, 2015
FullRange='AX20:AX50378';   %Aug 29 - March 8, 2014-2015

%Column Numbers
DateTimeNum=1;

[FullDataNumeric]=xlsread(file, sheet, FullRange);

% Input Date/Time Data

%Numeric Date in MATLAB Time (Date)
TDate=FullDataNumeric(:,DateTimeNum)+datenum('30-Dec-1899'); %Time in CST

clear FullDataNumeric


%% Calculate ETo
[Date_hr, T_hr]=HOUR_AVERAGE(Date, T);
[~,RH_hr]=HOUR_AVERAGE(Date, RH);
[~,u_2_hr]=HOUR_AVERAGE(Date, u_2);
[~,u_1_hr]=HOUR_AVERAGE(Date, u_1);
[~,pyran_hr]=HOUR_AVERAGE(Date, pyran);
[~,J_hr]=HOUR_AVERAGE(Date, J);
ETo_hr=CALC_ET0(Date_hr, T_hr, RH_hr, u_2_hr, u_1_hr, pyran_hr, J_hr);

%% Synchronize Data
% All dates will be synchronized to the Weather Station and ETo Date
```

```
%5 minute increment
inc=datenum([0 0 0 0 5 0]);
Tray_Synch=zeros(length(Date),n_Trays);
TC_Synch=zeros(length(Date),n_TC);

for i=1:length(Date)
    for j=1:length(TDate)
        if TDate(j)-inc/2 <= Date(i) && TDate(j)+inc/2 > Date(i)
            Tray_Synch(i,:)=Tray(j,:);
            TC_Synch(i,:)=TC(j,:);
            break;
        end
    end
end

clear Tray TC


%cleanse tray data
Tray_Synch=Tray_Synch.*(Tray_Synch>Min_Tray_Weight).*(Tray_Synch<Max_Tray_Weight);

%Amount of water in each tray (mm)
Tray_Synch_mm=(((Tray_Synch-
repmat(Tmin,size(Tray_Synch,1),1))/lb_per_ft3)/A_Tray)*in_per_ft*mm_per_in;

%Amount of water in each tray (HOURLY) (mm)
[~,Tray_Synch_hr]=HOUR_AVERAGE_SCALE(Date,Tray_Synch);
Tray_Synch_hr_mm=(((Tray_Synch_hr-
repmat(Tmin,size(Tray_Synch_hr,1),1))/lb_per_ft3)/A_Tray)*in_per_ft*mm_per_in;


%% Model Runs
switch choice
    case 1
        fprintf('\nPlotting Thermocouple, Tray, ET, and Precip Data\n');

        %% Average Thermocouple Temperatures

        %White (TPO) Roof Temperatures in C
        WhiteSubslab=TC_Synch(:,16); %White Sub-slab Temperature in C
        WhiteSurface=(TC_Synch(:,2)+TC_Synch(:,1))/2; %Average White Surface Temperature
in C
        WhiteAmbient=(TC_Synch(:,12)+TC_Synch(:,13))/2; %Average White Ambient Air
Temperature in C

        %Green Roof Temperatures in C
        GreenSubslab=TC_Synch(:,14); %Green Sub-slab Temperature in C
        GreenBenMedia=(TC_Synch(:,9)+TC_Synch(:,11))/2; %Average Green Beneath Media
Temperature in C
        GreenVegSurface=TC_Synch(:,10); %Green Vegetative Surface Temnperature in C
        GreenAmbient=(TC_Synch(:,8)+TC_Synch(:,3))/2; %Average Green Ambient Air
Temperature in C

        %Black (EPDM) Roof Temperatures in C
        BlackSubslab=TC_Synch(:,15); %Black Sub-slab Temperature in C
        BlackSurface=(TC_Synch(:,7)+TC_Synch(:,5))/2; %Average Black Surface Temperature
in C
        BlackAmbient=(TC_Synch(:,6)+TC_Synch(:,4))/2; %Average Black Ambient Air
Temperature in C


        %Cumulative Reference Evapotranspiration (CumETo)
        CumETo_hr=cumsum(ETo_hr); %in mm


        %% Plot

        %Plot Thermocouple Data
        figure;
        plot(Date,WhiteSubslab,'c-');
```

```
        datetick('x','mm/dd HH:MM','keeplimits');
        hold on;
        plot(Date,GreenSubslab,'g-');
        plot(Date,BlackSubslab,'k-');
        legend('White Roof Sub-Slab Temperature','Green Roof Sub-Slab Temperature',
'Black Roof Sub-Slab Temperature');
        xlabel('Date/Time');
        ylabel('Temperature ( ^oC)');
        title('Sub-slab Temperatures');

        figure;
        plot(Date,WhiteSurface,'c-');
        datetick('x','mm/dd HH:MM','keeplimits');
        hold on;
        plot(Date,GreenBenMedia,'g--');
        plot(Date,GreenVegSurface,'g-');
        plot(Date,BlackSurface,'k-');
        legend('White Roof Surface Temperature','Green Roof Beneath Media
Temperature','Green Roof Vegetative Surface Temperature', 'Black Roof Surface
Temperature');
        xlabel('Date/Time');
        ylabel('Temperature ( ^oC)');
        title('Surface Temperatures');

        figure;
        plot(Date,WhiteAmbient,'c-');
        datetick('x','mm/dd HH:MM','keeplimits');
        hold on;
        plot(Date,GreenAmbient,'g-');
        plot(Date,BlackAmbient,'k-');
        legend('White Roof Ambient Air Temperature','Green Roof Ambient Air Temperature',
'Black Roof Ambient Air Temperature');
        xlabel('Date/Time');
        ylabel('Temperature ( ^oC)');
        title('Ambient Air Temperatures');

         figure;
        plot(Date,WhiteAmbient,'c-');
        datetick('x','mm/dd HH:MM','keeplimits');
        hold on;
        plot(Date,WhiteSurface,'y-');
        plot(Date,WhiteSubslab,'r-');
        legend('Ambient Air Temperature','Surface Temperature', 'Sub-slab Temperature');
        xlabel('Date/Time');
        ylabel('Temperature (^oC)');
        title('White TPO Roof Temperatures');

        figure;
        plot(Date,BlackAmbient,'c-');
        datetick('x','mm/dd HH:MM','keeplimits');
        hold on;
        plot(Date,BlackSurface,'k-');
        plot(Date,BlackSubslab,'r-');
        legend('Ambient Air Temperature','Surface Temperature', 'Sub-slab Temperature');
        xlabel('Date/Time');
        ylabel('Temperature (^oC)');
        title('Black EPDM Roof Temperatures');

        figure;
        plot(Date,GreenAmbient,'c-');
        datetick('x','mm/dd HH:MM','keeplimits');
        hold on;
        plot(Date,GreenVegSurface,'g-');
        plot(Date,GreenBenMedia,'g--');
        plot(Date,GreenSubslab,'r-');
        legend('Ambient Air Temperature','Vegetative Surface Temperature','Beneath Media
Temperature', 'Sub-slab Temperature');
        xlabel('Date/Time');
        ylabel('Temperature (^oC)');
        title('Green Roof Temperatures');
```

```
        %Plot Tray Data
        figure;
        plot(Date,Tray_Synch(:,1),'k:'); %GAF Unplanted
        datetick('x','mm/dd HH:MM','keeplimits');
        hold on;
        plot(Date,Tray_Synch(:,2),'r:'); %Arkalyte Unplanted
        plot(Date,Tray_Synch(:,3),'g:'); %GAF Planted
        plot(Date,Tray_Synch(:,4),'b:'); %Arkalyte Planted
        plot(Date,Tray_Synch(:,5),'k-'); %GAF Unplanted
        plot(Date,Tray_Synch(:,6),'r-'); %Arkalyte Unplanted
        plot(Date,Tray_Synch(:,7),'g-'); %GAF Planted
        plot(Date,Tray_Synch(:,8),'b-'); %Arkalyte Planted
        legend('GAF Unplanted','Arkalyte Unplanted', 'GAF Planted', 'Arkalyte
Planted','GAF Unplanted','Arkalyte Unplanted', 'GAF Planted', 'Arkalyte Planted');
        xlabel('Date/Time');
        ylabel('Weight (lb)');
        title('Load Cell Weights');

        figure;
        plot(Date,Tray_Synch_mm(:,1),'k:');
        datetick('x','mm/dd HH:MM','keeplimits');
        hold on;
        plot(Date,Tray_Synch_mm(:,2),'r:'); %Arkalyte Unplanted
        plot(Date,Tray_Synch_mm(:,3),'g:'); %GAF Planted
        plot(Date,Tray_Synch_mm(:,4),'b:'); %Arkalyte Planted
        plot(Date,Tray_Synch_mm(:,5),'k-'); %GAF Unplanted
        plot(Date,Tray_Synch_mm(:,6),'r-'); %Arkalyte Unplanted
        plot(Date,Tray_Synch_mm(:,7),'g-'); %GAF Planted
        plot(Date,Tray_Synch_mm(:,8),'b-'); %Arkalyte Planted
        legend('GAF Unplanted','Arkalyte Unplanted', 'GAF Planted', 'Arkalyte Planted');
        xlabel('Date/Time');
        ylabel('Storage (mm)');
        title('Tray Storage');

        %Plot Thermocouple Data and Tray Data
        figure;
        hAx=plotyy(Date,Tray_Synch_mm(:,8),[Date, Date, Date, Date],[WhiteSurface,
GreenBenMedia, GreenVegSurface, BlackSurface]); %Arkalyte Planted
        hold on;
        legend('Arkalyte Planted','White Roof Surface Temperature','Green Roof Beneath
Media Temperature','Green Roof Vegetative Surface Temperature', 'Black Roof Surface
Temperature');
        xlabel('Date/Time');
        title('Scale Weights');
        datetick(hAx(1));
        ylabel(hAx(2),'Temperature ( ^oC)');
        datetick(hAx(2));
        ylabel(hAx(1),'Tray Water Content (mm)');

        figure;
        plot(Date_hr, CumETo_hr,'g-');
        datetick('x','mm/dd','keeplimits');
        legend('Cumulative Reference Evapotranspiration (ETo)');
        xlabel('Date/Time');
        ylabel('Cumulative ET_0 (mm)');
        title('Cumulative ET_0 vs. Time');


        %Plot Precipitation Data
        figure;
        plot(Date, CumPrecip,'b-');
        datetick('x','mm/dd','keeplimits');
        legend('Cumulative Precipitation');
        xlabel('Date/Time');
        ylabel('Cumulative Precipitation (mm)');
        title('Cumulative Precipitation vs. Time');


        % MASTER PLOT -- Plot Thermocouple Data and Tray Data
        figure;
```

```
        hAx=plotyy([Date, Date, Date,
Date],[WhiteSurface,GreenBenMedia,GreenVegSurface,BlackSurface],[Date_hr', Date_hr',
Date_hr'],[Tray_Synch_hr_mm(:,7),CumETo_hr, CumPrecip_hr]);
        legend('White Roof Surface Temperature','Green Roof Beneath Media
Temperature','Green Roof Vegetative Surface Temperature', 'Black Roof Surface
Temperature','Storage','Cumulative ETo','Cumulative Precipitation');
        xlabel('Date/Time');
        datetick(hAx(1));
        ylabel(hAx(1),'Temperature ( ^oC)');
        datetick(hAx(2));
        ylabel(hAx(2),'Storage, ETo, Precip (mm)');


    case 2
            %% Compare Buckets and Scales
        fprintf('\nComparing the Runoff Measured in the Buckets to the Runoff Reported by
Scales\n');

        BUCKET_VERIFY(Date, Precip, Tray_Synch);

    case 3
        %% Crop Coefficient Model
        fprintf('\nModeling Crop Coefficent\n');

        %Number of variables to fit
        n_vars=1;

        %Calculate months to fit
        [t_min(1),t_min(2)]=datevec(Date_hr(1));%Starting Month & Year
        [t_max(1),t_max(2)]=datevec(Date_hr(length(Date_hr)));%Ending Month & Year

        n_months=t_max(1)*12+t_max(2)-t_min(1)*12-t_min(2); %Number of months

        if Monthly_flag==1
            Monthly_inc=1;
        else
            Monthly_inc=n_months;
        end

        %Fit=zeros(n_Trays,n_months/Monthly_inc);
        %Month=zeros(n_Trays,n_months/Monthly_inc);
        %Year=Month;

        for tray=1:n_Trays;
            %Remove Data When Raining
            screen_counter=0;
            Tray_Synch_Screened_mm=zeros(size(ETo_hr));
            Tray_Synch_Screened=zeros(size(ETo_hr));
            ETo_Screened=zeros(size(ETo_hr));
            Date_Screened=zeros(size(ETo_hr));
            del_weight=zeros(size(ETo_hr));

            %Gather Data for Fitting
            for i=1:length(Date_hr)-1
                if Precip_Instantaneous_hr(i)==0 && Tray_Synch_hr_mm(i,tray)>0 &&
Tray_Synch_hr_mm(i+1,tray)>0 && ETo_hr(i)>0 && abs(Tray_Synch_hr_mm(i,tray)-
Tray_Synch_hr_mm(i+1,tray))<Max_Tray_ET %&& Tray_Synch_hr_mm(i,tray)-
Tray_Synch_hr_mm(i+1,tray)>0
                    screen_counter=screen_counter+1;
                    Tray_Synch_Screened_mm(screen_counter)=Tray_Synch_hr_mm(i,tray);
                    Tray_Synch_Screened(screen_counter)=Tray_Synch_hr(i,tray);
                    ETo_Screened(screen_counter)=ETo_hr(i);
                    Date_Screened(screen_counter)=Date_hr(i);
                    del_weight(screen_counter)=Tray_Synch_hr_mm(i,tray)-
Tray_Synch_hr_mm(i+1,tray); %The true change in tray weights
                end
            end
            Tray_Synch_Screened_mm=Tray_Synch_Screened_mm(1:screen_counter);
            Tray_Synch_Screened=Tray_Synch_Screened(1:screen_counter);
            ETo_Screened=(ETo_Screened(1:screen_counter));
            Date_Screened=Date_Screened(1:screen_counter);
```

```
            del_weight=del_weight(1:screen_counter);


            %Guess and bounds
            Guess=1;
            Lower=0;
            Upper=100;


            %Calculate months to fit
            [t_min(1),t_min(2)]=datevec(Date_Screened(1));%Starting Month & Year
            [t_max(1),t_max(2)]=datevec(Date_Screened(length(Date_Screened)));%Ending
Month & Year

            n_months=t_max(1)*12+t_max(2)-t_min(1)*12-t_min(2); %Number of months

            if Monthly_flag==1
                Monthly_inc=1;
            else
                Monthly_inc=n_months+1;
            end


            %Loop through each month, uniquely identified using
            %year*12+month
            [Date_Screened_Year, Date_Screened_Month]=datevec(Date_Screened);

            loop_counter=0;
            for t=t_min(1)*12+t_min(2):Monthly_inc:t_max(1)*12+t_max(2)
                loop_counter=loop_counter+1;
                start_index=0;
                end_index=0;
                for i=1:length(Date_Screened)-1

                    if start_index==0 &&
t==Date_Screened_Year(i)*12+Date_Screened_Month(i)
                        start_index=i;
                    elseif t==Date_Screened_Year(i)*12+Date_Screened_Month(i) &&
t<Date_Screened_Year(i+1)*12+Date_Screened_Month(i+1)
                        end_index=i;
                        break;
                    elseif i==length(Date_Screened)-1
                        end_index=i+1;
                    end
                end

                Month(tray,loop_counter)=rem(t-1,12)+1;
                Year(tray,loop_counter)=ceil(t/12)-1;

                %Skip months with no data
                if start_index==0 || end_index==0
                    fprintf('Month %i/%i had no
data\n',Month(loop_counter),Year(loop_counter));
                    break;
                end

                %Do the fitting
                %Fit(tray,:)=lsqcurvefit(@(Guess,
ETo_Dry)ET_MODEL(Guess,ETo_Dry,Tray_Synch_Dry),Guess,ETo_Dry,log10(del_weight),Lower,Uppe
r);


%Fit(tray,:)=patternsearch(@(Guess)ET_MODEL_PS(Guess,ETo_Screened,Tray_Synch_Screened,
(del_weight),1),Guess,[],[],[],[],Lower,Upper);
                Fit(tray,loop_counter)=ga(@(Guess)ET_MODEL_PS(Guess,Dry_wt(tray),
Water_wt(tray),
ETo_Screened(start_index:end_index),Tray_Synch_Screened(start_index:end_index),
(del_weight(start_index:end_index)),1),n_vars,[],[],[],[],Lower,Upper);

                %Plot results
```

```
                ET_pred=ET_MODEL_PS(Fit(tray,loop_counter),Dry_wt(tray), Water_wt(tray),
ETo_Screened(start_index:end_index),Tray_Synch_Screened(start_index:end_index),[],0);
%predicted log10 ET
                Residual=ET_pred-(del_weight(start_index:end_index)); %residual from fit

                if Plot_flag==1
                    figure;
                    set(gcf, 'Position', get(0,'Screensize')); % Maximize figure

                    subplot(3,3,1);
                    plot(ETo_Screened(start_index:end_index),Residual,'b.');
                    xlabel('ET_0');
                    ylabel('Residual');

                    subplot(3,3,2);
                    plot(ET_pred,Residual,'b.');
                    xlabel('Predicted ET');
                    ylabel('Residual');
                    title(['Tray',num2str(tray),'
Date:',num2str(Month(tray,loop_counter)),'/',num2str(Year(tray,loop_counter))]);

                    subplot(3,3,3);
                    plot(ET_pred,del_weight(start_index:end_index),'g.');
                    xlabel('Predicted ET');
                    ylabel('Tray Measured ET');
                    hold on;
                    plot([0.0001 max(ET_pred)],[0.0001 max(ET_pred)],'k-');
                    legend('Data','1:1 Line');

                    subplot(3,3,4);
                    plot(Date_Screened(start_index:end_index),Residual,'r.-');
                    axis([min(Date_Screened(start_index:end_index))
max(Date_Screened(start_index:end_index)) min(Residual) max(Residual)]);
                    datetick('x',6);
                    ylabel('Residual');
                    xlabel('Date');

                    subplot(3,3,5);

plot(Date_Screened(start_index:end_index),del_weight(start_index:end_index),'k-');
                    axis([min(Date_Screened(start_index:end_index))
max(Date_Screened(start_index:end_index)) min(del_weight(start_index:end_index))
max(del_weight(start_index:end_index))]);
                    datetick('x',6);
                    ylabel('Tray Measured ET');
                    xlabel('Date');

                    subplot(3,3,6);

plot(ETo_Screened(start_index:end_index),del_weight(start_index:end_index),'r.');
                    xlabel('ET_0');
                    ylabel('Tray Measured ET');

                    subplot(3,3,7);

plot(Date_Screened(start_index:end_index),del_weight(start_index:end_index),'k.');
                    hold on;

plot(Date_Screened(start_index:end_index),ETo_Screened(start_index:end_index),'g.');
                    xlabel('Date');
                    ylabel('Tray Weight or ET_0 (mm)');
                    datetick('x',6);
                    legend('Tray','ET_0');

                    subplot(3,3,8);

plot(Date_Screened(start_index:end_index),(Tray_Synch_Screened(start_index:end_index)-
Dry_wt(tray))./Water_wt(tray),'k.');
                    hold on;
                    plot(Date,Precip_Instantaneous/10,'b-');
                    xlabel('Date');
```

```
                    ylabel('Fraction of Saturation or Precip (cm)');
                    legend('Fraction Saturated','Precipitation');
                    axis([min(Date_Screened(start_index:end_index))
max(Date_Screened(start_index:end_index)),0,1.2]);
                    datetick('x',6,'keeplimits');
                end
            end

        end

        fprintf('\nTray\tYear\tMonth\tKc\n');
        for i=1:n_Trays
            for j=1:loop_counter
                fprintf('%3i\t\t%i\t%i%8.2f\n',i,Year(i,j),Month(i,j),Fit(i,j));
            end
        end

        % Plot Monthly Data
        if Monthly_flag==1
            figure;
            plot(Month(1,:),Fit(1,:),'bo');
            hold on;
            plot(Month(2,:),Fit(2,:),'ro');
            plot(Month(3,:),Fit(3,:),'go');
            plot(Month(4,:),Fit(4,:),'ko');
            plot(Month(5,:),Fit(5,:),'bd');
            plot(Month(6,:),Fit(6,:),'rd');
            plot(Month(7,:),Fit(7,:),'gd');
            plot(Month(8,:),Fit(8,:),'kd');
            xlabel('Month');
            ylabel('K_c');
            legend('Tray 1','Tray 2','Tray 3','Tray 4','Tray 5','Tray 6','Tray 7','Tray
8');
        end
    otherwise
        fprintf('\nImproper Selection\n');

end


function [ Time_out, Var_out ] = HOUR_SUM( Time_in, Var_in )
%HOUR_SUM Takes 5 minute data and sums over an hour
% Time_in is the input date/time
% Time_out is the output date/time
% Var is the variable to be summed
% The sum at 1PM consists of the average of all values between 1:00PM
% and 2:00PM

%% Calculate Time_out
Min_date=ceil(min(Time_in)); %first date, rounded to the next day
Max_date=floor(max(Time_in)); %last date, rounded to midnight

inc=1/24; %hourly increment

Time_out=Min_date:inc:Max_date;

%% Find and average

%Flags for finding values
start_flag=0;
end_flag=0;
start_loop=1;

Var_out=zeros(length(Time_out),size(Var_in,2));

for i=1:length(Time_out)
    for j=start_loop:length(Time_in)
        if start_flag==0 && Time_in(j)>=Time_out(i)
            start_flag=j;
        elseif Time_in(j+1)>=Time_out(i)+inc
            end_flag=j;
```

```
            %Check for missing data/jumps in the data
            if start_flag==0 || Time_in(j+1)>=Time_out(i)+2*inc
                Var_out(i,:)=0;
            else
                start_loop=start_flag; %no need to return to 1 each time, instead carry
on where we left off
                Var_out(i,:)=sum(Var_in(start_flag:end_flag,:));
            end
            %Reset flags
            start_flag=0;
            end_flag=0;
            break;
        end
    end
end
```

```
function [ Time_out, Var_out ] = HOUR_AVERAGE( Time_in, Var_in )
%HOUR_AVERAGE Takes 5 minute data and averages over an hour
% Time_in is the input date/time
% Time_out is the output date/time
% Var is the variable to be averaged. It may be a matrix, provided the
% temporal data are the rows
% The average at 1PM consists of the average of all values between 12:50PM
% and 1:10PM

%% Calculate Time_out
Min_date=ceil(min(Time_in)); %first date, rounded to the next day
Max_date=floor(max(Time_in)); %last date, rounded to midnight

inc=1/24; %hourly increment

Time_out=Min_date:inc:Max_date;

%% Find and average
avg_buffer=10/60/24; %in minutes

%Flags for finding values
start_flag=0;
end_flag=0;
start_loop=1;

Var_out=zeros(length(Time_out),size(Var_in,2));

for i=1:length(Time_out)
    for j=start_loop:length(Time_in)
        if start_flag==0 && Time_in(j)>=Time_out(i)-avg_buffer
            start_flag=j;
        elseif Time_in(j+1)>=Time_out(i)+avg_buffer
            end_flag=j;

            %Check for missing data/jumps in the data
            if start_flag==0 || Time_in(j+1)>=Time_out(i)+2*avg_buffer
                Var_out(i,:)=NaN;
            else
                start_loop=start_flag; %no need to return to 1 each time, instead carry
on where we left off
                Var_out(i,:)=mean(Var_in(start_flag:end_flag,:));
            end
            %Reset flags
            start_flag=0;
            end_flag=0;
            break;
        end
    end
end
```

```
function [ ETo ] = CALC_ET0(Date, T, RH, u_2, u_1, pyran, J  )
%CALC_ET0 - Calculates the ETo
%   ETo is in mm and will be >=0
%   Date is the date/time in CST -- Assumes hourly input
%   T is the temperature in deg C
%   RH is the relative humidity (%)
%   u_2 is the windspeed at 2 m above ground (m/s)
%   u_1 is the windspeed at 1 m above ground (m/s)
%   pyran i sthe pyranometer data (W/m^2)
%   J is the day of the year


%% Constants
J_per_MJ=10^6;
hr_per_day=24;
min_per_hr=60;
s_per_hr=3600;
mm_per_m=1000;
kg_per_m3=1000;

%elevation above sea level (z)
z=342; %in m
%latitude (latitude)
latitude=37.9562; %in degrees
%longitude of the center of the local time zone (Lz)
Lz=90; %in degrees
%longitude of the measurement site (Lm)
Lm=91.772674; %in degrees

%latent heat of vaporization (lambda)
lambda=2.45; %in MJ*kg^-1
%ratio of molecular weight of water vapor/dry air (epsilon)
epsilon=0.622; %unitless

%solar constant (Gsc)
Gsc=0.0820; %in MJ*m^-2*min^-1
%albedo for reference crop (alpha)
alpha=0.23; %dimensionless
%Stefan-Boltzmann constant (sigma)
sigma=4.903*10^-9; %in MJ*K^-4*m^-2*day^-1
sigma=sigma/hr_per_day; %in MJ*K^-4*m^-2*hr^-1
%length of calculation period (t1)
t1=60/min_per_hr; %in hours

%height of wind mesurement above surface for u_1(z_wind)
z_wind=1; %in m

%reference crop height
h=0.12; %in m
%height of wind measurements (z_m)
z_m=2; %in m
%height of humidity measurements (z_m)
z_h=1; %in m
%von Karman's constant (k)
k=0.41; %unitless
%bulk surface resistance (r_s)[Eq. 5]
r_s=70; %in s*m^-1
r_s=r_s/s_per_hr; %in hr*m^-1

%specific gas constant (R)
R=0.287; %in kJ*kg^-1*K^-1


%% Psychiometric Constant (constant value)

%atmospheric pressure (P) [Eq. 7]
P=101.3*((293-0.0065*z)/293)^5.26; %in kPa
%specific heat constant (c_p)
c_p=1.013*10^-3; %in MJ*kg^-1*C^-1
%psychiometric constant (gamma) [Eq. 8]
```

```
gamma=(c_p*P)/(epsilon*lambda); %in kPa*C^-1



%% Saturation Vapor Pressure Deficit and Slope Vapor Pressure Curve

%saturation vapor pressure at the air temperature (e_s)[Eq. 11]
e_s=0.6108*exp((17.27*T)./(T+237.3)); %in kPa
%actual vapor pressure (e_a) [Eq. 10]
e_a=e_s.*(RH/100); %in kPa
%saturation vapor pressure deficit (e_s-e_a)
%slope of saturation vapor pressure curve (Delta) [Eq. 13]
Delta=(4098*(0.6108*exp((17.27*T)./(T+237.3))))./(T+237.3).^2; %in kPa*C^-1



%% Radiation and Heat Flux

%latitude [Eq. 22]
fi=(pi/180)*latitude; %in radians
%inverse relative distance Earth-Sun (d_r) [Eq. 23]
d_r=1+0.033*cos((2*pi/365).*J); %unitless
%solar declinaion (delta) [Eq. 24]
delta=0.409*sin((2*pi/365).*J-1.39); %unitless
%sunset hour angle (w_s) [Eq. 25]
w_s=acos((-1*tan(fi).*tan(delta))); %in radians
%standard clock time at midpoint of period (t)
t=zeros(length(Date),1);
for i=1:length(Date);
    if i==length(Date);
        t(i)=t(i-1)+t1; %in hours
    else
    t(i)=((mean([Date(i),Date(i+1)]))-floor(Date(i)))*24; %in hours
    end
end
%seasonal angle variable (b) [Eq. 33]
b=(2*pi.*(J-81))/364; %in radians
%seasonal correction for solar time (Sc) [Eq. 32]
Sc=0.1645*sin(2.*b)-0.1255*cos(b)-0.025*sin(b); %unitless
%solar time angle at midpiont of period (w) [Eq. 31]
w=(pi/12)*((t+0.06667.*(Lz-Lm)+Sc)-12); %in rad
%solar time angle at beginning of period (w1) [Eq. 29]
w1=w-(pi.*t1/24); %in radians
%solar time angle at end of period (w2) [Eq. 30]
w2=w+(pi.*t1/24); %in radians
%daylight hours (N) [Eq.34]
N=(24/pi).*w_s; %in hours
%Is it daylight or nighttime?
IsNighttime=w<-w_s | w>w_s; %0 means Daytime, 1 means Nighttime
%extraterrestrial radiaiton (Ra) [Eq. 28]
Ra=~IsNighttime.*(12*60/pi)*Gsc.*d_r.*((w2-
w1)*sin(fi).*sin(delta)+cos(fi).*cos(delta).*(sin(w2)-sin(w1))); %in MJ*m^-2*hr^-1

%solar radiation (Rs)
Rs=~IsNighttime.*pyran./J_per_MJ.*s_per_hr*t1; %in MJ*m^-2*hr^-1
    %"~" turns o to 1 and 1 to 0 from IsNighttime true/false statement
Rs=max(0,Rs); %in MJ*m^-2*hr^-1

%clear sky solar radiation (Rso) [Eq. 37]
Rso=(0.75+2*10^-5*z).*Ra; %in MJ*m^-2*hr^-1
Rso=max(0,Rso); %in MJ*m^-2*hr^-1



%relative shortwave radiation (Rs/Rso)
Rs_Rso=min(1,Rs./Rso);

%estimate Nighttime Rs_Rso
Daycounter=0;
TempDayRs_Rso=zeros(24*60/t1,1);
for i=1:length(Date)-1;
```

```
    if w(i) <= w_s(i)-0.52 && w(i)>= w_s(i)-0.79; %Daytime averaging of cloudiness
        Daycounter=Daycounter+1;
        TempDayRs_Rso(Daycounter)=Rs_Rso(i);
    elseif IsNighttime(i)==1; %Nighttime
        if Daycounter>0
            AvgDayRs_Rso=mean(TempDayRs_Rso(1:Daycounter));
            Rs_Rso(i)=AvgDayRs_Rso;
        else
            Rs_Rso(i)=0.5; %Default value
            fprintf('No nighttime Rs_Rso available on %s, using default value of
%3.1f.\n',datestr(Date(i)),Rs_Rso(i));
        end

        if IsNighttime(i+1)==0; %Sunrise: Flag=1
            Daycounter=0;
            clear AvgDayRs_Rso;
            clear TempDayRs_Rso;
            TempDayRs_Rso=zeros(24*60/t1,1);
        end
    end
end


%net shortwave radiation (Rns) [Eq. 38]
Rns=(1-alpha).*Rs; %in MJ*m^-2*hr^-1
%net outgoing longwave radiation (Rnl) [Eq. 39]
Rnl=sigma.*(T+273.16).^4.*(0.34-0.14.*sqrt(e_a)).*(1.35.*(Rs_Rso)-0.35); %in MJ*m^-2*hr^-
1
%net radiation (Rn) [Eq. 40]
Rn=Rns-Rnl; %in MJ*m^-2*hr^-1
%soil heat flux for hourly or shorter periods (Ghr) [Eqs. 45 & 46]
Ghr=~IsNighttime.*0.1.*Rn+IsNighttime.*0.5.*Rn; %0.1*Rn for Daylight, 0.5*Rn for
Nighttime



%% Wind Speed

%calculated wind speed at 2m above surface (u2)from 1 m wind speed data
u2=u_1.*(4.87/(log(67.8.*z_wind-5.42))); %in m*s^-1
%wind speed at z=2m above surface used for subsequent caluations (u_z)
Isu_2zero=u_2==0; %1 means u_2=0, 0 means u_2~=0
u_z=~Isu_2zero.*u_2+Isu_2zero.*u2; %in m*s^-1



%% Reference Crop Aerodynamic Resistance & Bulk Surface Resistance

%zero plane displacement height (d)
d=(2/3)*h;
%roughness length governing momentum transfer (z_om)
z_om=0.123*h; %in m
%roughness length governing transfer of heat and vapor (z_oh)
z_oh=0.1*z_om; %in m
%aerodynamic resistance (r_a) [Eq. 4]
r_a=(log((z_m-d)/z_om)*log((z_h-d)/z_oh))./(k^2.*u_z); %in s*m^-1
r_a=r_a/s_per_hr; %in hr*m^-1


%% Reference Evapotranspiration

%virtual temperature (T_Kv) [Eq. on pg 26 of FAO56]
T_Kv=1.01.*(T+273);
%mean air density (rho_a) [Eq. on pg 26 of FAO56]
rho_a=P./(T_Kv*R); %in kg*m^-3
%Reference Evapotranspiration (ETo) [Eq. 3]
ETo_per_time=(1/lambda).*((Delta.*(Rn-Ghr)+rho_a.*c_p.*((e_s-
e_a)./r_a))./(Delta+gamma.*(1+(r_s./r_a))))*(mm_per_m/kg_per_m3); %in mm/hr
ETo=ETo_per_time.*t1; %in mm
ETo=max(0,ETo); %in mm
```

```
%Plot Solar Radiation Data
figure;
plot(Date,Rs,'b-');
datetick('x','mm/dd', 'keeplimits');
hold on;
plot(Date,Rso,'r-');
legend('Solar Radiaiton (Rs)','Clear Sky Solar Radiation (Rso)');
xlabel('Date/Time');
ylabel('Radiation (MJ m^-^2 hr^-^1)');
title('Solar Radiation vs. Clear Sky Solar Radiation');

figure;
plot(Date,Rs_Rso,'b-');
datetick('x','mm/dd','keeplimits');
legend('Ratio of Solar Radiation to Clear Sky Solar Radiation (Rs/Rso)');
xlabel('Date/Time');
ylabel('Ratio (Rs/Rso)');
title('Rs/Rso vs. Time');

%Plot Evapotranspiration Data
figure;
plot(Date,ETo,'g-');
datetick('x','mm/dd','keeplimits');
legend('Reference Evapotranspiration (ETo)');
xlabel('Date/Time');
ylabel('ETo (mm)');
title('ETo vs. Time');


end



function [ Time_out, Var_out ] = HOUR_AVERAGE_SCALE( Time_in, Var_in )
%HOUR_AVERAGE_SCALE Takes 5 minute data and averages over an hour
% Time_in is the input date/time
% Time_out is the output date/time
% Var is the variable to be averaged. It may be a matrix, provided the
% temporal data are the rows
% The average at 1PM consists of the average of all values between 12:50PM
% and 1:10PM

%% Calculate Time_out
Min_date=ceil(min(Time_in)); %first date, rounded to the next day
Max_date=floor(max(Time_in)); %last date, rounded to midnight

inc=1/24; %hourly increment

Time_out=Min_date:inc:Max_date;

%% Find and average
avg_buffer=10/60/24; %in minutes

%Flags for finding values
start_flag=0;
end_flag=0;
start_loop=1;

Var_out=zeros(length(Time_out),size(Var_in,2));

for i=1:length(Time_out)
    for j=start_loop:length(Time_in)
        if start_flag==0 && Time_in(j)>=Time_out(i)-avg_buffer
            start_flag=j;
        elseif Time_in(j+1)>Time_out(i)+avg_buffer
            end_flag=j;

            %Check for missing data/jumps in the data
            if start_flag==0 || Time_in(j+1)>=Time_out(i)+2*avg_buffer
                Var_out(i,:)=NaN;
```

```
            else
                start_loop=start_flag; %no need to return to 1 each time, instead carry
on where we left off
                Var_out(i,:)=mean(Var_in(start_flag:end_flag,:));
            end
            %Reset flags
            start_flag=0;
            end_flag=0;
            break;
        end
    end
end
```

```
function [ET] = ET_MODEL_PS ( fitting, Dry_wt, Water_wt, ET0, Tray_wt, Del_wt, Fit_flag )
%ET_MODEL Calculates the amount transpired from a tray
%   ET0: synchronized ET0, in log 10, instantaneous (mm)
%   fitting: vector of parameters to be fit
Kc=fitting(1);
%   Kc: a scalar crop coefficient for the tray (-)
%   Water_wt: Water weight of saturated tray (will have units of Tray_wt)
%   Dry_wt: Dry weight of tray (will have units of Tray_wt)
%   Tray_wt: The actual tray weight to determine percent saturation
%   Del_wt: The measured change in weight synched to ET0 (in mm)
%   Fit_flag: 1 if Kc is to be fit, 0 if not to be fit

%% Calculate Percent of Saturation
Per_sat=abs(Tray_wt-Dry_wt)/(Water_wt);
%Per_sat=max([Per_sat;zeros(size(Per_sat))]);
%Per_sat=min([Per_sat;ones(size(Per_sat))]);

%% Calculate ET
%ET0=10.^ET0;
ET=Kc*ET0.*Per_sat;
%ET=log10(ET);

% Calculate sum of squares error for fitting
if Fit_flag==1
    SSE=sum((ET-Del_wt).^2);
    ET=SSE;
end
```

APPENDIX B

MATLAB OUTPUT FOR 08/30/14-09/03/14, 12/13/14-12/17/14, & 01/11/15-01/15/15

Ambient Air Temperatures for the Three Roofs from 08/30/14-09/03/14 based on 5-minute Interval Data

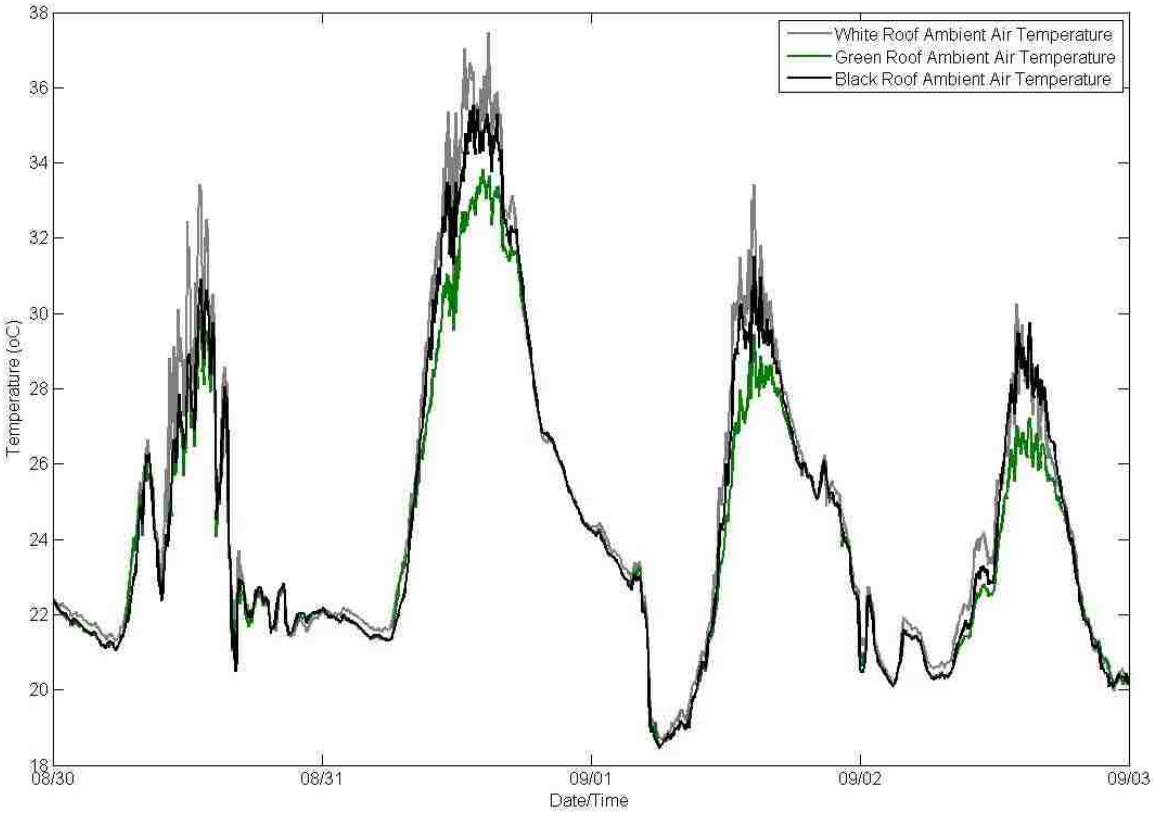

Surface Temperatures for the Three Roofs from 08/30/14-09/03/14 based on 5-minute Interval Data

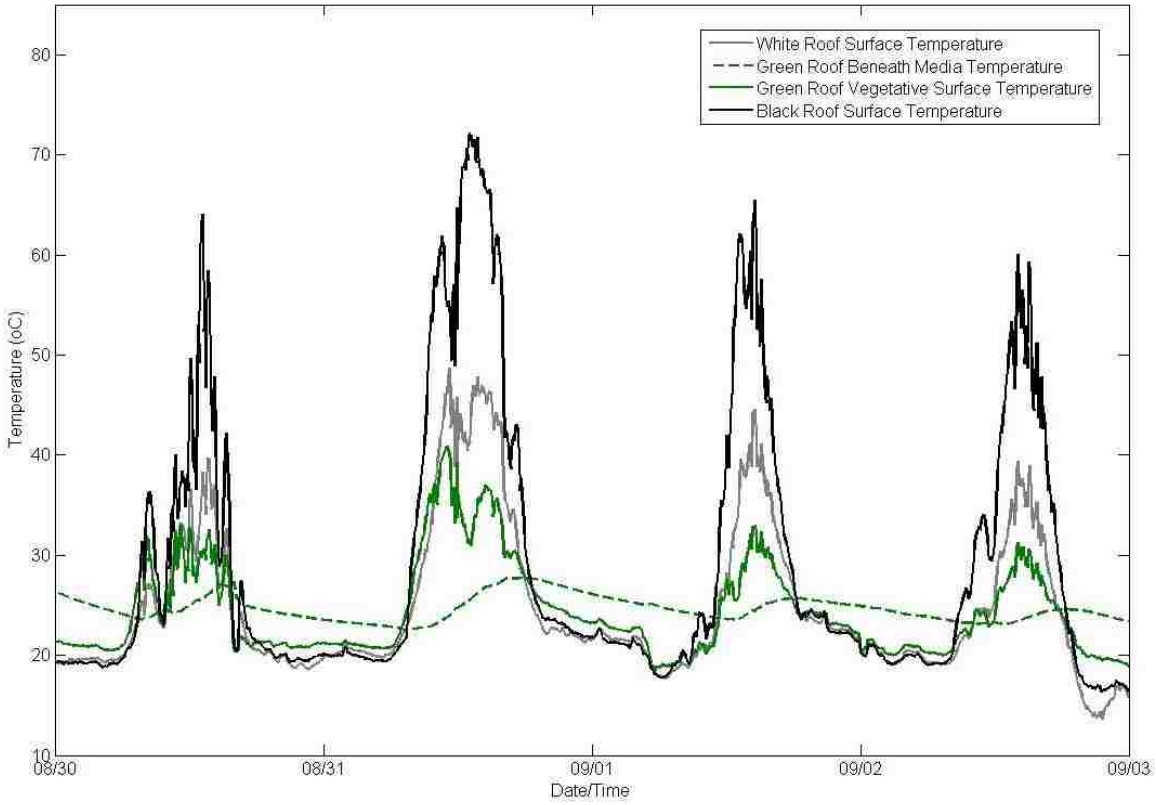

Sub-slab Temperatures for the Three Roofs from 08/30/14-09/03/14 based on 5-minute Interval Data

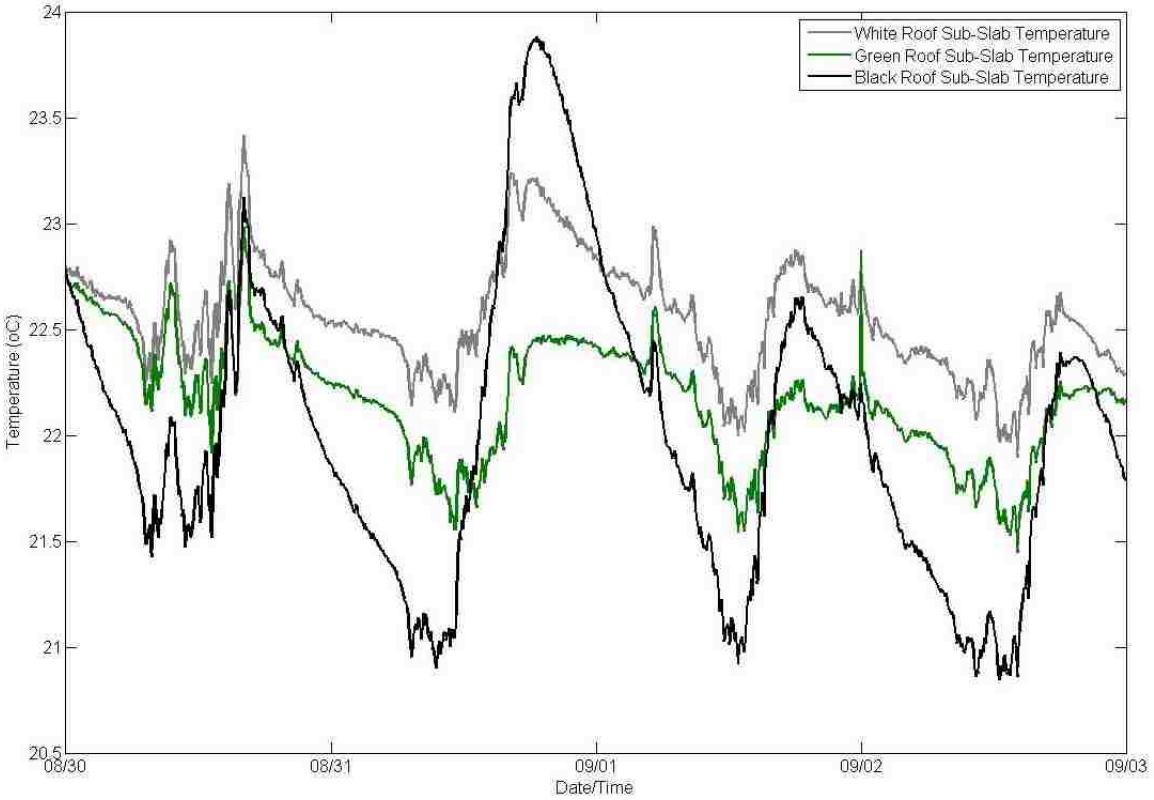

White TPO Roof Temperatures from 08/30/14-09/03/14 based on 5-minute Interval Data

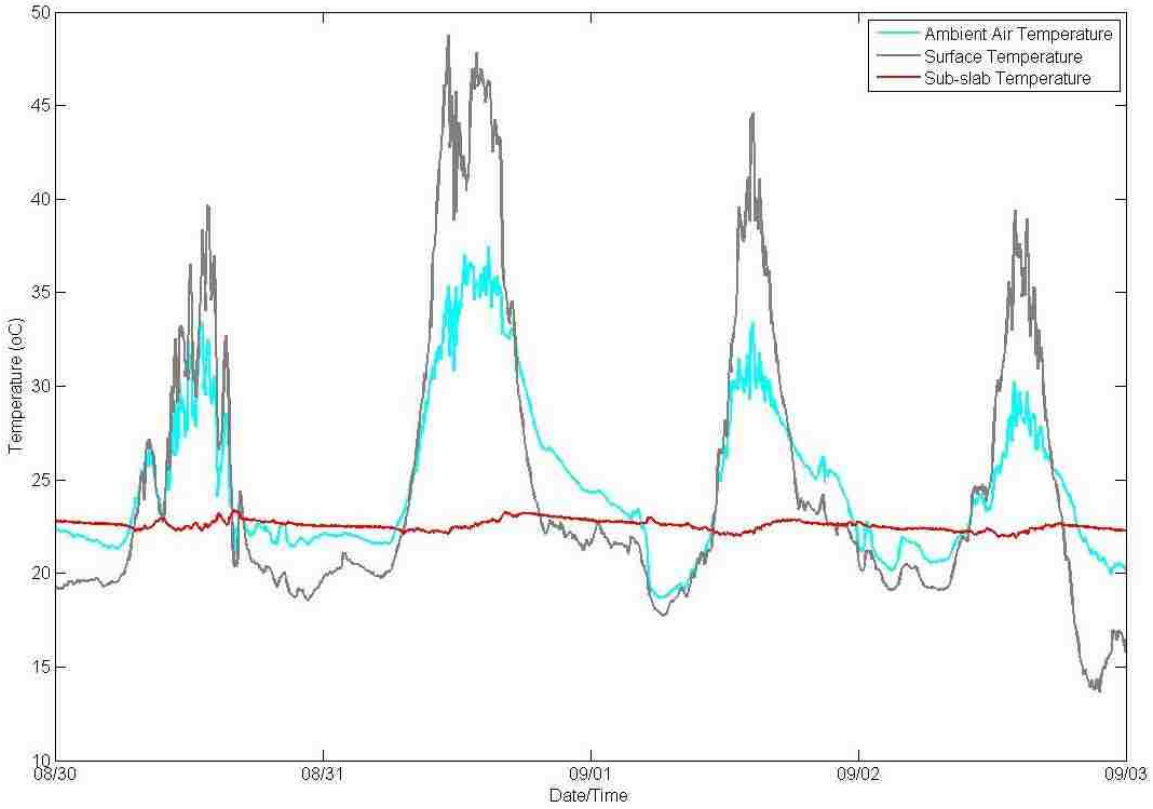

Black EPDM Roof Temperatures from 08/30/14-09/03/14 based on 5-minute Interval Data

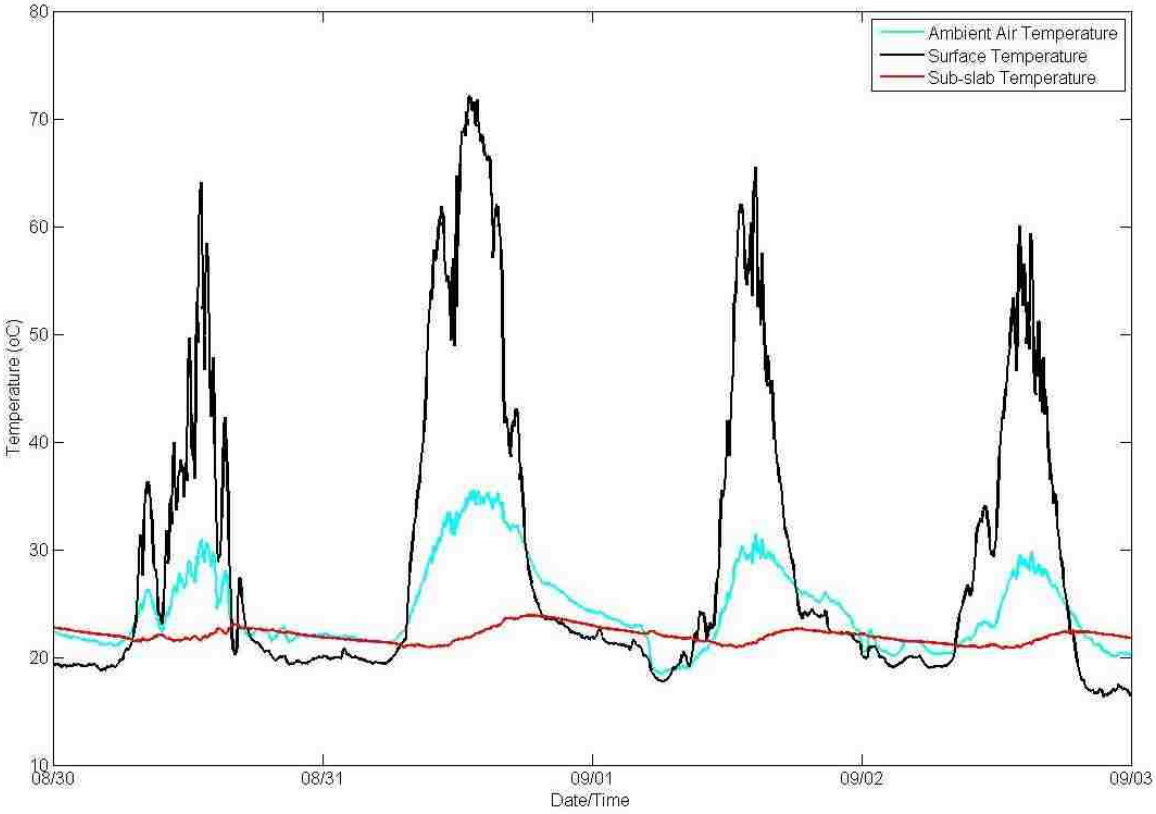

Green Roof Temperatures from 08/30/14-09/03/14 based on 5-minute Interval Data

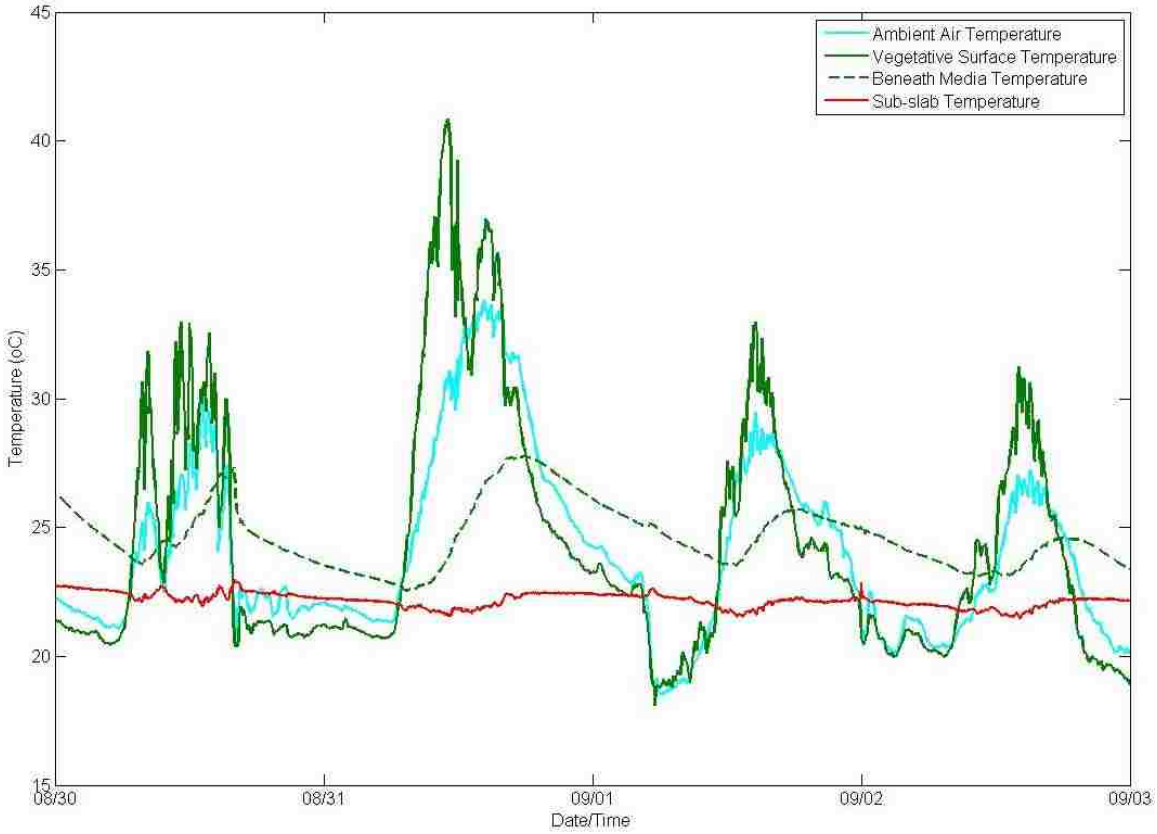

Ratio of Measured Solar Radiation to Clear Sky Solar Radiation from 08/30/14-09/03/14 based on Hourly-Averaged Data

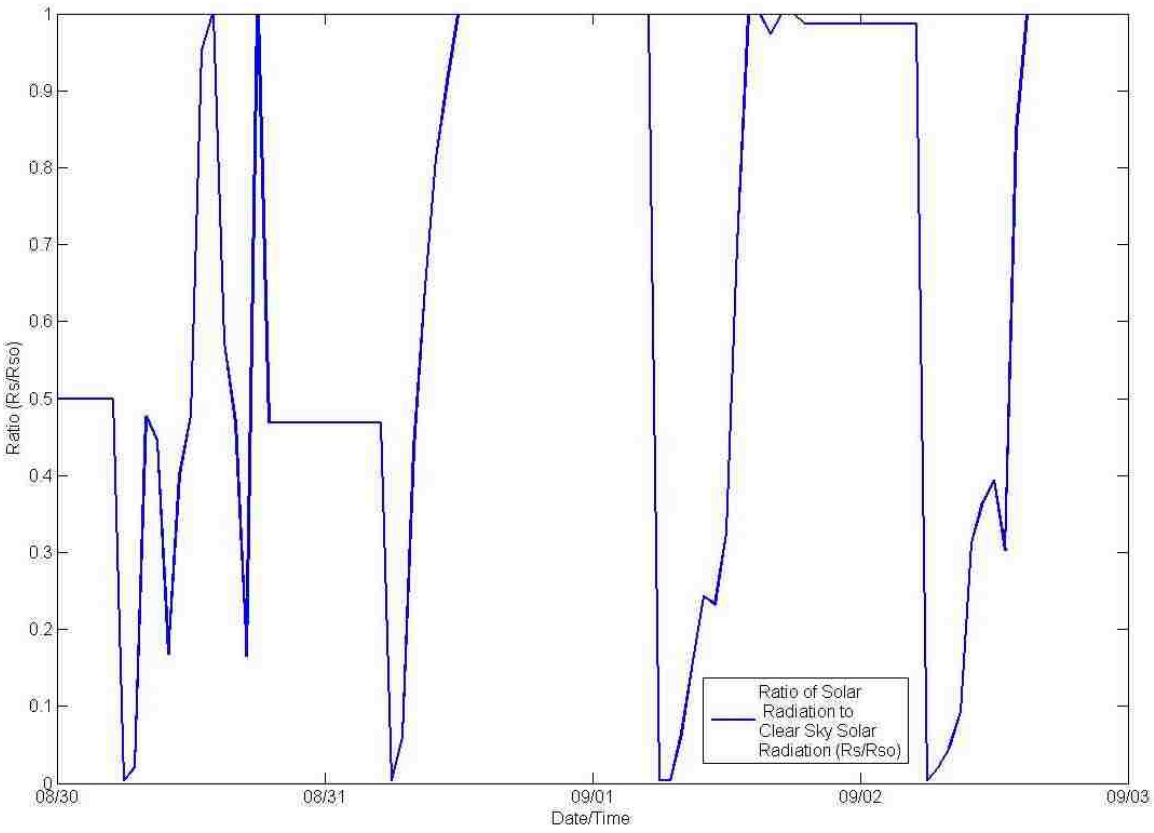

Measured Solar Radiation and Clear Sky Solar Radiation from 08/30/14-09/03/14 based on Hourly-Averaged Data

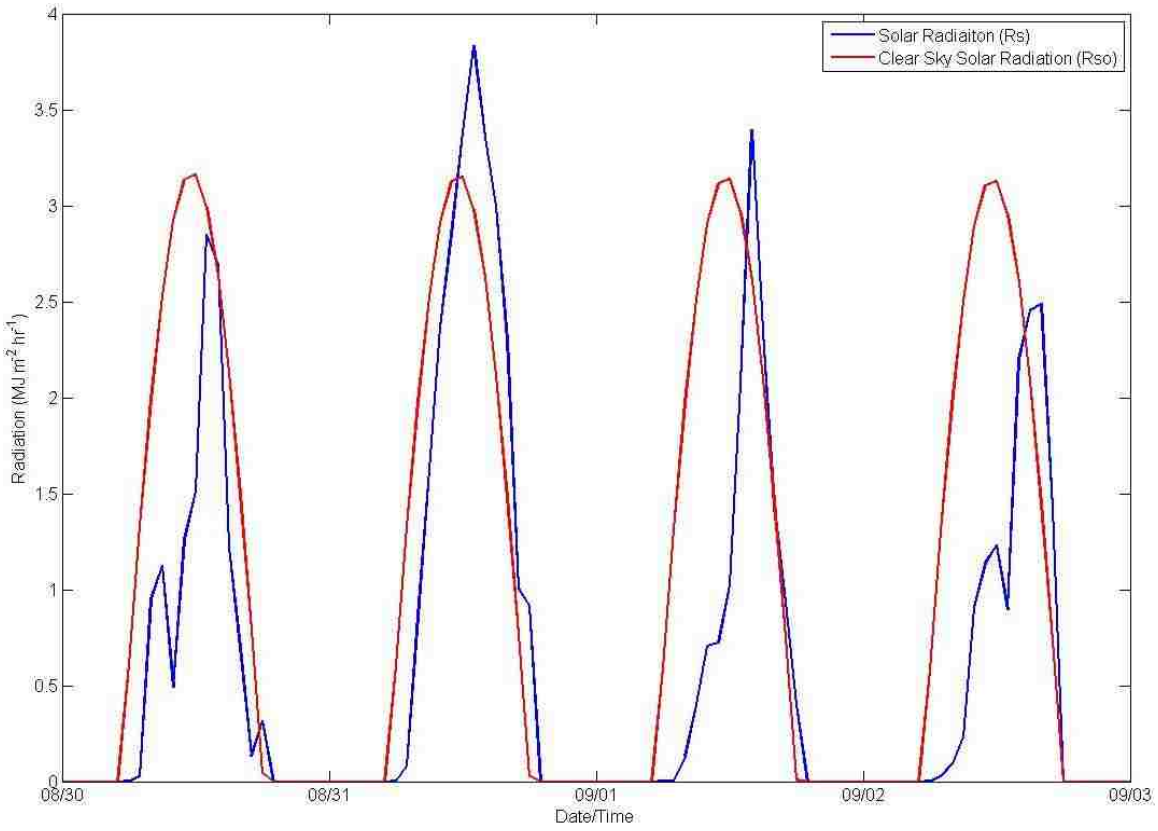

Reference Evapotranspiration from 08/30/14-09/03/14 based on Hourly-Averaged Data

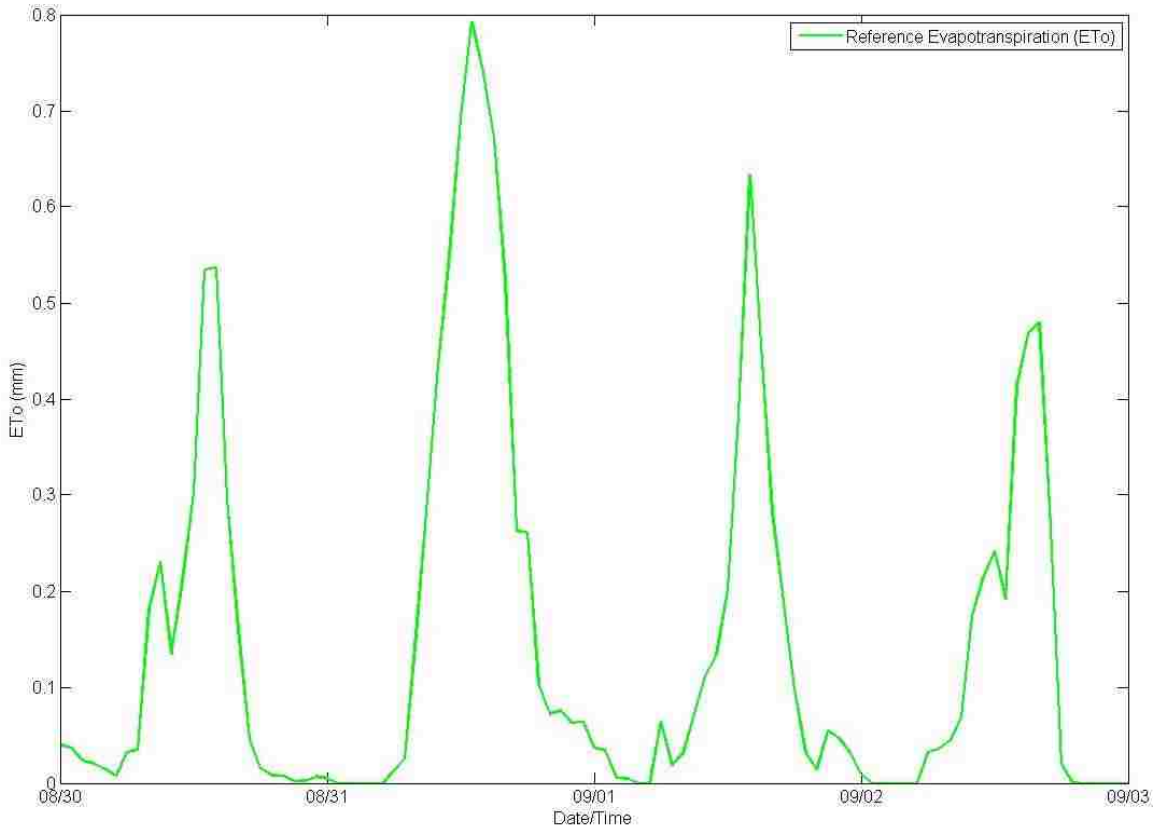

Cumulative Reference Evapotranspiration from 08/30/14-09/03/14 based on Hourly-Averaged Data

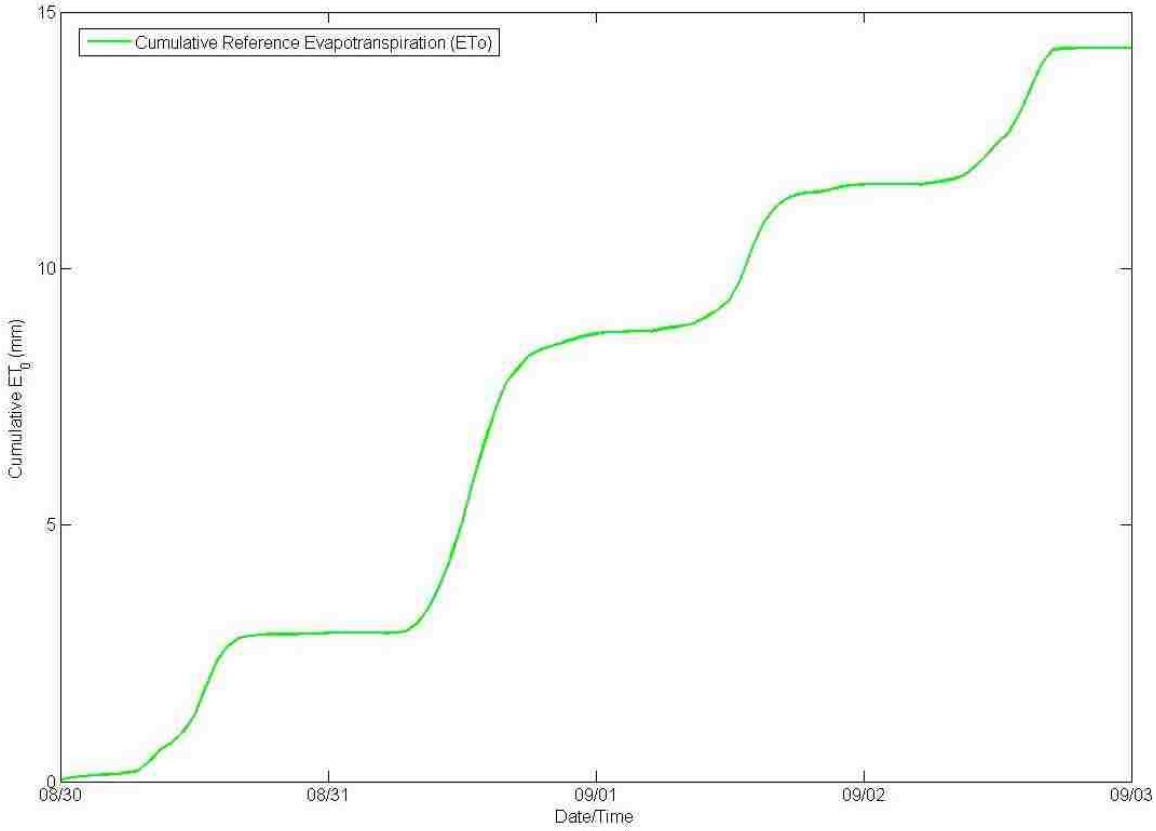

Cumulative Precipitation from 08/30/14-09/03/14 based on 5-minute Interval Data

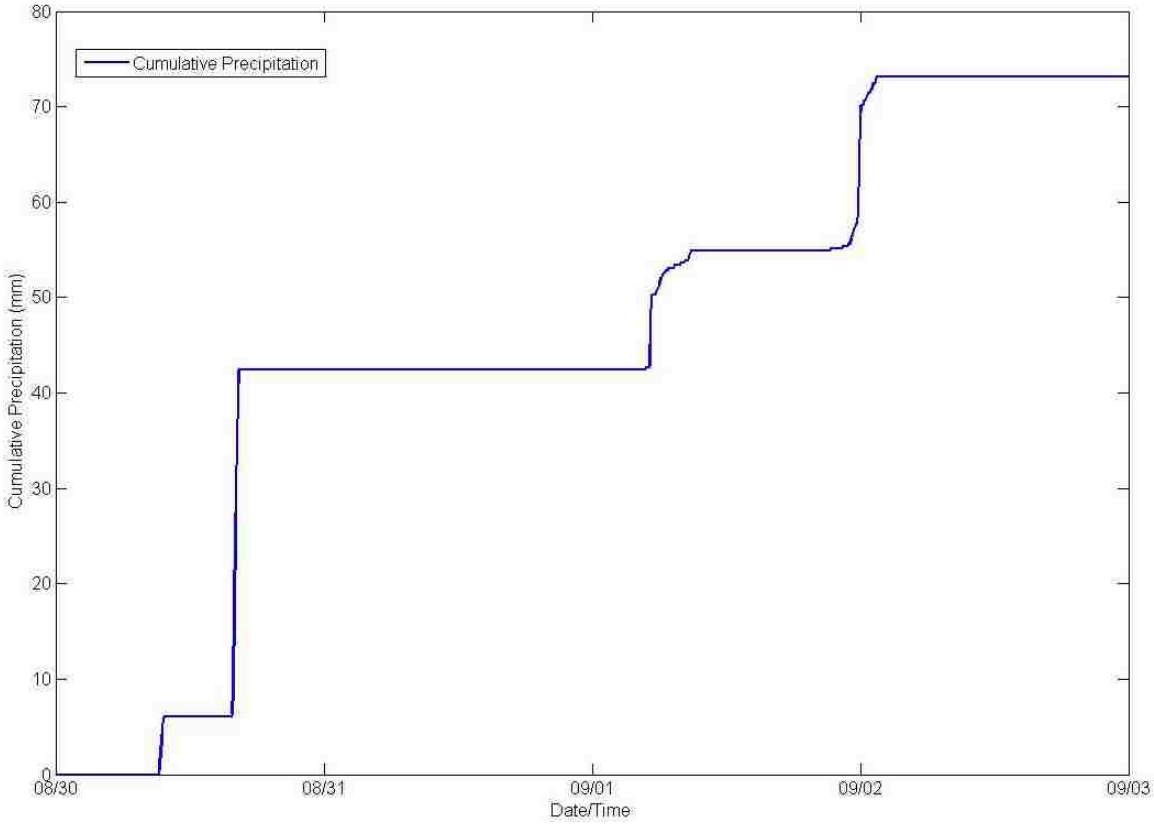

Surface Temperatures of the Three Roof Surfaces as well as Cumulative Precipitation, Reference Evapotranspiration, and Water Storage in the Media for 08/30/14-09/03/14

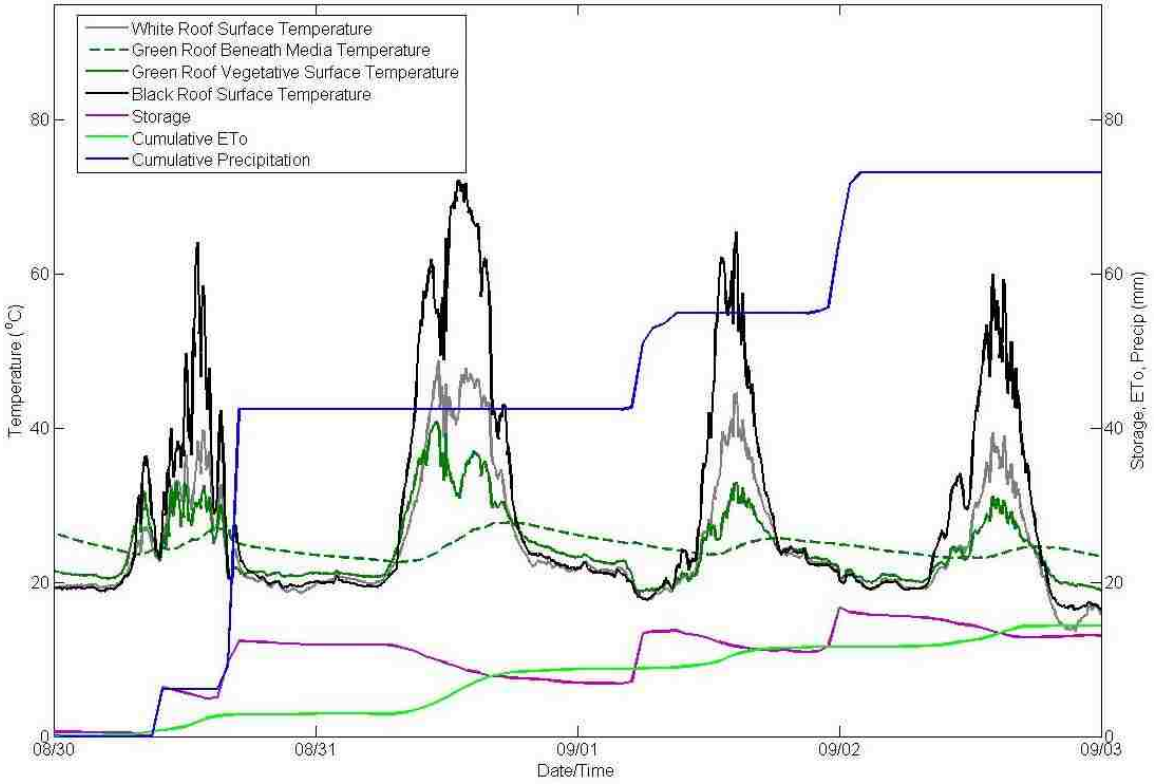

Ambient Air Temperatures for the Three Roofs from 12/13/14-12/17/14 based on 5-minute Interval Data

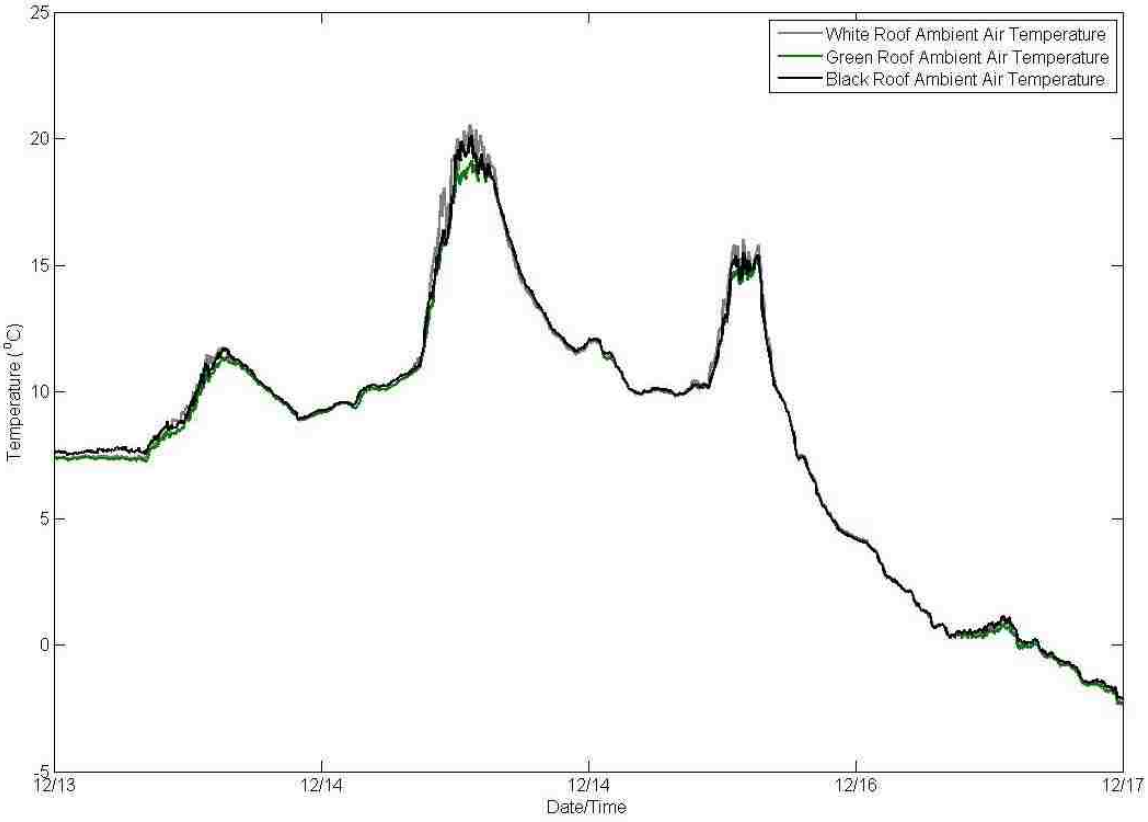

Surface Temperatures for the Three Roofs from 12/13/14-12/17/14 based on 5-minute Interval Data

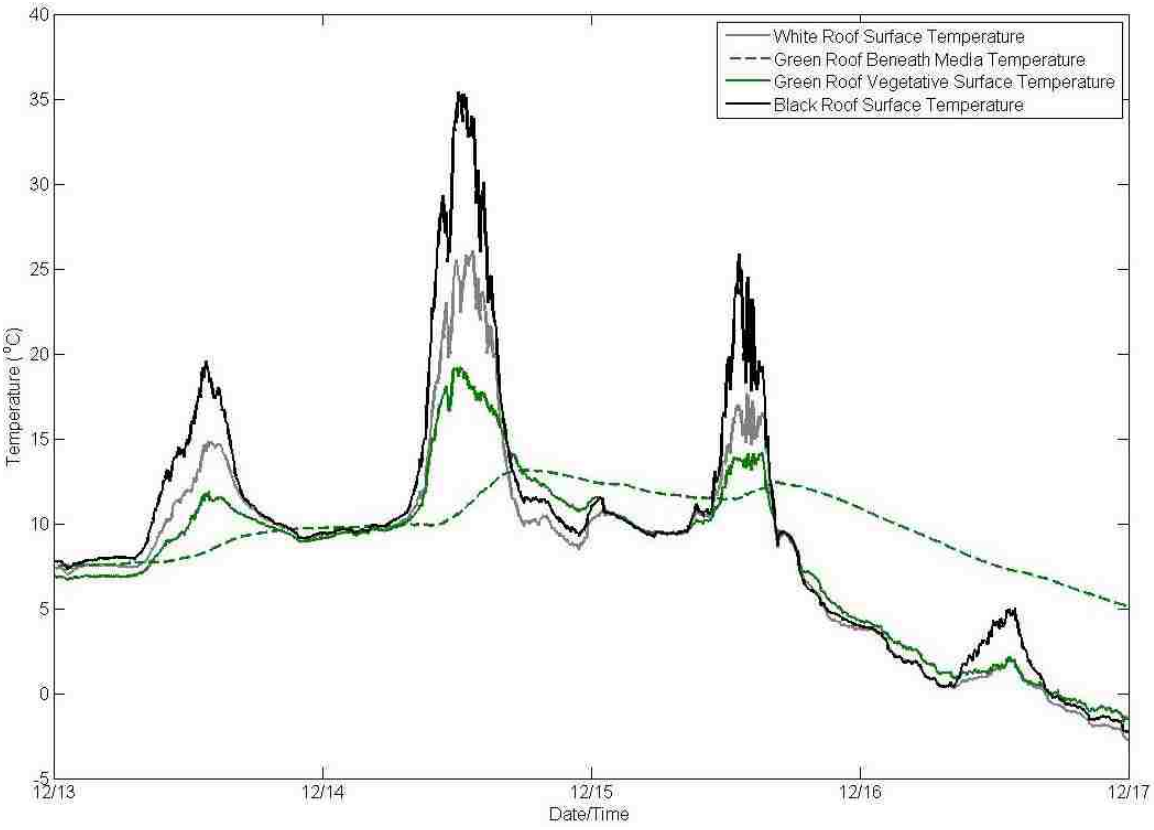

Sub-slab Temperatures for the Three Roofs from 12/13/14-12/17/14 based on 5-minute Interval Data

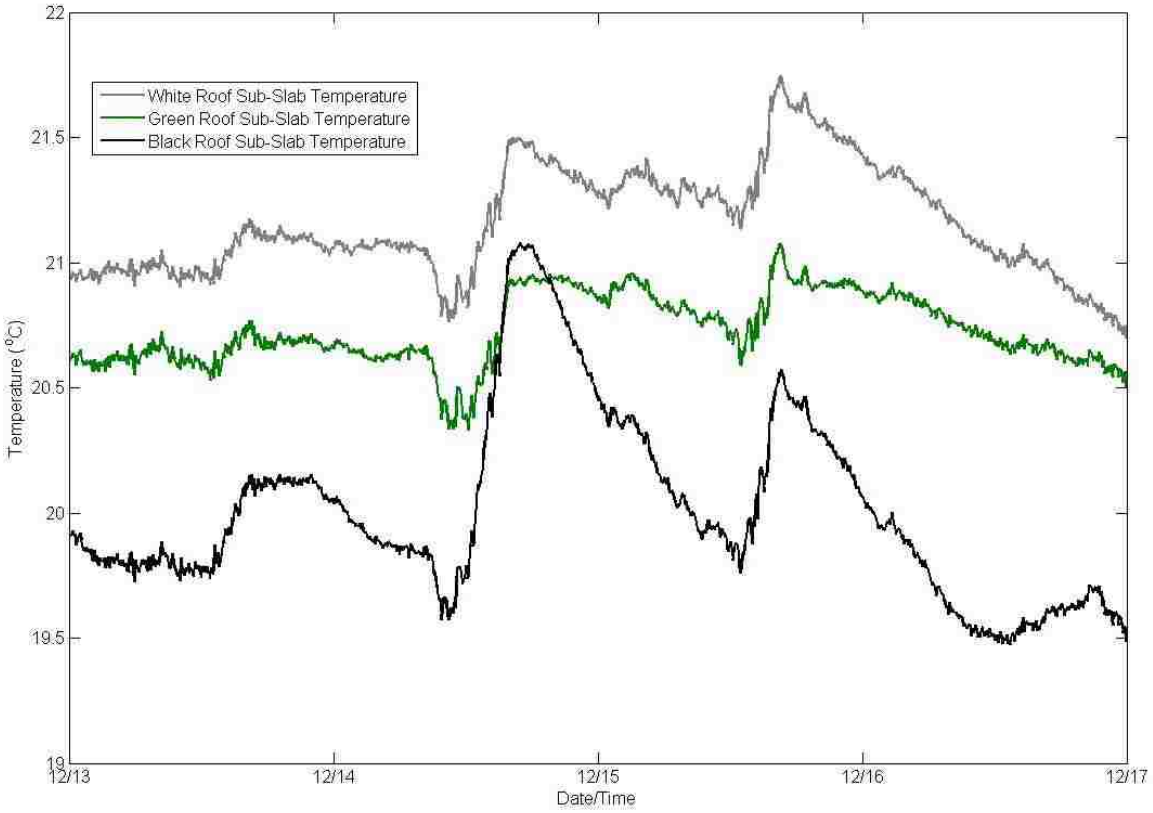

White TPO Roof Temperatures from 12/13/14-12/17/14 based on 5-minute Interval Data

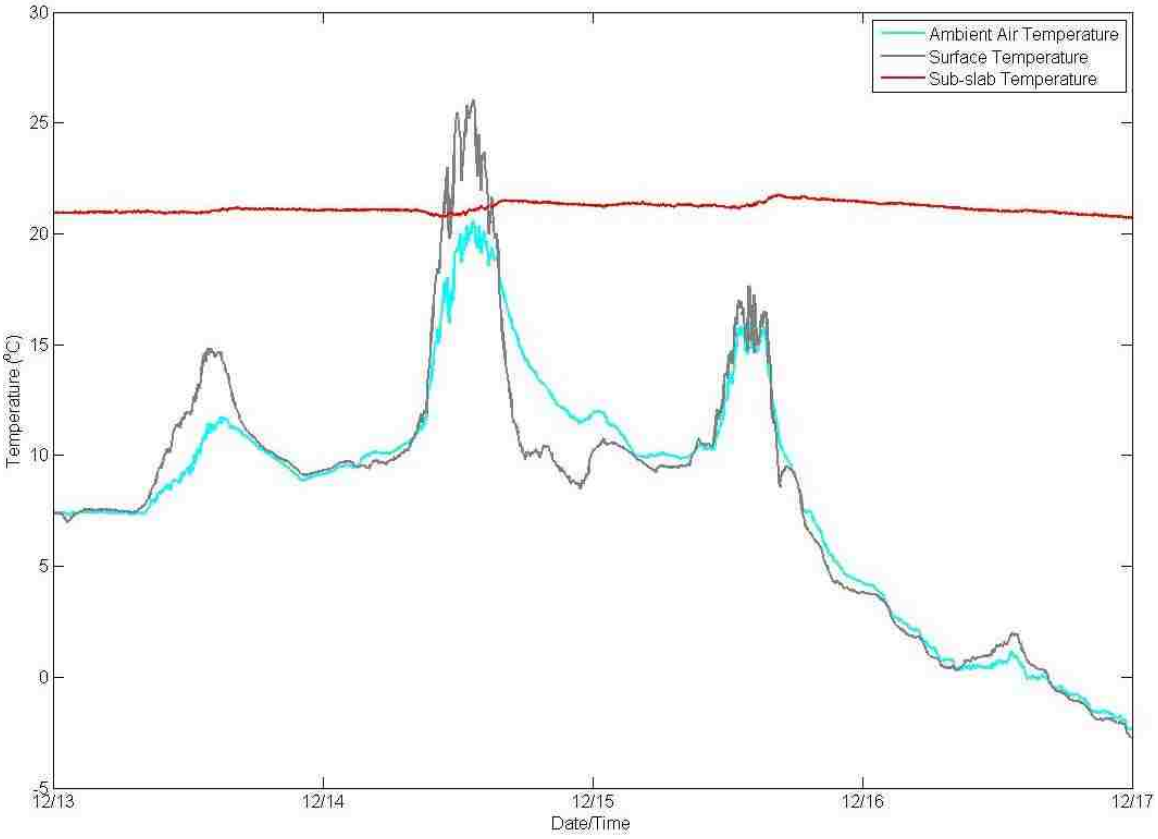

Black EPDM Roof Temperatures from 12/13/14-12/17/14 based on 5-minute Interval Data

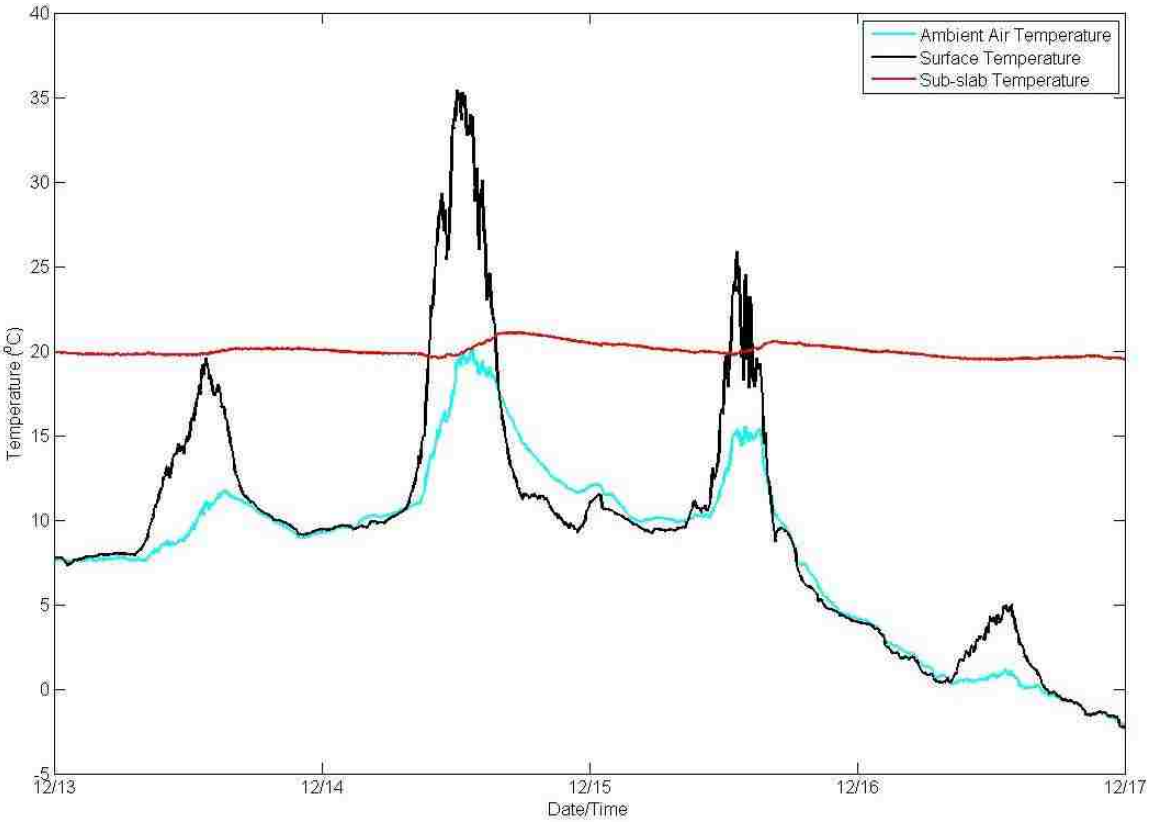

Green Roof Temperatures from 12/13/14-12/17/14 based on 5-minute Interval Data

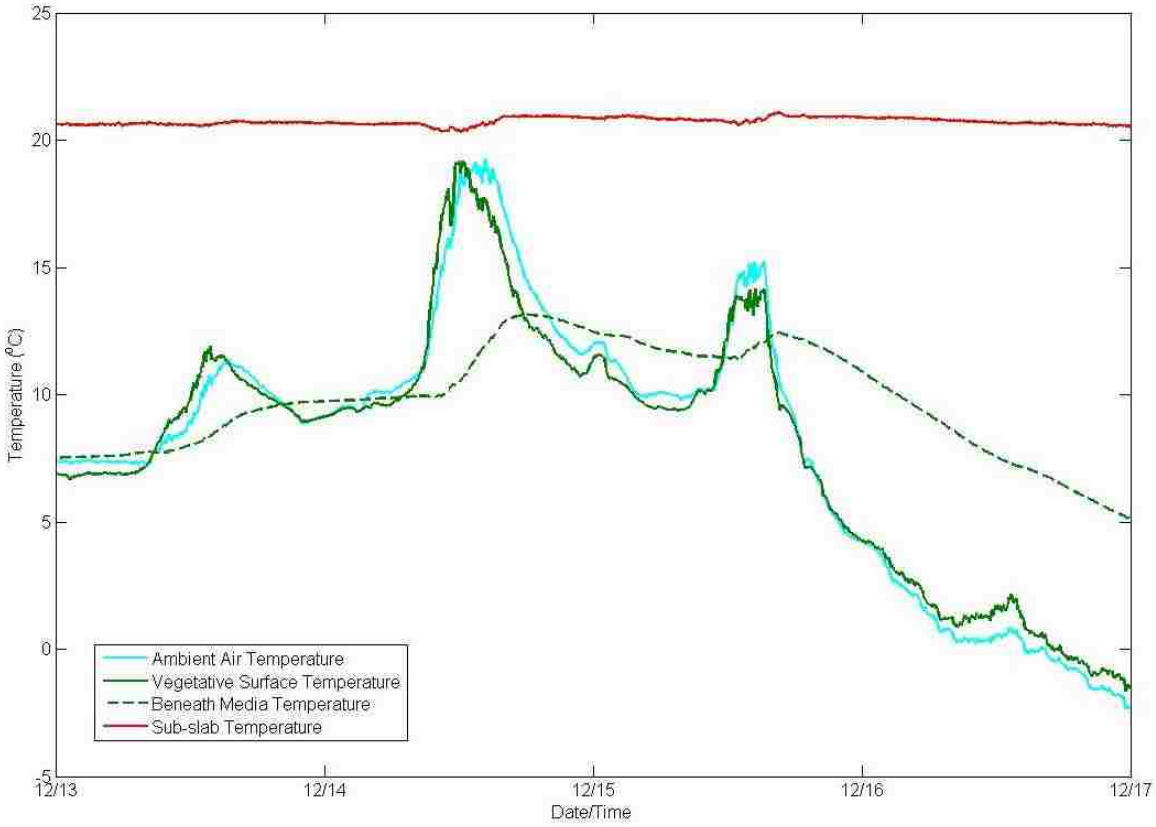

Ratio of Measured Solar Radiation to Clear Sky Solar Radiation from 12/13/14-12/17/14 based on Hourly-Averaged Data

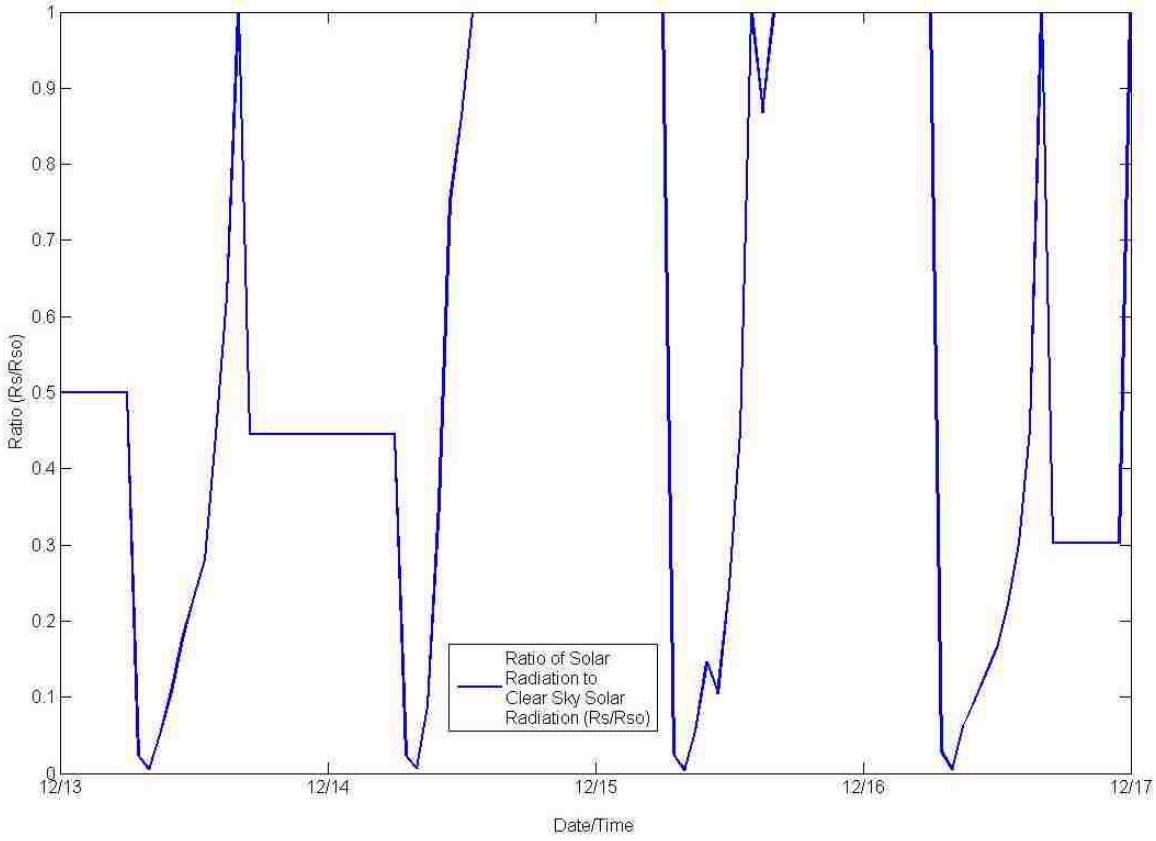

Measured Solar Radiation and Clear Sky Solar Radiation from 12/13/14-12/17/14 based on Hourly-Averaged Data

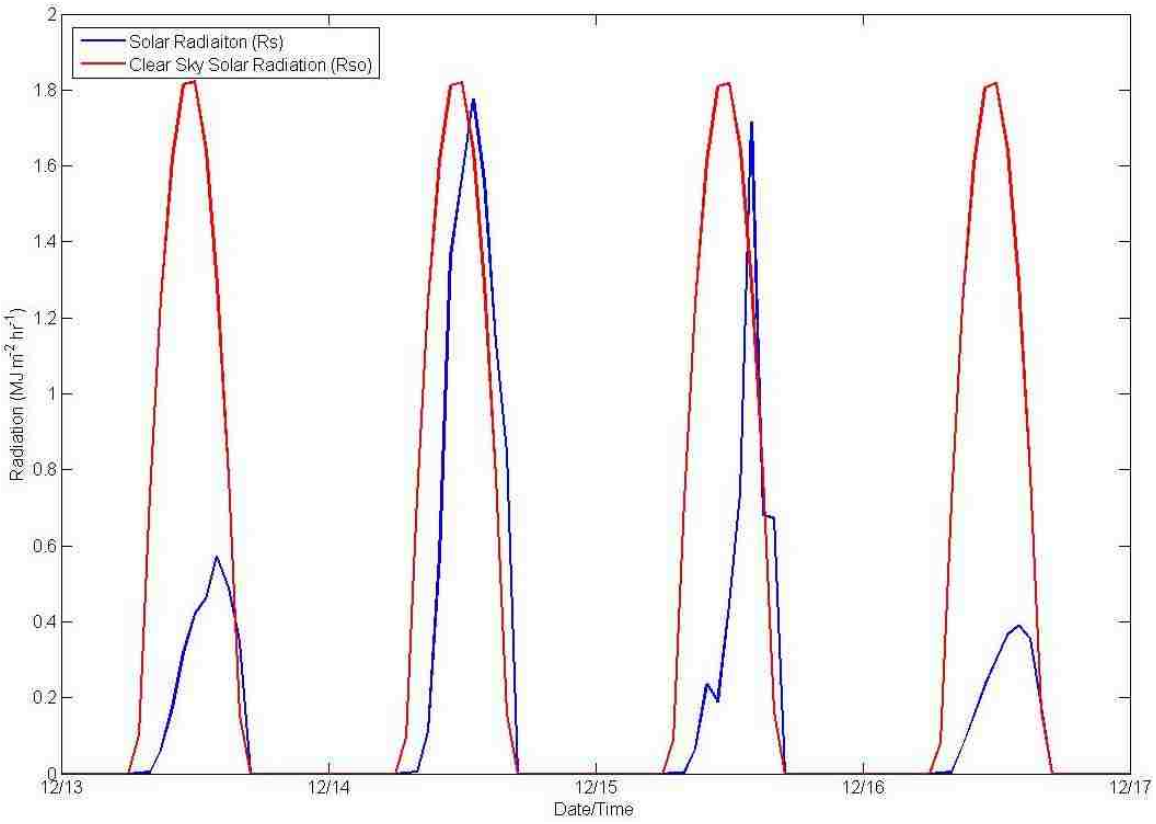

Reference Evapotranspiration from 12/13/14-12/17/14 based on Hourly-Averaged Data

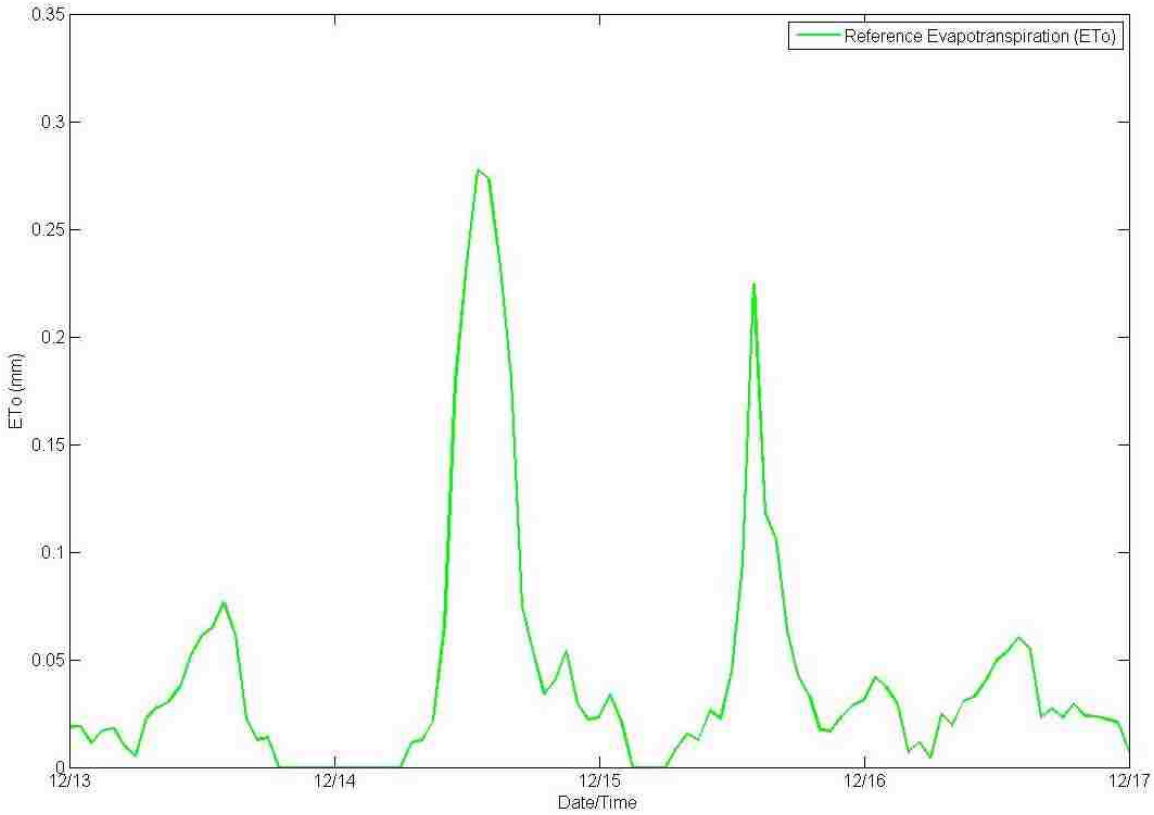

Cumulative Reference Evapotranspiration from 12/13/14-12/17/14 based on Hourly-Averaged Data

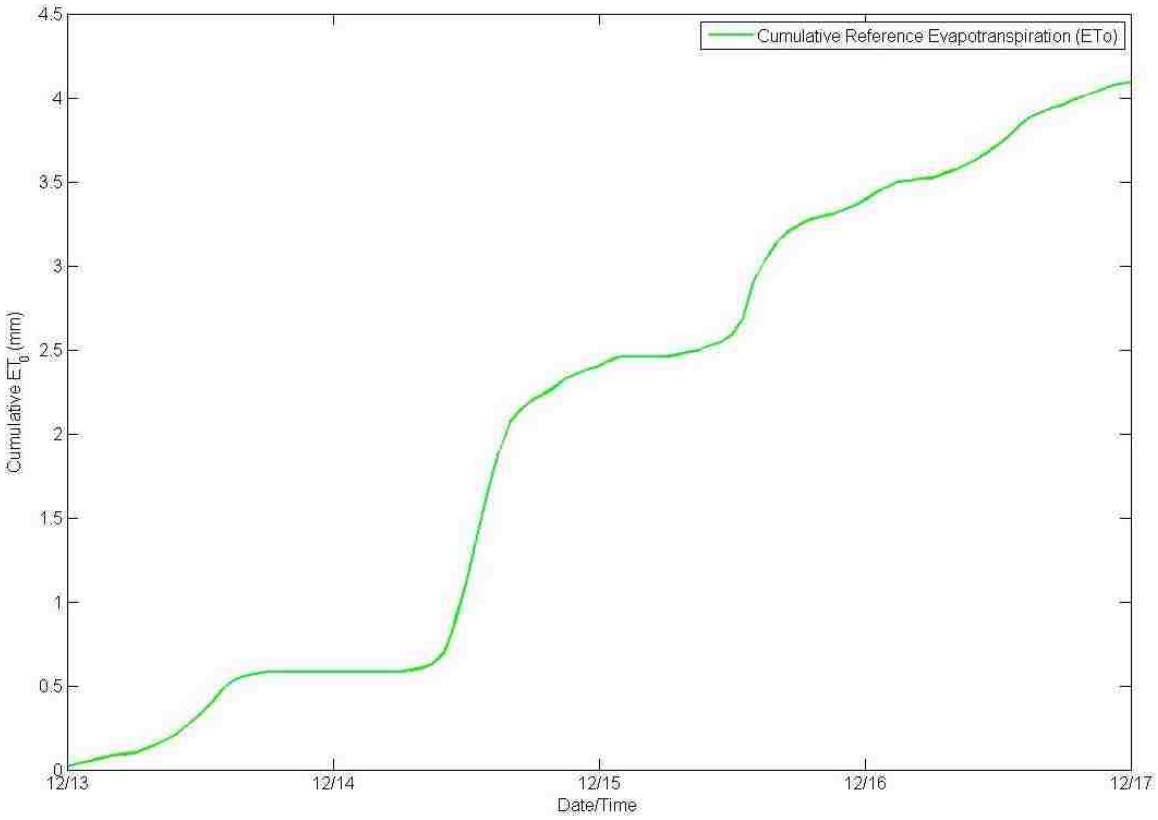

Cumulative Precipitation from 12/13/14-12/17/14 based on 5-minute Interval Data

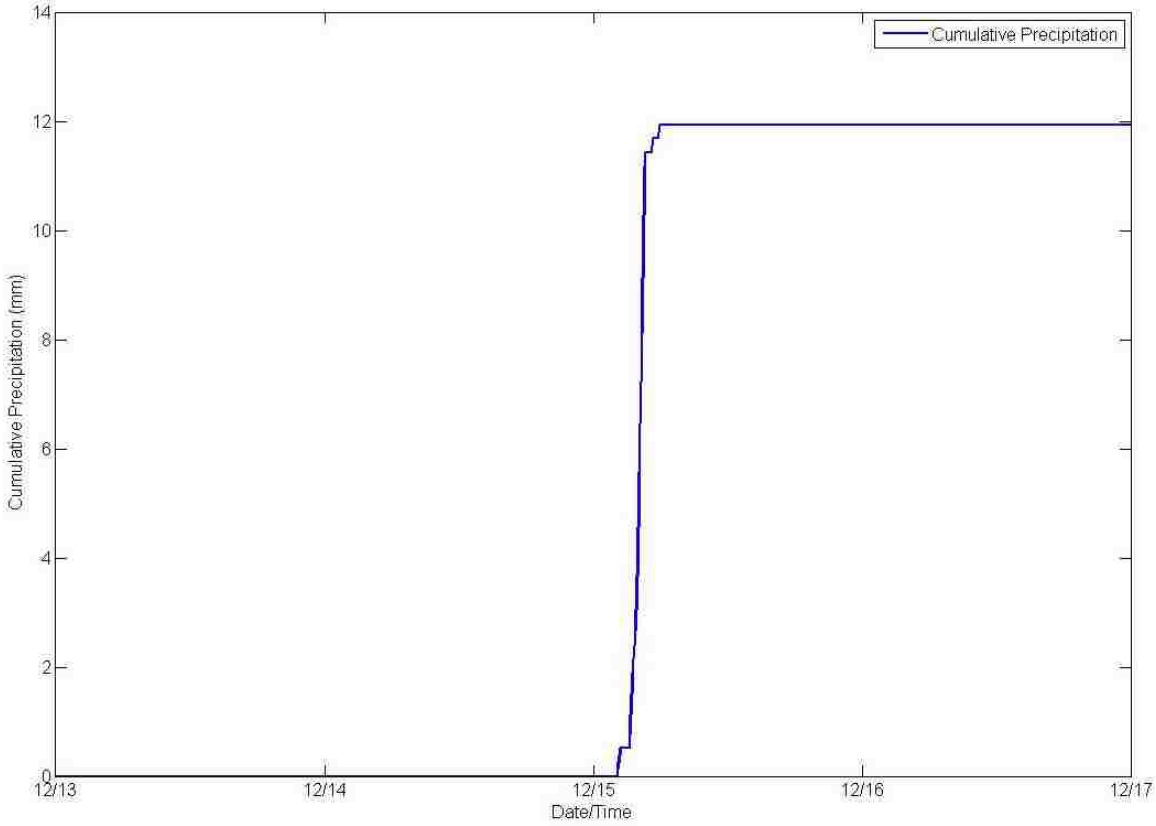

Surface Temperatures of the Three Roof Surfaces as well as Cumulative Precipitation, Reference Evapotranspiration, and Water Storage in the Media for 12/13/14-12/17/14

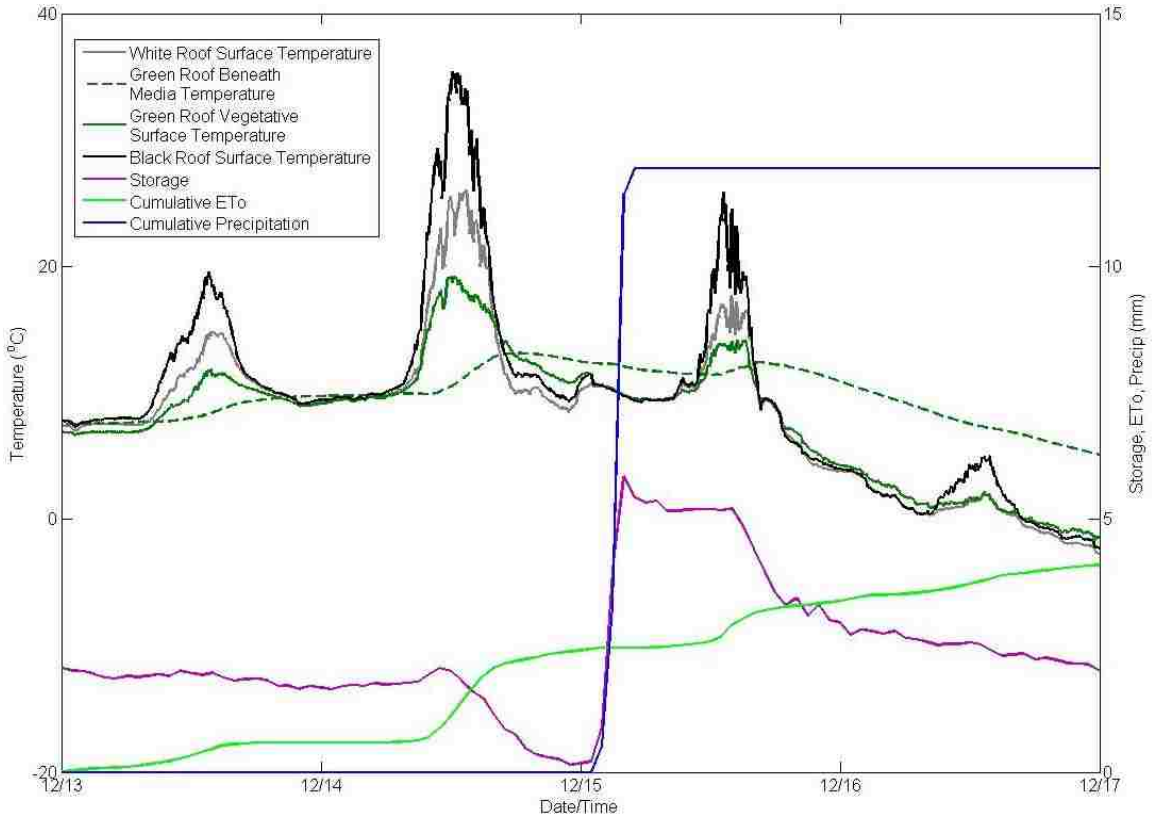

Ambient Air Temperatures for the Three Roofs from 01/11/15-01/15/15 based on 5-minute Interval Data

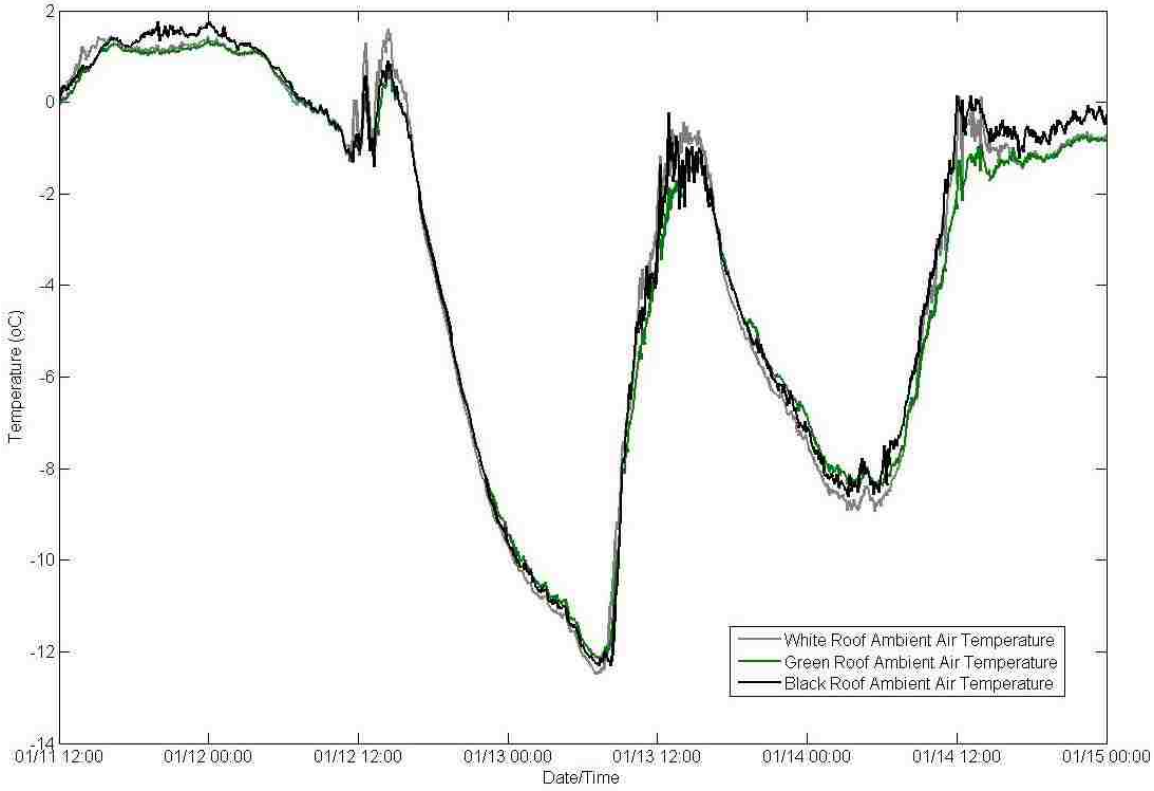

Surface Temperatures for the Three Roofs from 01/11/15-01/15/15 based on 5-minute Interval Data

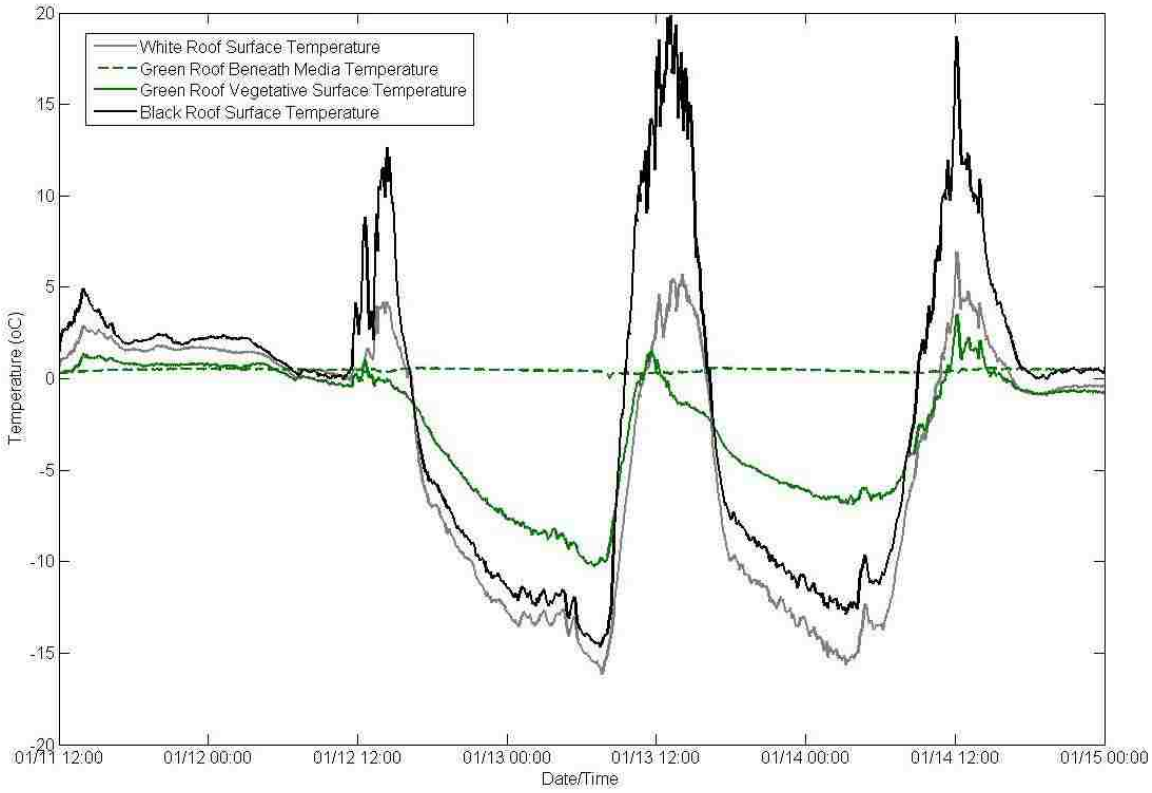

Sub-slab Temperatures for the Three Roofs from 01/11/15-01/15/15 based on 5-minute Interval Data

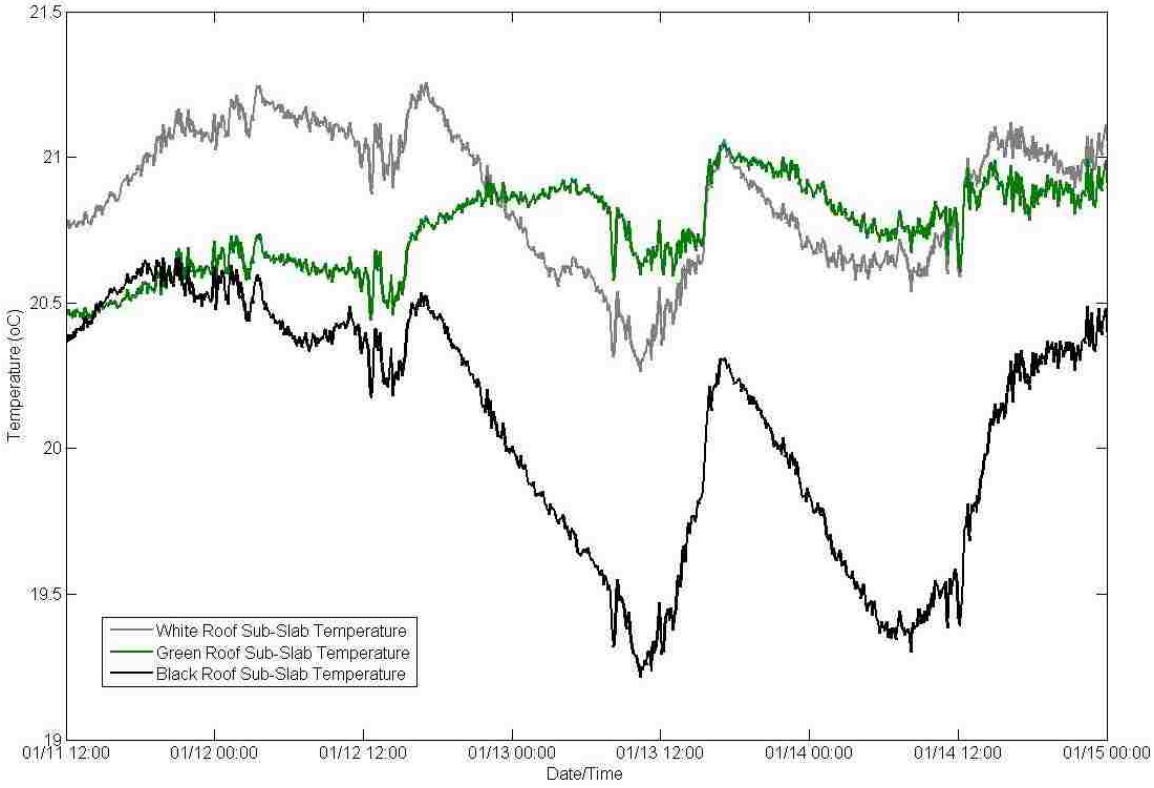

White TPO Roof Temperatures from 01/11/15-01/15/15 based on 5-minute Interval Data

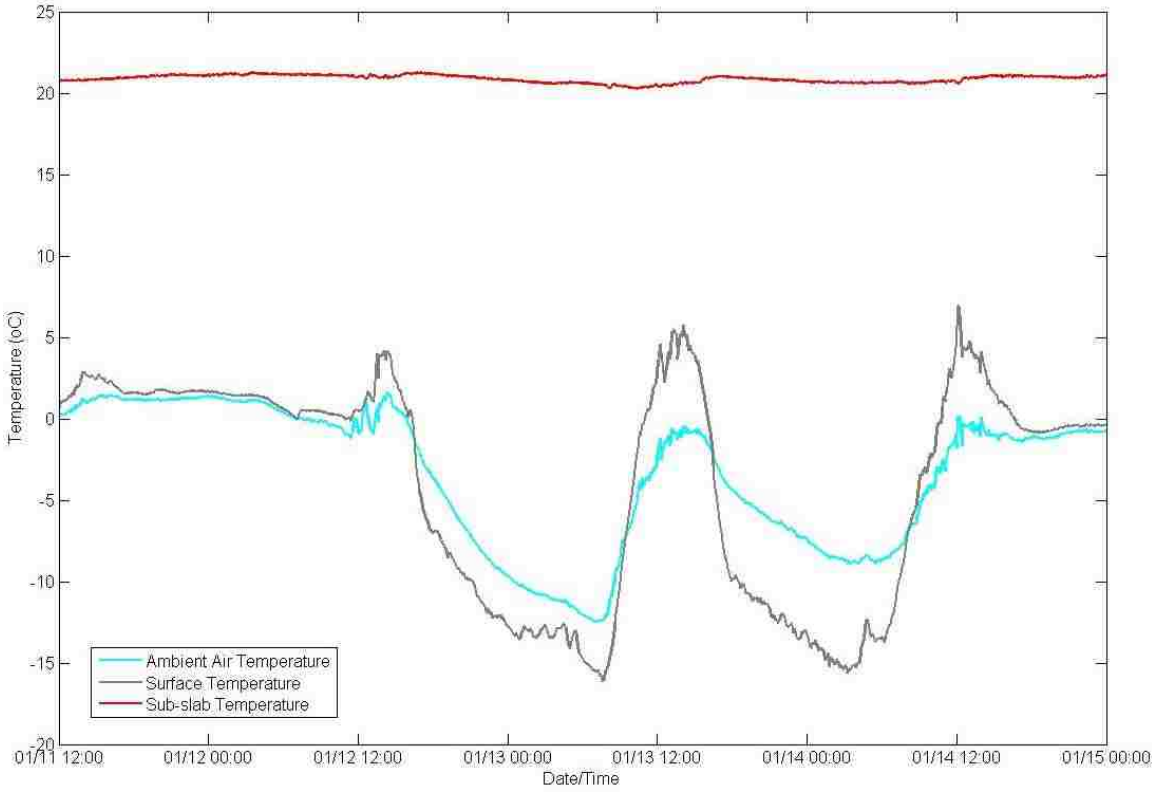

Black EPDM Roof Temperatures from 01/11/15-01/15/15 based on 5-minute Interval Data

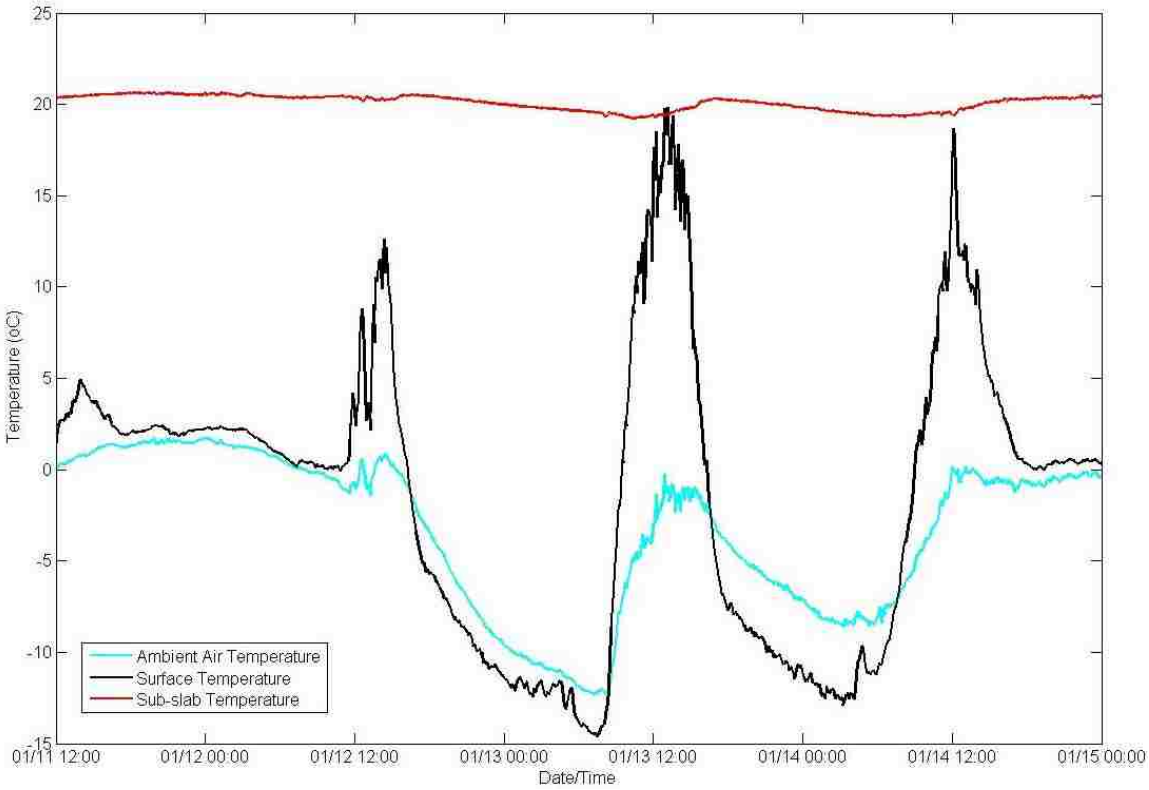

Green Roof Temperatures from 01/11/15-01/15/15 based on 5-minute Interval Data

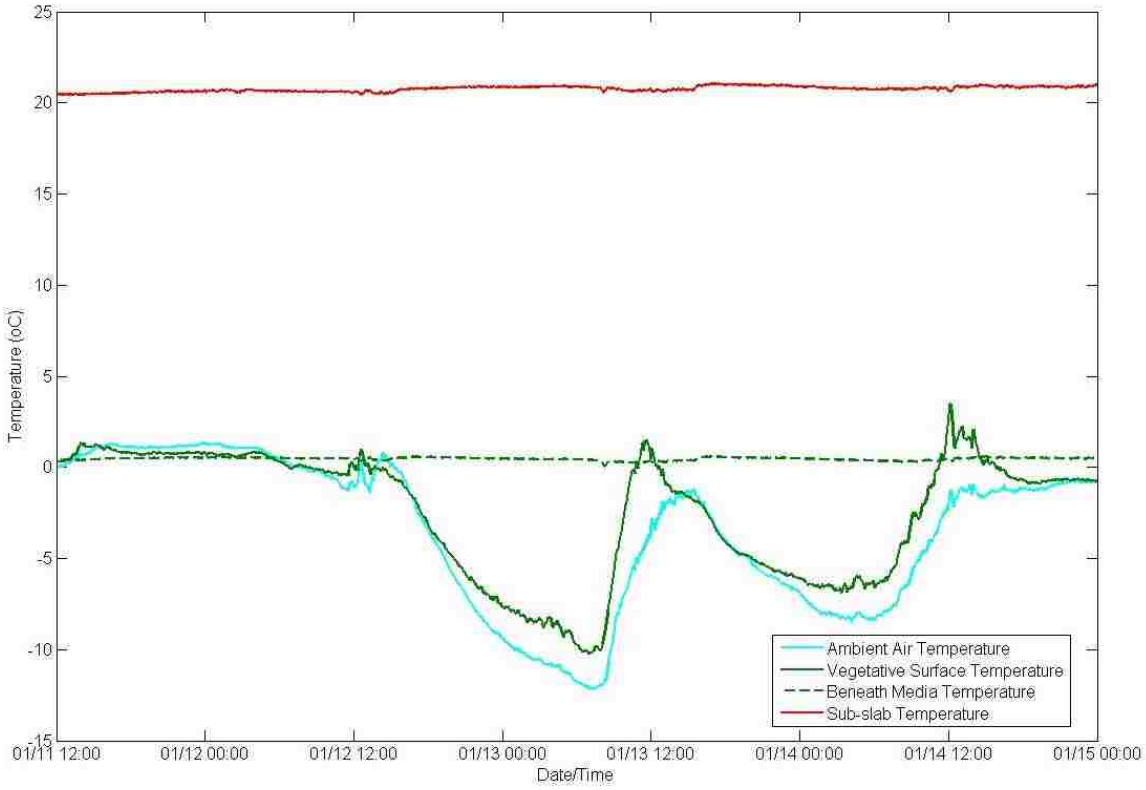

Ratio of Measured Solar Radiation to Clear Sky Solar Radiation from 01/12/15-01/15/15 based on Hourly-Averaged Data

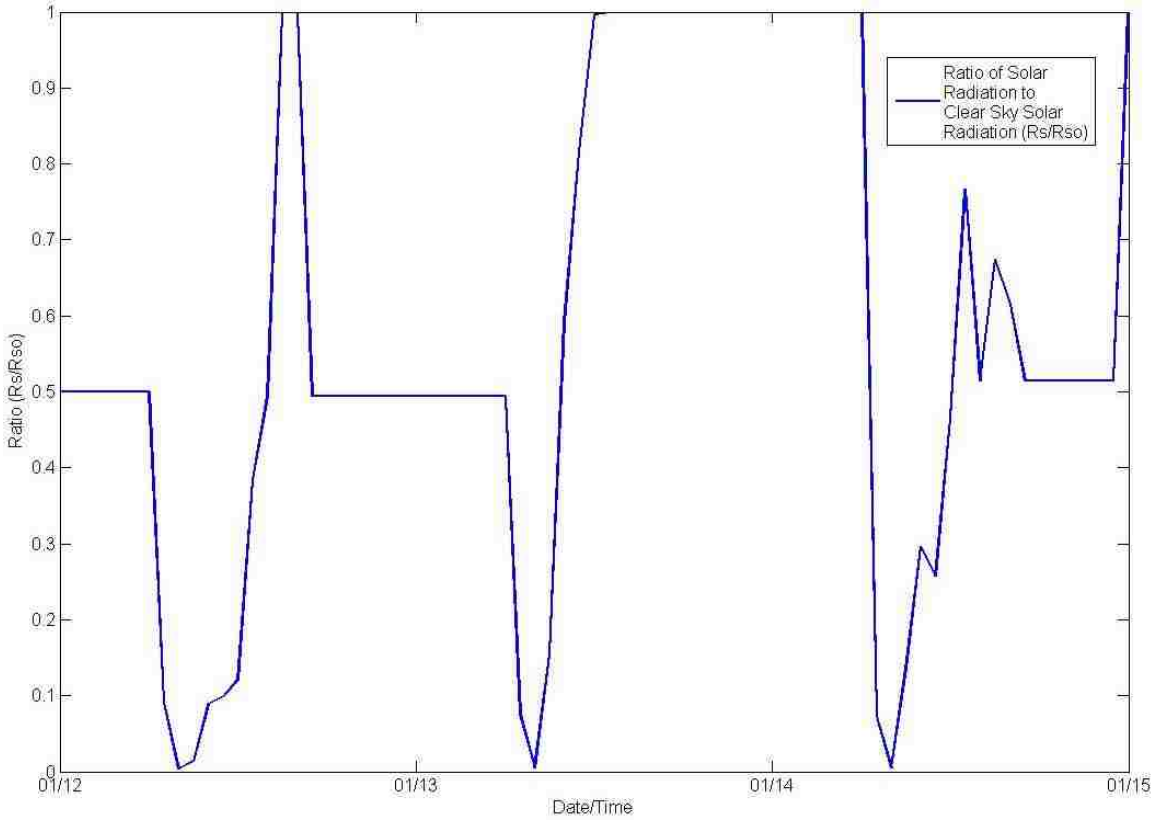

Measured Solar Radiation and Clear Sky Solar Radiation from 01/12/15-01/15/15 based on Hourly-Averaged Data

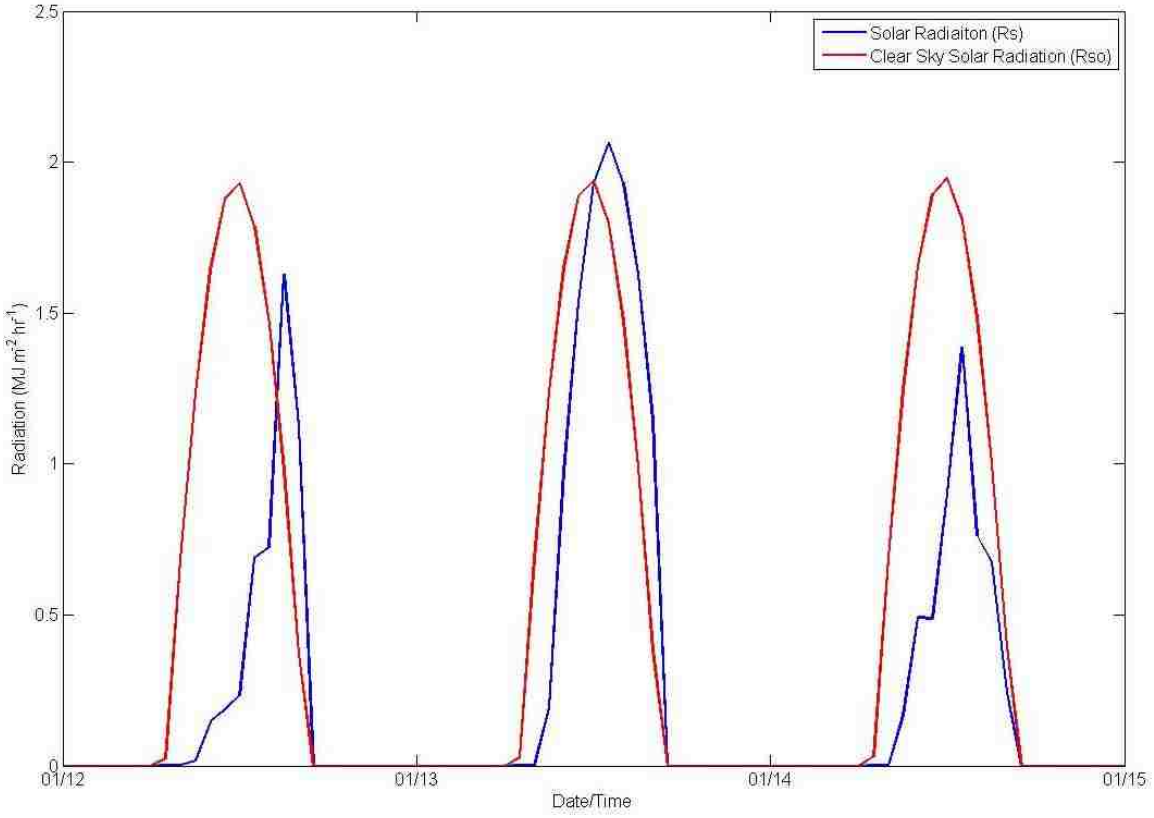

Reference Evapotranspiration from 01/12/15-01/15/15 based on Hourly-Averaged Data

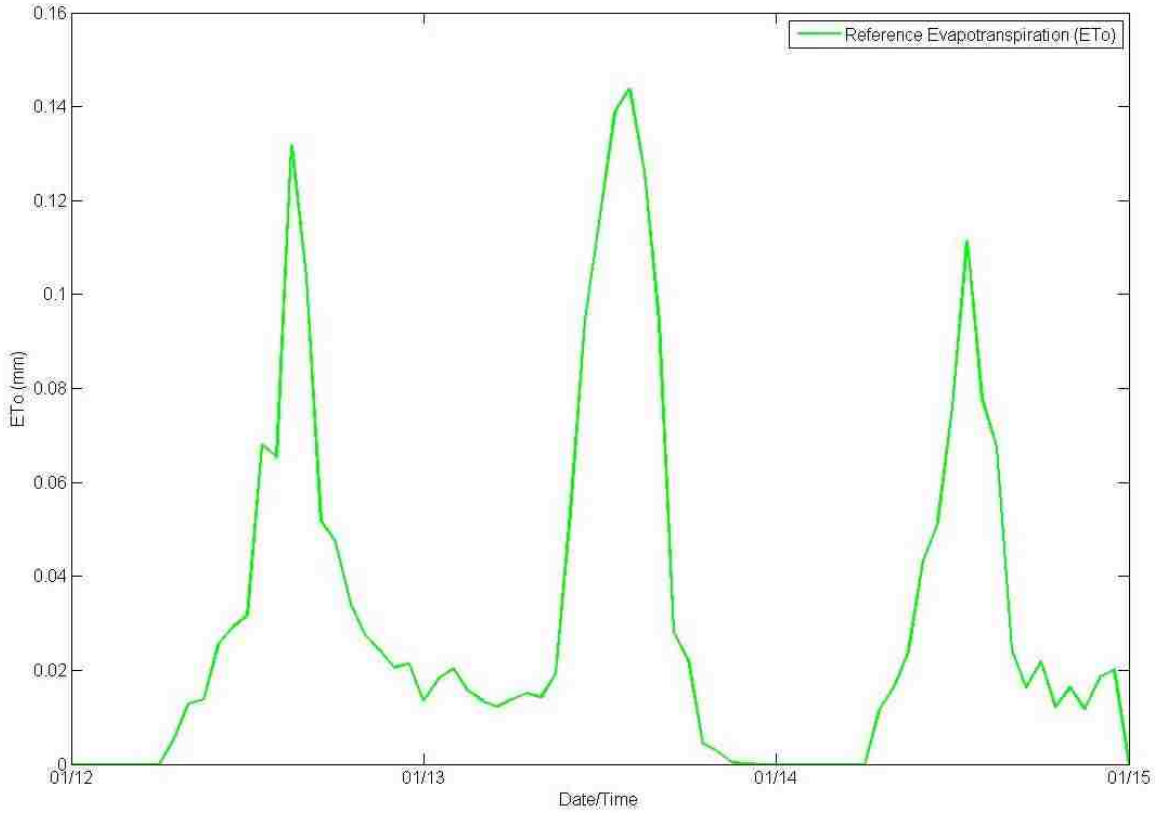

Cumulative Reference Evapotranspiration from 01/12/15-01/15/15 based on Hourly-Averaged Data

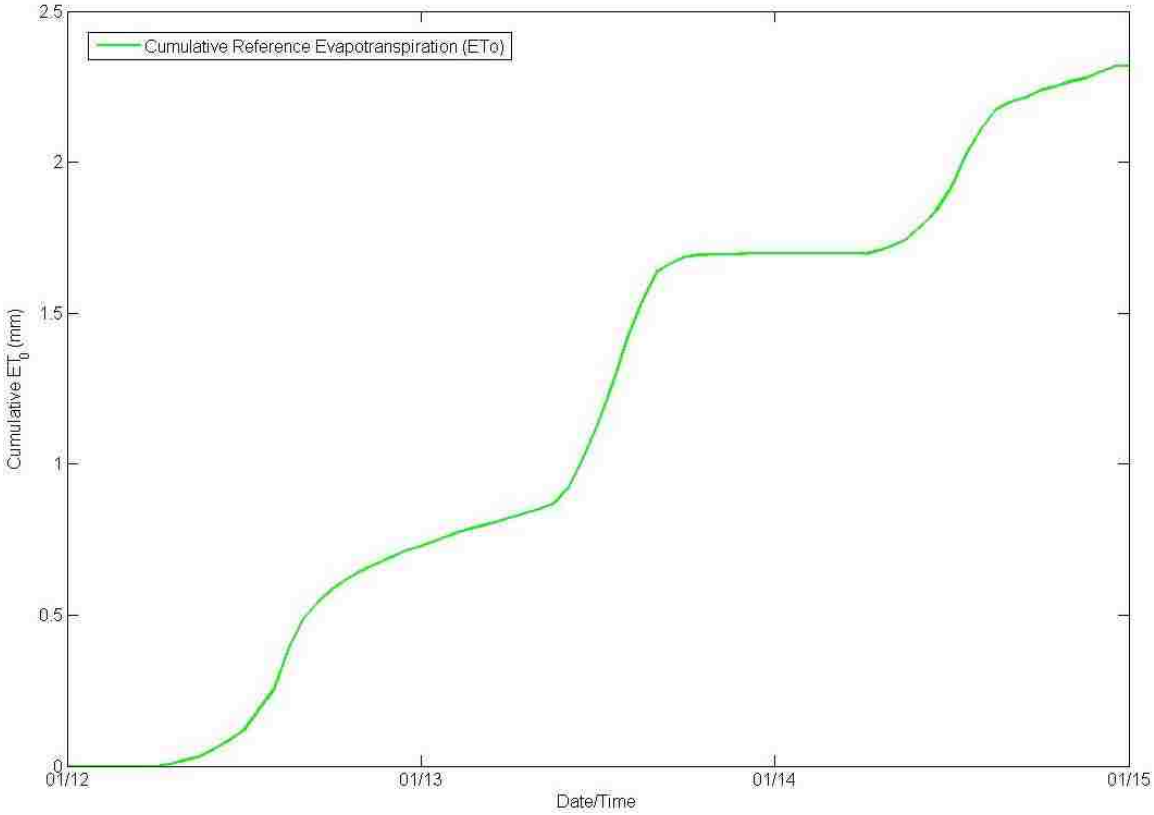

Cumulative Precipitation from 01/11/15-01/15/15 based on 5-minute Interval Data

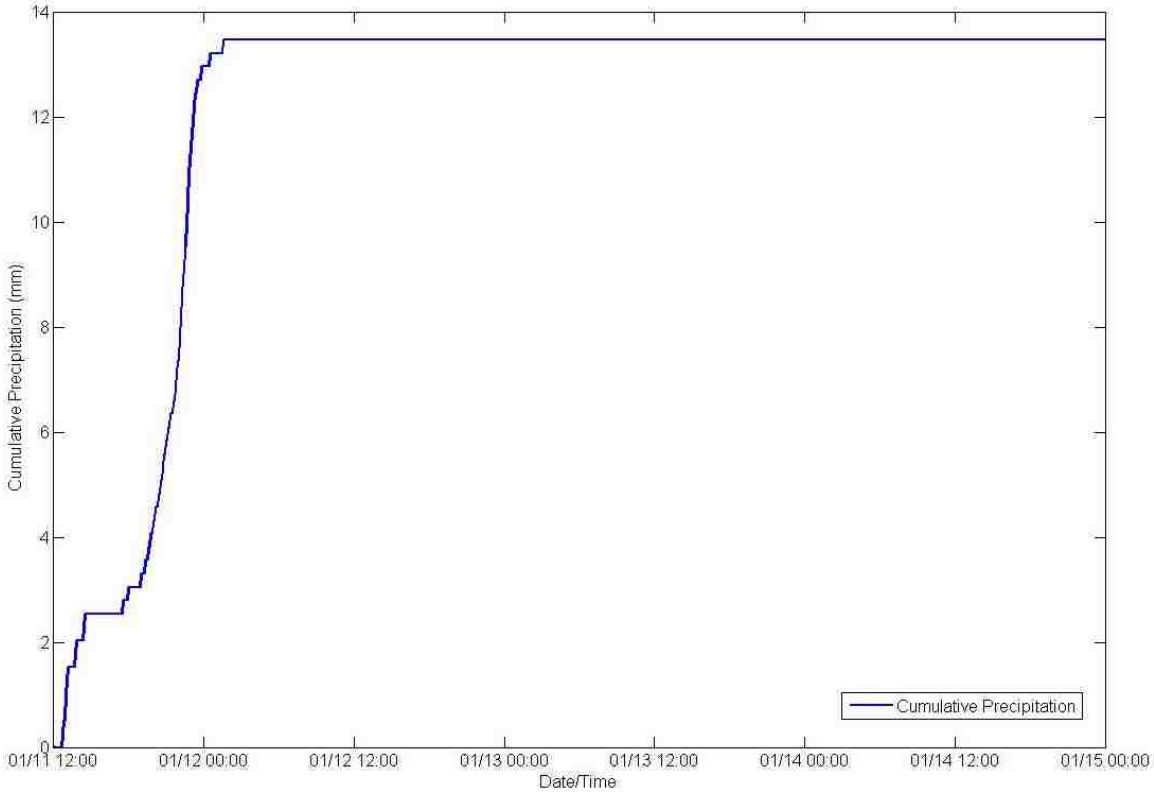

Surface Temperatures of the Three Roof Surfaces as well as Cumulative Precipitation, Reference Evapotranspiration, and Water Storage in the Media for 01/11/15-01/15/15

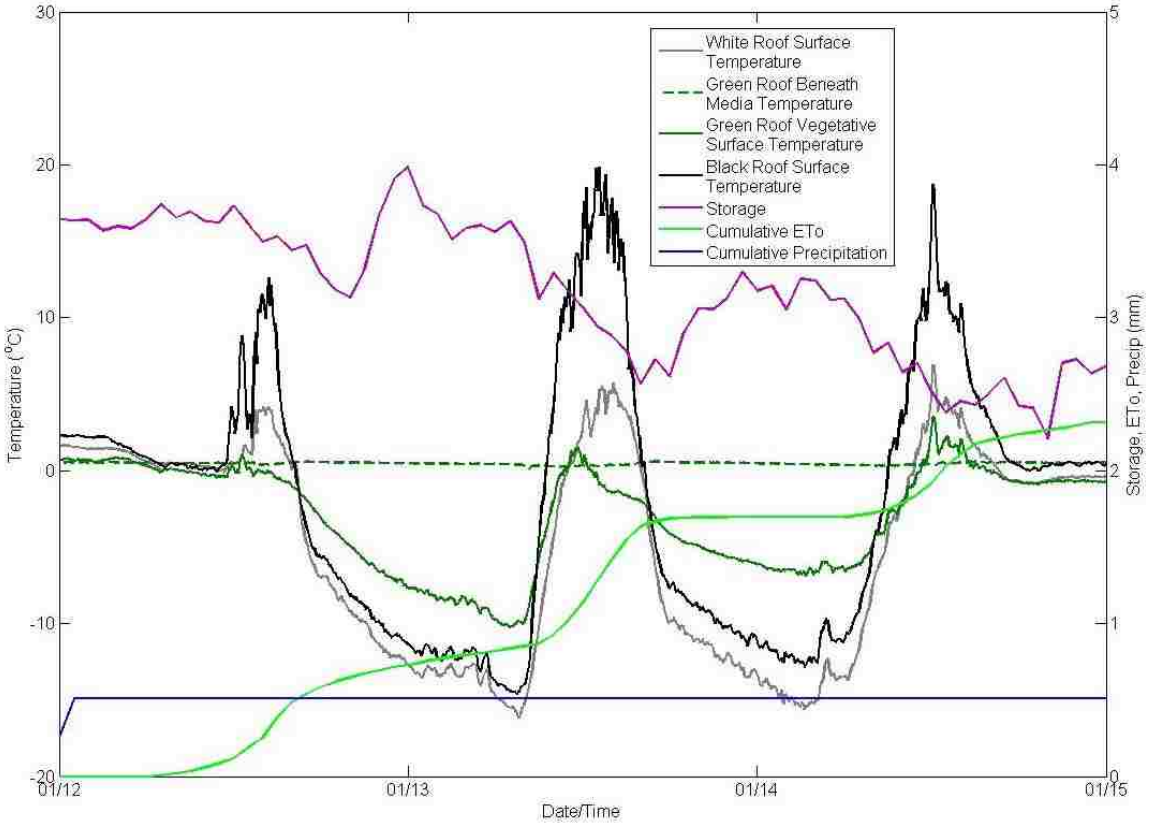

BIBLIOGRAPHY

Akan, A. O., and R. J. Houghtalen 2003 Urban Hydrology, Hydraulics, and Stormwater Quality: Engineering Applications and Computer Modeling. Hoboken, NJ: J. Wiley & Sons.

Akbari, H., and S. Konopacki 2005 Calculating energy-saving potentials of heat-island reduction strategies. Energy Policy 33(6):721-756.

Akbari, H., M. Pomerantz, and H. Taha 2001 Cool surfaces and shade trees to reduce energy use and improve air quality in urban areas. Solar Energy 70(3):295-310.

Allen, R. G., L.S. Pereira, D. Raees, and M. Smith 1998 FAO Irrigation and Drainage Paper No. 56. Pp. 333. Rome, Itlay.

Beck, D. A., G. R. Johnson, and G. A. Spolek 2011 Amending greenroof soil with biochar to affect runoff water quantity and quality. Environmental Pollution 159(8-9):2111-2118.

Bedient, P. B. , W. C. Huber, and B. E. Vieux 2013 Hydrology and Floodplain Analysis. Upper Saddle River, NJ: Pearson Education, Inc.

Bell, C. L., F. W. Brownell, R. E. Cardwell, D. R. Case, K. A. Ewing, J. J. O. King, S. W. Landfair, D. K. McCall, M. L. Miller, K. J. Nardi, A. P. Olney, T. Richini, J. M. Scagnelli, J. M. Spensley, D. M. Steinway, and R. R. von Oppenfeld 2014 Environmental Law Handbook. United States of America: Bernan Press.

Berndtsson, J. C. 2010 Green roof performance towards management of runoff water quantity and quality: A review. Ecological Engineering 36(4):351-360.

Berndtsson, J. C., T. Emilsson, and L. Bengtsson 2006 The influence of extensive vegetated roofs on runoff water quality. Science of the Total Environment 355(1 3):48-63.

Bledsoe, B. P., and C. C. Watson 2001 Effects of urbanization on channel instability. Journal of the American Water Resources Association 37(2):255-270.

Booth, D. B., and C. R. Jackson 1997 Urbanization of aquatic systems: Degradation thresholds, stormwater detection, and the limits of mitigation. Journal of the American Water Resources Association 33(5):1077-1090.

Brooks, K. N., P F. Ffolliott, H. M. Gregersen, and L. F. DeBano 2003 Hydrology and the Management of Watersheds. Ames, Iowa: Blackwell Publishing Professional.

Brunekreef, B., and S. T. Holgate 2002 Air pollution and health. Lancet 360(9341):1233 1242.

CArE Department of Civil, Architectural, and Environmental Engineering 2014 Missouri S&T Green Roof. Missouri University of Science and Technolgy. http://care.mst.edu/facilities/greenroof/ Jan. 4, 2015.

Chen, X. L., H. M. Zhao, P. X. Li, and Z. Y. Yin 2006 Remote sensing image-based analysis of the relationship between urban heat island and land use/cover changes. Remote Sensing of Environment 104(2):133-146.

Chow, V. T., D. R. Maidment, and L. W. Mays 1988 Applied Hydrology. United States of America: McGraw-Hill, Inc.

Dousset, B., and F. Gourmelon 2003 Satellite multi-sensor data analysis of urban surface temperatures and landcover. ISPRS Journal of Photogrammetry and Remote Sensing 58(1-2):43-54.

EISA 2007 Energy Independence and Security Act of 2007. Pp. 129. One Hundred Tenth Congress of the United States of America.

EPA 2004 Report to Congress on the Impacts and Control of CSOs and SSOs. United States Environmental Protection Agency, Office of Water (4203).

EPA, U.S. 2014 United States Environmental Protection Agency

greenerheights.wordpresss.com 2012 The Structure of Green Roofs: Greener heights.

Harper, G. E., M. A. Limmer, W. E. Showalter, and J. G. Burken 2014 Nine-month evaluation of runoff quality and quantity from an experiential green roof in Missouri, USA. Ecological Engineering.

Hathaway, A. M., W. F. Hunt, and G. D. Jennings 2008 A field study of green roof hydrologic and water quality performance. Transactions of the ASABE 51(1):37 44.

Holzman, D. C. 2012 Accounting for nature's benefits: the dollar value of ecosystem services. Environmental health perspectives 120(4):A152-157.

Luckett, K. 2009 Green Roof Construction and Maintenance. U.S.A: The McGraw-Hill Companies, Inc.

Lundholm, J., S. Tran, and L. Gebert 2015 Plant functional traits predict green roof ecosystem services. Environmental Science and Technology 49(4):2366-2374.

Michalak, A. M., E. J. Anderson, D. Beletsky, S. Boland, N. S. Bosch, T. B. Bridgeman, J. D. Chaffin, K. Chao, R. Confesor, I. Daloglu, J. V. DePinto, M. A. Evans, G. L. Fahnenstiel, L. He, J. C. Ho, L. Jenkins, T. H. Johengen, K. C. Kuo, E. LePorte, X. Liu, M. R. McWilliams, M. R. Moore, D. J. Posselt, R. P. Richards, D. Scavia, A. L. Steiner, E. Verhamme, D. M. Wright, and M. A. Zagorski 2013 Record setting algal bloom in Lake Erie caused by agricultural and meteorological trends consistent with expected future conditions. Proceedings of the National Academy of Sciences of the United States of America 110(16):6448-6452.

Morgan, S., I. Alyaseri, and W. Retzlaff 2011 Suspended solids in and turbidity of runoff from green roofs. International Journal of Phytoremediation 13(SUPPL.1):179-193.

Morgan, S., S. Celik, and W. Retzlaff 2013 Green roof storm-water runoff quantity and quality. Journal of Environmental Engineering (United States) 139(4):471-478.

Nagase, A., and N. Dunnett 2012 Amount of water runoff from different vegetation types on extensive green roofs: Effects of plant species, diversity and plant structure. Landscape and Urban Planning 104(3-4):356-363.

Palomo Del Barrio, E. 1998 Analysis of the green roofs cooling potential in buildings. Energy and Buildings 27(2):179-193.

PCAST, The President's Council of Advisors on Sience and Technology 2011 Sustaining Environmental Capital: Protecting Society and the Economy. Executive Office of the President.

Rabotyagov, S. S., C. L. King, P. W. Gassman, N. N. Rabalais, and R. E. Turner 2014 The economics of dead zones: Causes, impacts, policy challenges, and a model of the gulf of Mexico Hypoxic Zone. Review of Environmental Economics and Policy 8(1):58-79.

Rosenzweig, C., W. Solecki, L. Parshall, S. gaffin, B. Lynn, R. Goldberg, J. Cox, and S. Hodge 2006 Mitigating New York City's heat island with urban forestry, living roofs, and light surfaces. 86th AMS Annual Meeting, Atlanta, GA, 2006.

Sailor, D. J. 2008 A green roof model for building energy simulation programs. Energy and Buildings 40(8):1466-1478.

Scavia, D., J. D. Allen, K. K. Arend S. Bartell, D. Beletsky, N. S. Bosch, S. b. Brandt, R. D. Briland, I. Daloglu, J. V. DePinto, D. M. Doland, M. A. Evans, T. M. Farmer, D. Goto, H. Han, T. O. Hook, R. Knight, S. A. Ludsin, D. Mason, A. M. Michalak, R. P. Richards, J. J. Roberts, D. K. Rucinski, E. Rutherford, D. J. Schwab, T. M. Sesterhenn, H. Zhang, and Y.Zhou 2014 Assessing and addressing the re-eutrophication of Lake Erie: Central basin hypoxia. Journal of Great Lakes Research 40(2):226-246.

Schnoor, J. L. 1996 Environmental Modeling: Fate and Transport of Pollutants in Water, Air, and Soil. United States of America: John Wiley & Sons, Inc.

Sproul, J., M. P. wan, B. H. Mandel, and A. H. Rosenfeld 2014 Economic comparison of white, green, and black flat roofs in the United States. Energy and Buildings 71:20-27.

Stovin, V., G. Vesuviano, and H. Kasmin 2012 The hydrological performance of a green roof test bed under UK climatic conditions. Journal of Hydrology 414-415:148 161.

Taha, H. 1997 Urban climates and heat islands: Albedo, evapotranspiration, and anthropogenic heat. Energy and Buildings 25(2):99-103.

Taha, H., S. Konopacki, and H. Akbari 1998 Impacts of lowered urban air temperatures on precursor emission and ozone air quality. Journal of the Air and Waste Management Association 48(9):860-865.

Takebayashi, H., and M. Moriyama 2007 Surface heat budget on green roof and high reflection roof for mitigation of urban heat island. Building and Environment 42(8):2971-2979.

USGBC 2015 LEED. U.S.G.B. Council, ed. Pp. Leadership in Energy & Environmental Design, Vol. 2015.

van Seters, T., L. Rocha, D. Smith, and G. MacMillan. 2009 Evaluation of green roofs for runoff retention, runoff quality, and leachability. Water Quality Research Journal of Canada 44(1):33-47.

VanWoert, N. D., et al. 2005 Green roof stormwater retention: Effects of roof surface, slope, and media depth. Journal of Environmental Quality 34(3):1036-1044.

Villarreal, E. L., A. Semadeni-Davies, and L. Bengtsson 2004 Inner city stormwater control using a combination of best management practices. Ecological Engineering 22(4-5):279-298.

WEF, Water Environment Federation, American Society of Civil Engineers ASCE, and Environmental & Water Resources Institute EWRI 2012 Design of Urban Stormwater Controls. U.S.A.: McGraw-Hill.

Wu, T., and R. E. Smith 2011 Economic benefits for green roofs: A case study of the skaggs pharmacy building, university of Utah. International Journal of Design and Nature and Ecodynamics 6(2):122-138.

VITA

Madison R. Gibler was born in Kansas City, Missouri to Kevin and Lori Gibler. Madison attended Oak Park High School in Kansas City, Missouri from 2006 to 2008 and Staley High School in Kansas City, Missouri from 2008 to 2010. She graduated from Staley High School in May 2010. In December 2013 Madison graduated summa cum laude from Missouri University of Science and Technology, located in Rolla, Missouri, with a Bachelor of Science in Civil Engineering. Madison graduated with a Master of Science in Environmental Engineering in May 2015 from Missouri University of Science and Technology.